Marcelo Augusto Christoffolete

DESIODASES DE IODOTIRONINAS

RELEVÂNCIA PARA A HOMEOSTASE DO HORMÔNIO TIROIDEANO E TECIDO ADIPOSO MARROM

Tese apresentada à Universidade Federal de São Paulo – Escola Paulista de Medicina para obtenção do título de Doutor em Ciências

São Paulo

2006

Marcelo Augusto Christoffolete

DESIODASES DE IODOTIRONINAS

RELEVÂNCIA PARA A HOMEOSTASE DO HORMÔNIO TIROIDEANO E TECIDO ADIPOSO MARROM

Tese apresentada à Universidade Federal de São Paulo – Escola Paulista de Medicina para obtenção do título de Doutor em Ciências

Orientador: Prof. Dr. Antonio C. Bianco
Coordenador : Prof. Dr. Sérgio Atala Dib

São Paulo

2006

Dedico esta tese à minha esposa Dani
e ao meu filho Guilherme, fontes
constantes de inspiração e apoio, sem eles
nada disso teria valido a pena.

Agradecimentos

Ao Professor Antonio Carlos Bianco pelo apoio oferecido durante minha estadia em seu laboratório e incentivo para a realização deste doutorado.

To the professor P. Reed Larsen for the scientific discussion and general advice

Ao professor Anselmo Sigari Moriscot, cujos ensinamentos passados durante meu mestrado foram fundamentais durante meu amadurecimento no doutorado.

À professora Miriam Oliveira Ribeiro, responsável pela minha iniciação científica e conselheira oficial desde então.

À professora Cecília Gouveia, pelos conselhos e apoio.

Aos antigos amigos que acompanharam de longe, Flávio-Rubia, Mauro-Elaine, Cristiano-Gisele, Márcio-Patrícia, Carlos-Elaine, Diego, Marcelo Leandro, Maurício, Gabriel, Flávio Borges, Patrícia Severino, Gisele Gianocco, Adriano, Bonadia.

To my international friends, Guy-Adriana, Dave-Patrícia, João Kulcsar, Luciana Lavallé, Sun Chul, Marc-Kelly, Sandra-Ulisses, Lisiane-Axel and Jon-Beth Winickoff.

To the friends in Lab; Brian (what to say??), Ann Marie (One big heart), John Harney (Wise Man, Oracle among others), Michelle, Steve, Monica, Cristina, Beatriz Freitas, Renata Pavan, Rogério, Miguel, Tatiana e Luciane Capelo.

Ao amigo Wagner pelas discussões, sugestões, cafés e principalmente amizade, a qual tornou a estadia muito mais agradável.

To the secretaries at the Thyroid Division, Anita and Birgit.

To a great friend I had the pleasure to meet, Serge.

À minha primeira assistente e grande amiga Fernanda Gazoni e seu marido Wilson.

À minha última assistente Vanessa Gonçalves.

À minha família, minha mãe Dina, irmãs Maisa e Marilda, irmão Marco, sogros João e Maria Alice, cunhadas Renata e Marcela e cunhado Tadeu.

Sumário

Resumo

As três desiodases de iodotironina catalizam a iniciação (D1, D2) e o término (D3) dos efeitos dos hormônios tireoideanos nos vertebrados. Enquanto D1 e D3 são proteínas de meia-vida longa localizadas na membrana plasmática, a D2 é uma proteína residente do retículo endoplasmático com meia-vida de apenas 20 min. Nesta série de estudos, foram investigados: (1) os efeitos causados pela combinação da disrupção do gene da D2 (*Dio2*$^{-/-}$) com a deficiência familiar de D1 (camundongos C3H) na homeostase do hormônio tiroideano e apesar da múltipla deficiência de D1 e D2, animais C3H-D2KO apresentam T3 sérico na faixa eutiroidea, sugerindo mecanismos compensatórios, que promovem (i) aumento de aproximadamente 2 vezes nos níveis de T4 sérico, comparando com camundongos da linhagem C57/BL6 (C57) e, (ii) aumento da atividade de D1 hepática e renal, 8,4 e 2,0 vezes, respectivamente, em comparação com animais C3H. E ainda, este mecanismo compensatório não depende de aumento da atividade da glândula tiróide ou diminuição do "clearance" de T3 mediado pela D3; (2) o papel da D2 no sistema de retroalimentação negativa do TSH mediado pelo T4 na pituitária, o qual se revelou fundamental neste sistema e que, apesar de sofrer degradação induzida pelo

substrato como em qualquer outro tecido que expressa D2, a alta taxa de síntese da enzima assegura atividade e, conseqüentemente, produção constante de T3, mesmo na vigência de doses de T4 muito acima do fisiológico; (3) a importância da geração de T3 adaptativa mediada pela D2 para a resposta termogênica do BAT, a qual não está limitada a mediar a responsividade à catecolaminas, mas também promover lipogênese no tecido, essencial para fornecer substrato para oxidação mitocondrial e, conseqüentemente, desacoplamento e geração de calor; (4) o papel da D2 na conversão da célula pré-adiposa marrom em célula madura, que confirmou *in vitro* a importância da D2 para a capacidade termogênica deste tipo celular e seu papel chave no recrutamento do programa de diferenciação, o qual, na ausência de D2, apresenta um déficit de ~25%.

Abstract

The three iodothyronine deiodinases catalyze the initiation (D1,D2) and termination (D3) of thyroid hormone effects in vertebrates. While D1 and D3 are long-lived plasma membrane proteins, D2 is an endoplasmic reticulum resident protein with a half-life of only 20 min. In these series of studies, we investigated: (1) the effects in thyroid hormone homeostasis caused by the combined targeted disruption of D2 gene (*Dio2-/-*) and inbred D1 deficiency (C3H mice), and despite the multiple D1 and D2 deficiency, C3H-D2KO animals present serum T3 in the euthyroid range, suggesting compensatory mechanisms that promote (i) ~2 fold increase in serum T4, when compared to C57/BL6 (C57) mice and (ii) increase in hepatic and renal D1 activity of 8.4 and 2.0 fold, respectively, when comparing to C3H animals. Furthermore, this compensatory mechanism does not depend on increased thyroidal activity or decreased in D3-mediated T3 clearance.; (2) D2 role in the T4-mediated TSH feedback in the pituitary, which place D2 in a pivotal role in this system, and despite being target to the substrate induced degradation as in any other D2-expressing tissue, the high rate of D2 synthesis assure activity, and consequently, constant T3 production, even at high doses of T4, well above the physiological levels; (3) the importance of

adaptive D2-mediated T3 generation to the BAT thermogenic response, which is not limited to mediate responsiveness to catecholamines, but also promote lipogenesis in the tissue, essential to make available substrate for mitochondrial oxidation and, consequently, uncoupling and heat generation; (4) D2 role in brown pre-adipocyte to mature cell conversion, confirming *in vitro* the importance of D2 to this cell type thermogenic capacity, and its key role in the differentiation program recruitment, which in D2 absence, presents a ~25% déficit.

I – Introdução

O principal produto de secreção da glândula tiróide é a tiroxina (T4), embora 5,3,3'-triiodotironina (T3) seja a forma biologicamente ativa. O T4 é considerado um pró-hormônio que precisa ser convertido em T3, através da retirada do iodo na posição 5' do anel fenólico ou desiodação do anel externo. Esta conversão é catalizada pelas desiodases de iodotironinas do tipo 1 (D1) e 2 (D2) (1). Em humanos, estas enzimas são responsáveis por 80% da produção diária de T3, enquanto em roedores a desiodação extra-tiroideana é responsável por cerca de 60% da produção diária de T3 (2).

O término da ação do hormônio tiroideano também depende em grande parte de desiodação, entretanto, neste processo, o iodo da posição 5 do anel tirosil é removido, sendo esta reação denominada desiodação do anel interno. Desta forma, tanto o pró-hormônio (T4) quanto o hormônio (T3) são inativados, resultando em 3,5',3'-triiodorironina (rT3) e 3,3'- diiodotironina (T2), respectivamente. Esta reação é catalizada pelo terceiro membro da família de desiodases, a desiodase do tipo 3 (D3) e em menor proporção pela D1 (1).

As três desiodases apresentam grande similaridade estrutural (~50% de identidade)(3). Todas são proteínas de membrana com peso molecular de 29-33 KDa(3). Elas também apresentam alta homologia na região do centro catalítico (4-6). Entretanto, apesar da grande similaridade reforçada por modelos tridimensionais (3), as três

desiodases possuem afinidade por substrato, cinética enzimática, meia vida e sensibilidade ao propiltiouracil (PTU) muito distintas e serão discutidas a seguir.

Desiodase de iodotironina do tipo 1 (D1)

A D1 foi a primeira a ser reconhecida por ensaios bioquímicos de conversão de T4 a T3 e foi a primeira das enzimas a ser clonada (1). Compreensivelmente, o conhecimento sobre as características bioquímicas da D1 é o mais extenso dentre as três desiodases (1). A característica principal da desiodação catalizada pela D1 é a sensibilidade à inibição por PTU (7). Outra característica importante é a capacidade de catalizar desiodaçao do anel interno, na via da inativação do hormônio tiroideano (8).

A reação catalizada pela D1 segue cinética do tipo ping-pong com dois substratos, o primeiro sendo a iodotironina e o segundo, um co-fator endógeno tiol. A primeira metade da reação constitui a desiodação da iodotironina, levando à formação de um possível intermediário selenoyl iodide. Este por sua vez é reduzido pelo co-fator tiol ainda não identificado, o qual regenera a enzima (5, 9-13). A D1 apresenta Km T4 em torno de 1 μM e Km rT3 em torno de 0.5 μM, e uma meia-vida de 8h (1, 3).

A D1 é expressa em vários tecidos em todos os vertebrados (14-16). Em ratos, a D1 é encontrada no fígado, rins, sistema nervoso central (SNC), hipófise anterior, tiróide, intestino e placenta (17). Em humanos, D1 está ausente no SNC, mas foi confirmada em

fígado, rins, tiróide e hipófise anterior, além de seu mRNA ser detectável por RT-PCR em células mononucleares circulantes (18).

A D1 localiza-se na membrana plasmática (19) com o centro catalítico no citoplasma. Devido à localização junto à membrana plasmática, é provavél que o T3 produzido pela D1 retorne rapidamente para o plasma, tendo pouco impacto na concentração intracelular de T3 e um impacto maior para os níveis séricos de T3.

Desiodase de iodotironina do tipo 2 (D2)

A D2 foi a desiodase clonada mais recentemente, razão pela qual o conhecimento de suas propriedades e funções tem se acumulado rapidamente (1). D2 cataliza exclusivamente a desiodação do anel externo e, ao contrário da D1, é muito menos sensivel à inibiçao por PTU (20-22). A reação catalizada pela D2 segue cinética do tipo seqüencial, de modo que iodotironina e o co-fator endógeno tiol são combinados com a enzima para que a reação aconteça (23). A D2 tem afinidade por T4 e rT3 em torno de 1 nM, e meia-vida de aproximadamente 20 min (3).

Em ratos, a atividade de D2 é encontrada na hipófise anterior, cérebro e tecido adiposo marrom (BAT) (20, 22-26). A atividade da D2 também é encontrada em gônadas, glândula pineal, timo, útero durante a gestação; em glândula mamária e esqueleto em camundongos e em artéria coronária e em músculo liso da aorta em humanos (27-32). mRNA e atividade de D2 são encontrados na cóclea de camundongos,

no oitavo dia pós-parto (33), sugerindo um papel da D2 no desenvolvimento coclear. De fato, animais *Dio2*$^{-/-}$ são quase surdos devido ao desenvolvimento incompleto da cóclea (34, 35). No córtex, mRNA da D2 é expresso predominantemente em astrócitos do lobo frontal de ratos recém-nascidos (36). A atividade da D2 também é alta em tanicitos e células ependimais ao longo do terceiro ventrículo (36-39). Uma via mono-sináptica também foi identificada entre células do núcleo arqueado, que expressam D2, e entre células neuroendócrinas, que secretam TRH no núcleo para-ventricular (40). Em humanos, D2 é expressa na tiróide, coração, cérebro, medula espinhal, músculo esquelético e placenta (4, 41-45).

A D2 é uma proteína residente do retículo endoplasmático (46) com o centro catalítico também localizado no citosol. D2 é alvo do sistema de ubiqüitinaçao, sendo esta a principal via de degradaçao da enzima, e será discutido com mais detalhes adiante (3). Devido à localização junto ao retículo endoplasmático, é provavél que o T3 produzido pela D2 seja preferencialmente translocado para o núcleo, o que explicaria o grande impacto na concentração intranuclear de T3 promovida pela D2, embora o efluxo de T3 para o plasma também ocorra, não descartando a D2 como fonte de T3 sérico (47-49). D2 é importante no cérebro, produzindo mais de 75% de todo o T3 nuclear no córtex cerebral de ratos (50). A presença de D2 no músculo esquelético em humanos provê uma fonte significante para o T3 extra-tiroideano produzido diariamente (41).

O papel da D2 na termogênese facultativa do tecido adiposo marrom

A exposição ao frio prontifica o hipotálamo a iniciar tremor muscular, o principal mecanismo involuntário na termogênese facultativa induzida pelo frio em humanos adultos e mamíferos de grande porte. Entretanto, o tremor muscular inevitavelmente causa perda de calor por convecção devido à oscilações corpóreas e é, conseqüentemente, uma forma menos econômica de geração de calor quando comparada com desacoplamento mitocondrial, principalmente em pequenos mamiferos com alta razão de área de superfície por massa corpórea (51). Por esta razão, a termogênese facultativa que não envolve tremor muscular é a principal fonte de calor em humanos recém-nascidos e pequenos mamíferos (51). Esta resposta também é iniciada no hipotálamo através da ativição do sistema nervoso simpático (SNS), aumentando a liberação de catecolaminas pelo corpo, principalmente no tecido adiposo marrom (BAT), o órgão chave dessa modalidade de termogênese facultativa. O BAT é intensamente inervado pelo SNS, e sua capacidade termogênica é grandemente atribuída à proteína desacopladora 1 (UCP-1), uma proteína mitocondrial que promove o vazamento de prótons do espaço intermembrana da mitocôndria, competindo com a menos abundante ATP sintase, desacoplando desta forma a oxidação de substratos energéticos da fosforilação de ADP (52-54).

A resposta normal da UCP-1 à exposição ao frio é abolida em ratos hipotiróideos (55-57), requerendo saturação completa dos receptores de hormônio tiroideano no BAT (56). A normalização dos níveis de UCP-1 em animais hipotiróideos com T3 exógeno requer doses que provocam hipertiroidismo sistêmico (58). Em contrapartida, os níveis de UCP-1 são normalizados com doses fisiológicas de T4, o que é explicado pela expressão

de D2 no BAT, a qual gera o T3 adicional necessário para a termogênese facultativa do BAT (26).

Outra função da D2 no tecido é proporcionar o aumento de 3 a 4 vezes na atividade de enzimas lipogênicas, i.é., enzima málica e glicose-6-fosfato desidrogenase, observado no tecido durante a exposição ao frio. Este fenômeno também é abolido em ratos hipotiróideos (56, 59). Durante a exposição ao frio, a lipogênese no BAT é muito ativa, sendo responsável por mais de 50% da *de novo* síntese de ácidos graxos no rato (60).

A análise mais detalhada do modelo animal hipotiróideo revela a grande limitação deste modelo, a qual resulta do aumento intrínseco da atividade do SNS. A liberação de norepinefrina (NE) na maioria dos tecidos é acelerada pelo hipotiroidismo, provavelmente para compensar o decréscimo generalizado à responsividade a NE (61). O aumento da liberação de NE causa desensitização adrenérgica, levando ao decréscimo da responsividade a NE (62, 63). É muito difícil discriminar os efeitos causados pelo hipotiroidismo dos eventos relacionados à desensitização.

Alternativamente, o camundongo com disrupção do gene da D2 (*Dio2*$^{-/-}$) constitui um sistema aperfeiçoado para o estudo das interações hormônio tiroideano-sistema adrenérgico (64, 65). Estes animais são sistemicamente eutiróideos, apresentando T3 sérico normal e T4 levemente elevado. Desta forma, estes animais não desenvolvem

adaptações homeostáticas a temperatura ambiente. Entretanto, a ausência da D2 prejudica a termogênese do BAT por eliminar a conversão adaptativa de T4 a T3 (64).

A termogênese facultativa do BAT está prejudicada nos animais *Dio2*$^{-/-}$, como demonstrado *in vivo* e *in vitro* (64). Quando expostos ao frio, os animais *Dio2*$^{-/-}$ apresentam hipotermia moderada e sobrevivem por aumentar a termogênese por tremor muscular. Estes efeitos podem ser revertidos pela administração de uma única dose saturante de T3 24, horas antes da exposição ao frio, demonstrando que a função crítica da D2 é catalizar a produção de T3 nestas células (64). Desta forma, ao contrário do modelo animal hipotiróideo, o animal *Dio2*$^{-/-}$ possibilita a melhor compreensão dos mecanismos pelos quais a D2 é um componente crítico da resposta termogênica do BAT (51).

Degradaçao da D2 pelo sistema proteassomal

A D2 é considerada a desiodase crítica na homeostase do T3 gerado por desiodação devido a sua plasticidade fisiológica. Por exemplo, a responsividade da D2 a AMP cíclico constitui a base para sua rápida estimulaçao adrenérgica no BAT, no músculo esquelético humano e na tiróide, associando a expressão de D2 ao sistema nervoso simpático e, expandindo o espectro de estímulos ambientais e endógenos que podem, potencialmente, influenciar a produção adaptativa de T3 (para revisão (1)).

Um grande número de mecanismos transcripcionais e pós-traducionais evoluíram para assegurar expressão limitada e controle rígido dos níveis de D2, os quais são inerentes à suas funções homeostáticas (3). Em vertebrados superiores, a extensão do mRNA da D2 é maior do que 6 Kb em comprimento, apresentando longas regiões 5'e 3' não codificadoras (66). "Splicing" alternativo é um dos mecanismos que controlam os níveis de D2, gerando mRNAs similares em tamanho aos principais 6 e 7 Kb, mas que não codificam a enzima ativa (66). Instabilidade da sequência AUUUA localizada na porção 3' não codificadora diminue a meia-vida do mRNA da D2 e a deleção desta região promove um aumento de, aproximadamente, 3,8 vezes da meia-vida do mRNA da D2 (66).

A razão atividade/mRNA da D2 é variável, indicando regulação pós-traducional substancial (67). De fato, a curta meia-vida (~20 min) é o que caracteriza o seu comportamento homeostático (68), e mais, esta meia-vida pode ser ainda menor devido a exposição à concentrações fisiológicas de seu substrato, o T4, e, em condições experimentais, rT3 e T3 (68-74). Isto constitui uma alça de retroalimentação rápida e potente, controlando de forma eficiente a produção de T3 e níveis intracelulares de T3 de acordo com a disponibilidade de T4. O potencial das iodotironinas para promover degradação da D2 reflete a afinidade da enzima pelo substrato, indicando que o complexo enzima-substrato é necessário para a perda de atividade da D2 (3).

A D2 após catalizar a conversão de T4 a T3, torna-se alvo do sitema de ubiqüitinação, o qual marca a enzima através da conjugação desta com ubiqüitinas. Após

ubiqüitinação, A D2 é extraída do retículo endoplasmático e encaminhada para degradação no citosol (75, 76). A maquinaria de ubiqüitinação é constituída de dois complexos inespecíficos (E1 e E2) e um terceiro complexo que garante especificidade (E3) (77, 78). Estudo recente identificou a SOCS-box containing WD-40 protein (WSB-1) como o componente do complexo E3 que promove a ubiqüitinação da D2 de forma específica (79).

A D2 ubiqüitinada pode ser resgatada por proteínas desubiqüitinadoras (VDU 1 e 2). Este mecanismo é bastante eficiente na amplificação da atividade da D2 e é bem ilustrado pela rápida estimulação da VDU 1 em BAT, nas primeiras horas de exposição ao frio, promovendo um salto na atividade da D2 que precede o aumento do próprio mRNA da D2 no tecido (80).

Desta forma, devido à ineficiência intrínseca na síntese de selenoproteínas, a desubiqitinação da D2 constitui vantagem bioquímica e fisiológica que possibilita rápido controle da ativação do hormônio tiroideano (3).

Desiodase de iodotironina do tipo 3 (D3)

A D3 é considerada a via principal de inativação de T3 e T4 porque a D1 tem capacidade limitada de promover desiodação do anel interno. A D3 por sua vez, promove exclusivamente a desiodação do anel interno, convertendo T4 a rT3 e T3 a 3,3'-T2, ambos biologicamente inativos (81). Esta enzima contribui para a homeostase do

hormônio tiroideano, protegendo tecidos da exposição ao excesso de hormônio tiroideano (3).

A reação catalizada pela D3, a exemplo da D2, também segue cinética do tipo seqüencial e é insensível à inibição por PTU (5, 82). A D3 isolada de microssomos do córtex cerebral de ratos apresenta afinidade por T3 em torno de 1 nM e uma afinidade menor por T4, em torno de 37 nM. A afinidade da D3 humana por T3 está em torno de 12 nM.(82) A D3 apresenta meia-vida de 12h (3).

Apesar da desiodação do anel interno, de forma generalizada, e da atividade de D3, em particular, terem sido descritas em vários tecidos, em um grande número de espécies animais, a maioria dos estudos realizados utilizam-se de ratos como modelo animal. No rato adulto, a D3 é encontrada predominantemente no SNC, pele e placenta, enquanto que no rato recém-nascido a D3 é encontrada no músculo esquelético, fígado e intestino (32, 83-87). A atividade da D3 também é detectada em fígado de fetos humanos, mas desaparece ao final da gestação (88). Com o uso da técnica de hibridação *in situ*, o mRNA da D3 foi identificado por todo o cérebro no SNC de ratos adultos, com alta expressão nos neurônios piramidais do hipocampo, células granulosas do núcleo dentado e camadas II-IV do córtex cerebral (89). É importante ressaltar que estas áreas do cérebro apresentam as concentrações mais altas de receptores de hormônio tiroideanos dentro do SNC e são fundamentais para o aprendizado, memória e funções cognitivas superiores (90-92). D3 também é encontrada na retina de fetos de ratos e, em menor quantidade, nos olhos de ratos adultos (93). D3 é encontrada em abundância na pele de ratos adultos (32,

94). D3 é também altamente expressa na placenta de ratos, de porquinhos-da-índia e de humanos (85, 95-98). O sítio de implantação do embriao é a região da placenta que apresenta a maior atividade de D3, aproximadamente o dobro de qualquer outra área (99). Na célula, a D3 localiza-se na membrana plasmática (19), mas a localizacao do centro catalítico ainda é controversa (19, 100). Devido à localização junto a membrana plasmática, esta enzima tem acesso facilitado ao hormônio tiroideano plasmático, explicando sua capacidade de inativar o T4 e T3 circulante em pacientes com hemangiomas e o bloqueio de hormônio tiroideano materno ao feto em desenvolvimento (101-103).

II - Objetivos

1 – Avaliar a homeostase do hormônio tiroideano em camundongos com disrupção do gene da desiodase do tipo 2, em deficiência familiar da desiodase do tipo 1;

2 – Investigar o papel da desiodase do tipo 2 no sistema de retroalimentação negativa no eixo hipofisário-tiróide;

3 – Investigar os mecanismos que explicam termogênese facultativa ineficiente do tecido adiposo marrom em animais com disrupção do gene da desiodase do tipo 2;

4 – Investigar o papel da desiodase do tipo 2 no desenvolvimento e função termogênica da célula adiposa marrom.

III – Primeiro Artigo

Title

MICE WITH IMPAIRED EXTRATHYROIDAL THYROXINE TO 3,5,3'-TRIIODOTHYRONINE (T3) CONVERSION MAINTAIN NORMAL SERUM T3 CONCENTRATIONS

Authors:

Marcelo A. Christoffolete, Rafael Arrojo e Drigo, Fernanda Gazoni, Susana M. Tente, Vanessa Goncalves, P. Reed Larsen, Antonio C. Bianco, Ann Marie Zavacki

Institutions:

Thyroid Section, Division of Endocrinology, Diabetes and Hypertension, Brigham and Women's Hospital, Boston MA 02115

Key words: deiodinase, thyroid hormone metabolism, thyroid hormone receptor, thyroid

Corresponding author:

Ann Marie Zavacki

Thyroid Section, Division of Endocrinology, Diabetes and Hypertension, Brigham and Women's Hospital, HIM 641, 77 Ave Louis Pasteur, Boston MA 02115

Phone: 671-525-5158

Fax: 617-731-4718

azavacki@rics.bwh.harvard.edu

Resumo

Em ordem para que a 3,5,3'-triiodotironina (T3) possa mediar seus efeitos biológicos, o pró-hormônio tiroxina (T4) deve ser ativado pela remoção de um iodo do anel externo pelas desiodases do tipo 1 ou 2 (D1 e D2). Para melhor definir os papéis da D1 e da D2 na homeostase do hormônio tiroideano, nós introduzimos a disrupção do gene Dio2 em linhagem C3H/HeJ (C3H) com baixa expressão de D1, gerando o camundongo C3H D2KO. Notavelmente, estes animais mantém níveis séricos de T3 eutiroideos, com crescimento normal e sem decréscimo na expressão de genes hepáticos responsivos ao T3. Contudo, o T4 está aumentado 1,2 vezes em relação aos já elevedos níveis de C3H, sendo 2,2 vezes acima dos níveis de camundongos C57BL/6J (C57), os quais apresentam expressam de D1 e D2 selvagem. O TSH do C3H-D2KO está aumentado 1,4 vezes em relação ao C3H, e ainda assim a captação de ^{125}I não indica diferença na atividade tiroideana entre estes animais. As atividades da D1 hepática e renal estavam bem abaixo do que em camundongos selvagens C57 (0,1 vezes para ambas), mas estavam aumentadas 8 e 2 vezes, respectivamente, em relação ao C3H. Além disso, atividade da D1 tiroideana e desiodase do tipo 3 (D3) do córtex cerebral estavam inalteradas entre camundongos C3H-D2KO e C3H. Em conclusão, camundongos C3H-D2KO apresentam notável aumento dos níveis de T4 sérico, e isto, em conjunto com baixa atividade residual de D1, poderiam desempenhar papel importante na manutenção de suas concentrações eutiroideas de T3 sérico. Entretanto, atividade tiroideana aumentada e/ou produção de T3 mediada por D1, ou um decréscimo da inativação de T3 mediado pela D3, não parecem participar da manutençao da homeostase do hormônio tiroideano nestes animais.

Mice With Impaired Extrathyroidal Thyroxine to 3,5,3'-Triiodothyronine (T3) Conversion Maintain Normal Serum T3 Concentrations

Marcelo A. Christoffolete, Rafael Arrojo e Drigo, Fernanda Gazoni, Susana M. Tente, Vanessa Goncalves, P. Reed Larsen, Antonio C. Bianco, Ann Marie Zavacki

Thyroid Section, Division of Endocrinology, Diabetes and Hypertension
Brigham and Women's Hospital, Boston MA 02115

Requests for reprints should be directed to A.M.Z.

Abbreviated title: C3H-D2KO Mice Maintain Euthyroid T3

Key words: deiodinase, thyroid hormone metabolism, thyroid hormone receptor, thyroid

This work was supported by NIH grants DK06576, DK65055, and DK36256

Corresponding author:
Ann Marie Zavacki
Thyroid Section,
Division of Endocrinology, Diabetes and Hypertension
Brigham and Women's Hospital
HIM 641
77 Ave Louis Pasteur
Boston MA 02115
Phone: 671-525-5158
Fax: 617-731-4718
azavacki@rics.bwh.harvard.edu

Abstract:

In order for 3,5,3'-triiodothyronine (T3) to mediate its biological effects, the pro-hormone thyroxine (T4) must be activated by removal of an outer-ring iodine by the type 1 or 2 deiodinases (D1 and D2). To further define the roles of D1 and D2 in thyroid hormone homeostasis, we backcrossed the targeted disruption of the *Dio2* gene into C3H/HeJ (C3H) mice with genetically low D1 expression, creating the C3H-D2KO mouse. Remarkably, these mice maintain euthyroid serum T3 levels, with normal growth and no decrease in expression of hepatic T3-responsive genes. However, T4 is increased 1.2-fold relative to the already elevated C3H levels, being 2.2-fold that C57BL/6J (C57) mice with wild type D1 and D2 expression. C3H-D2KO TSH is increased 1.4-fold relative to C3H, yet thyroidal ^{125}I uptake indicates no difference in thyroidal activity between these mice. C3H-D2KO hepatic and renal D1 activities were well below those observed in wild type C57 mice (~0.1-fold for both), but were increased 8-fold and 2-fold respectively relative to C3H mice. Additionally, thyroidal D1, and cerebral cortical type 3 deiodinase activity (D3) were unchanged between C3H-D2KO and C3H mice. In conclusion, C3H-D2KO mice have notably elevated serum T4 levels, and this, in conjunction with residual low D1 activity, could play an important role in the maintenance of their euthyroid serum T3 concentrations. However, increased thyroidal activity and/or thyroidal D1-mediated T3 production, or a decrease in D3-mediated T3 clearance, do not appear to play a role in the maintenance of thyroid hormone homeostasis in these mice.

Introduction:

Thyroxine (T4) is the major product secreted by the thyroid gland, yet 3,5,3'-triiodothyronine (T3) is the ligand for thyroid hormone receptor (TR) (1). Thus, T4 must be converted to T3 by the type 1 or 2 iodothyronine deiodinases (D1 or D2) to mediate its biological effects (reviewed in (2)). In humans, approximately 80% of daily T3 production is derived from extrathyroidal D1- and D2-mediated T4 to T3 conversion, while in rodents, 60% of their daily T3 production is *via* this pathway (reviewed in (2)).

Three rodent models exist where the effects of deiodinase deficiency on extrathyroidal T4 to T3 conversion may be studied. These include the C3H/HeJ (C3H), *Dio1*$^{-/-}$ (D1KO) and *Dio2*$^{-/-}$ (D2KO) mice. In C3H mice, a decreased expression of the *Dio1* gene results in both liver and kidney D1 activities being reduced to ~10-20% that of most wild type mice, e.g. C57/BL6 (C57)(3-6). These mice have no obvious phenotypic abnormalities despite their relative deficiency of D1, with serum T3 and TRH-stimulated TSH levels being normal, however, T4 is increased by ~60 % (3). Pituitary D2 activity is also decreased by ~50% in these mice, presumably due to high T4 levels increasing T4-mediated proteosomal degradation of this enzyme (3, 7, 8).

D1KO mice with a targeted disruption of the *Dio1* gene are very similar to C3H, with normal serum T3 and TSH, while T4 is elevated (9). These mice have no obvious abnormalities, however a detailed analysis of these animals has revealed they are slightly heavier than wild type siblings, and have greater fecal iodothyronine excretion (9).

Mice with a targeted disruption of the *Dio2* gene are also apparently euthyroid, with normal serum T3 and hepatic D1 activity, although elevation in serum T4 and TSH indicates a central insensitivity to T4 (10). D2KO mice exhibit isolated hypothyroidism

in tissues that depend on D2-catalyzed T4 to T3 conversion to regulate thyroid status, i.e. brain, and brown adipose tissue. Thus, these animals have elevated TSH, are deaf, and are unable to sustain their body temperature during cold exposure as a result of impaired energy expenditure (10-12).

Still, it is remarkable that there are no further abnormalities in any of these mice. This leads one to wonder, is the T3 generating capacity of the remaining D1 and/or D2 in these animals able to compensate such that more severe defects are not manifested? Further, what would happen if both D1 and D2 activity were impaired? To address this question, we backcrossed the targeted disruption of the *Dio2* gene into a C3H background to generate the C3H-D2KO mice. Our results indicate that remarkably, despite very low D1 activity and no D2 expression, C3H-D2KO mice maintain euthyroid plasma T3 levels, and no apparent additional phenotypic abnormalities exist in these animals.

Materials and Methods:

Animal Treatment Protocols

Animals were maintained and experiments were performed according to protocols approved by the Animal Care and use Committee of Harvard Medical School in compliance with NIH standards. C57BL/6J (C57) or C3H/HeJ (C3H) mice were obtained from Jackson Labs (Bar Harbor, ME). Mice were fed normal chow and housed under a 12-hour light 12-hour dark cycle at 22 ^{0}C. For all experiments shown male mice of approximately 8-weeks of age were used unless otherwise indicated.

Generation of Dio1$^{C3H/C3H}$-Dio2$^{-/-}$, C3H-D2KO and C57-D2KO mice

Male mice homozygous for a targeted disruption of the *Dio2* gene (*Dio2*$^{-/-}$) (10) were mated with C3H females, and the resulting *Dio*1$^{WT/C3H}$-*Dio*2$^{+/-}$ heterozygotes were interbred to generate *Dio*1$^{WT/WT}$-*Dio*2$^{+/+}$, *Dio*1$^{C3H/C3H}$-*Dio*2$^{+/+}$, *Dio*1$^{WT/WT}$-*Dio*2$^{-/-}$, and *Dio*1$^{C3H/C3H}$-*Dio*2$^{-/-}$ mice. To generate C3H-backcrossed animals, male *Dio2*$^{-/-}$ mice were mated with C3H females to create F1, with the resulting male *Dio2*$^{-/+}$ heterozygotes being crossed with a C3H female 3 more times to generate the F4. F4 *Dio2*$^{-/+}$ heterozygous females were then mated with C3H males to ensure the Y chromosome was also C3H-derived in the F5 offspring. Heterozygous F5 males and females were then interbred to generate animals predicted to be 97 % C3H (13) and these animals are referred to as C3H-D2KO mice. A similar strategy was used to generate animals where the targeted disruption of the *Dio2* allele was backcrossed into a C57 background, and these animals are referred to as D2KO mice in this manuscript.

Genotyping

Animals were tailed at 3 weeks of age, and genomic DNA was extracted using DNAzol (Invitrogen, Carlsbad CA) following the manufacturer's instructions. Mice were genotyped by PCR using the following strategies:

Dio1: 50 ng of genomic DNA was amplified using Platinum GenoTYPE Tsp DNA polymerase (Invitrogen, Carlsbad CA) following the manufacturer's specifications with the following modifications: reactions contained 32 μM dATP, dCTP, dTTP and 40 μM 7-deaza-dGTP (Roche, Indianapolis, IN), and 0.2 μl α-^{32}P dCTP (6000Ci/mmol, New England Nuclear, Boston MA), 1x PCR Enhancer solution (Invitrogen, Carlsbad CA), 2.5 mM $MgSO_4$, 2.5% DMSO, and 0.4 μM sense and anti-sense primers (sense: 5'-GCAGCGTCCATTCTCATTTAC-3', anti-sense 5'-TCTTAACGGACTGCCCAGG-3'). PCR products were resolved on a 10% TBE buffered acrylamide gel (BioRad), which was then dried and exposed to film.

Dio2: 50 ng of genomic DNA was amplified using the Red Taq DNA polymerase (Sigma, St. Louis MO) following the manufacture's protocol using a mix containing the following primers: WT sense primer (5'-GTTTAGTCATGGAAGCAGCACTATG–3'), D2KO sense primer (5'-CGTGGGATCATTGTTTTTCTCTTG-3') and common anti-sense primer (5'–CATGGCGTTAGCCAAAACTCATC-3') (14). Fragments were resolved by 1.5% agarose gel electrophoresis.

T3, T4, and TSH measurements and T3-charcoal uptake

Serum T3 values were either measured as described previously (15, 16) using a standard curve prepared by diluting a known amount of T3 into charcoal-stripped mouse serum (Sigma, St. Louis, MO) and primary anti-T3 antibody at a 1/100,000 final concentration or by using the same standard curve with COAT-A-COUNT total T3 kit (DPC, Los Angeles, CA). Serum T4 values, and ^{125}I T3 charcoal uptake to assess serum T3 binding proteins were measured as described previously (16). TSH was determined using the rat TSH ^{125}I Biotrak Assay System from Amersham Biosciences (Piscataway, NJ) with slight modifications (17), with samples all falling within the linear range of a curve generated by the serial dilution of hypothyroid mouse serum.

D1, D2, and D3 assays

Deiodinase assays were performed as described previously (18). Briefly, tissues were sonicated in buffer containing 0.1 M KPO_4, 1 mM EDTA, 0.25 M sucrose and 10 mM DTT. Protein concentrations were determined by Biorad Protein Assay reagent (Biorad, Hercules CA), and the following conditions were used: for D1 assays 5-15 μg of liver, 15-50 μg of kidney, 3-6 μg of thyroid and 20-150 μg of pituitary were assayed with a final concentration of 10 mM DTT and 500 nM ^{125}I rT3, for D2 assays 20-125 μg of cerebral cortex or 50 μg of pituitary was assayed with a final concentration of 20 mM DTT, 5.0 nM ^{125}I T4, and 1 mM PTU, and for D3 assays 20-125 μg of cerebral cortex protein was assayed with 10 mM DTT, 10 nM ^{125}I T3, and 1 mM PTU.

Thyroidal radioiodine uptake

Mice were injected with 15,000 cpm/ g body weight $Na^{125}I$ (New England Nuclear, Boston MA) intraperitoneally. 2 hours after injection (at a time where uptake was determined to be maximal and in a stationary phase, data not shown) mice were sacrificed and serum and thyroid were collected and counted. Data are expressed as thyroidal cpm/ cpm 1 ml serum.

Real-time PCR

Real-time PCR was performed as described previously using the QuantiTect SYBR Green PCR kit on an I-Cycler (Biorad, Hercules CA) (16).

Statistical analysis

When two groups were compared, statistical significance was determined using a two-tailed student's t-test, while when multiple groups were compared one-way Analysis of Variance (ANOVA) with a Newman-Keuls post-test was used (Prism 4, GraphPad Software, San Diego CA).

Results:

Two strategies were used to create mice with the C3H Dio1 allele and a targeted disruption of the Dio2 gene

A mouse with low levels of D1, and without D2, was generated by crossing the D1 deficient C3H/HeJ (C3H) mouse with mice that have a targeted disruption of the *Dio2* gene, to generate *Dio*1$^{WT/C3H}$-*Dio*2$^{+/-}$ heterozygous animals. These heterozygotes were interbred, and mice homozygous for both the C3H *Dio1* allele and the targeted disruption of the *Dio2* gene were identified. In order to distinguish the *Dio1* allele, we used PCR primers flanking a previously described ~150 bp insertion located in the second intron of the C3H *Dio*1 gene (4) (Fig. 1A). For D2 genotyping, we used 5' sense primers either directed against sequences in the wild type *Dio*2 gene or the inserted neomycin gene, and a common *Dio*2 anti-sense primer. This resulted in a 396 bp PCR product for the wild type *Dio2* allele, while the amplicon for the neomycin-containing disrupted *Dio2* gene is 450 bp (Fig. 1B).

Mice homozygous for both the C3H *Dio1* allele and a disruption of the *Dio2* gene (*Dio*1$^{C3H/C3H}$-*Dio*2$^{-/-)}$ were born at the expected Mendelian frequency. Strikingly, serum T3 levels were not different in any of the mice generated from this cross, including the *Dio*1$^{C3H/C3H}$-*Dio*2$^{-/-}$ mice (Table 1). Serum T4 levels were increased 73% in *Dio*1$^{wt/wt}$-*Dio*2$^{-/-}$ mice lacking the *Dio2* gene ($p<0.05$), and 62% in *Dio*1$^{C3H/C3H}$-*Dio*2$^{+/+}$ mice containing the C3H allele of the *Dio1* gene ($p < 0.05$) relative to wild type siblings, in accordance with previous results (3, 6, 10). However, in *Dio*1$^{C3H/C3H}$-*Dio*2$^{-/-}$ mice, T4 levels were even further elevated, being double that of wild type littermates ($p<0.01$). TSH was not different between wild type littermates and mice containing the C3H allele

of the *Dio1* gene (Table 1). Serum TSH of mice lacking a functional *Dio2* gene was elevated by 34%, although this was not significantly different from wild type littermates, however, serum TSH levels of the *Dio*1$^{C3H/C3H}$-*Dio*2$^{-/-}$ mice were ~50% higher that of wild type siblings ($p< 0.01$).

Measurement of hepatic D1 activity confirmed no difference between wild type littermates and mice with a targeted disruption of the *Dio2* gene as described previously (data not shown) (10). D1 activity was greatly decreased in *Dio*1$^{C3H/C3H}$-*Dio*2$^{+/+}$ mice in agreement with earlier results being less than 1 % that of wild type siblings (3, 6). D1 was also decreased in *Dio*1$^{C3H/C3H}$-*Dio*2$^{-/-}$ mice to 7 % that of wild type siblings. While the D1 activity in *Dio*1$^{C3H/C3H}$-*Dio*2$^{+/+}$ and *Dio*1$^{C3H/C3H}$-*Dio*2$^{-/-}$ mice was not significantly different, the trend for slightly increased D1 activity in *Dio*1$^{C3H/C3H}$-*Dio*2$^{-/-}$ mice did raise concerns that the low expression of the *Dio1* gene in C3H mice might be influenced by other *trans*-factors not directly linked to the polymorphisms found in the C3H *Dio1* gene alone (6).

Due to this concern, and to the limitations imposed by the small number of animals homozygous for both markers generated in each cross (1/16), we decided to employ a second strategy for creating mice with low D1 expression lacking the *Dio2* gene. Thus, mice with a targeted disruption of the *Dio2* gene were backcrossed with C3H mice for 5 generations, generating animals with a genetic background predicted to be 97 % C3H-derived, and these animals are referred to as C3H-D2KO mice (13). A similar strategy was used to generate animals where the targeted disruption of the *Dio2* allele was backcrossed into a C57 background with wild type expression of the *Dio1* allele, and these animals will be referred to as D2KO mice (6).

C3H-D2KO mice have normal serum T3 values, while T4 is elevated

C3H and C3H-D2KO mice have litters that are comparable in size (5.6 ± 0.9 vs. 4.6 ± 0.7 pups/litter, mean ± SEM, $p>0.05$), suggesting that no defects in embryonic development or fertility are associated with this genotype. C3H-D2KO male mice were slightly heavier and longer than C3H mice, weighing 14% more at 56 days of age ($p<0.01$), and being 9.1 versus 8.6 cm in length ($p<0.01$).

Remarkably, as with the first strategy, measurement of serum T3 showed no difference between male C57, D2KO, C3H and C3H-D2KO, indicating that despite a deficiency of both D1 and D2, C3H-D2KO mice maintain normal serum T3 levels ($p>0.05$) (Fig. 2A). Additionally, charcoal T3 uptake assays were not significantly different between any of the groups, suggesting that the free fraction of serum T3 is not different between any of these animals (data not shown). T4 was increased 50% in the D2KO mice relative to that of C57 ($p<0.05$), while that of the C3H-D2KO mice was slightly increased by 16% ($p<0.01$) when compared to the already elevated C3H T4 values (Fig. 2B). Strikingly, when C3H-D2KO serum T4 is compared to that of C57, T4 is doubled in the C3H-D2KO mice. These results are mirrored when one compares the T3/T4 ratio on a mouse by mouse basis, with the ratios being 0.14 ± 0.1, 0.10 ± 0.1, 0.09 ± 0.1 and 0.08 ± 0.01 for C57, D2KO, C3H and C3H-D2KO mice respectively, indicating a progressive increase in T4 levels, while T3 remains unchanged.

Serum TSH levels were not different between C3H and C57 mice (Fig. 2C). In agreement with previous results, serum TSH in D2KO mice was elevated, being over twice that of C57 controls ($p<0.05$) (Fig. 2C) (10). TSH levels of C3H-D2KO mice were

increased to a lesser extent than that of the D2KO mice, being increased by 40% relative to C3H ($p<0.01$).

To determine if the observed increases in TSH correlated with increased thyroidal activity, thyroidal ^{125}I uptake was performed (Fig. 2D). No significant difference was observed between C57 and D2KO or C3H and C3H-D2KO animals, although there appeared to be more ^{125}I uptake in mice with a C3H versus a C57 background.

Measurement of deiodinase activity in C57, D2KO, C3H, and C3H-D2KO mice

C3H and C3H-D2KO hepatic D1 activities were both reduced when compared to C57, being 1% and 11% that of C57 respectively (Table 2). Unexpectedly, hepatic D1 activity was significantly increased (8.4-fold) in C3H-D2KO mice relative to C3H ($p< 0.01$). Since D1 is a very sensitive marker of peripheral thyroid status (16) levels of other hepatic thyroid hormone responsive genes were also assessed. However, measurement of mRNA expression of both spot 14 and α-glycerol phosphate dehydrogenase (α-GPD) by real-time PCR (16) showed no change between C3H and C3H-D2KO mice (1.75 ± 0.67 vs. 1.64 ± 0.82 for spot 14 and 0.60 ± 0.33 vs. 0.47 ± 0.12 for α-GPD, mean target gene expression/β actin expression ± SEM, n=5 animals/group).

Measurement of renal D1 showed a decrease in C3H and C3H-D2KO activity compared to C57 levels, and yet again, C3H-D2KO activity was increased relative to C3H, being doubled ($p<0.01$). While renal D1 activity was also decreased in D2KO mice when compared to C57, this difference was not found to be significant ($p>0.05$). Thyroidal D1 activity was not significantly different between C57 and D2KO or C3H and

C3H-D2KO mice. Notably, mice with a C3H background had approximately one-half the thyroidal D1 activity of mice with a C57 background.

In accordance with previous results, D2 activity in cerebral cortex and pituitary was decreased in C3H when compared to C57 (Table 2) (6). Cerebral cortical D3 was not different between C57 and D2KO mice, unlike previous reports where it is elevated (Table 2) (10). However, D3 activity was the same between C3H and C57 mice, in agreement with previous results (3).

Discussion:

Mice with isolated D1 (C3H or D1KO) or D2 deficiency (D2KO) maintain normal levels of serum T3 with few phenotypic consequences (3, 6, 10, 19). It seemed possible, however, that this adaptive capacity of the T3-generating system would be seriously jeopardized in mice resulting from the cross of the C3H and D2KO animals, and thus, the C3H-D2KO mouse was developed *via* two strategies. However, these mice still maintain euthyroid serum T3 values, exhibit normal growth and reproduction, and have no change in hepatic expression of the T3-responsive marker genes spot 14 and α-GPD.

How do C3H-D2KO mice maintain normal serum T3 levels? One possibility might be increased thyroidal production of T3. However, our data indicate that C3H-D2KO have no change in ^{125}I uptake relative to C3H mice, suggesting no increase in thyroid activity in these animals (Fig. 2D). Additionally, the TSH-inducible thyroidal D1 activity of C3H-D2KO is unchanged relative to C3H, making it unlikely that C3H-D2KO mice have more T4 to T3 conversion within this tissue, and hence more T3 production (Table 2).

T3 can be inactivated by inner-ring deiodination *via* D3 or D1, and thus a decrease in T3 clearance rates could also play a role in maintaining euthyroid serum T3 levels in the C3H-D2KO mice (2). However, cerebral cortical D3 levels of C3H-D2KO animals are not different from that of C3H or C57 mice (Table 2), suggesting that there is no change in D3-mediated T3 clearance in these animals. Further, D1KO mice have no change in their clearance rates of physiological amounts of T3, thus it is not likely that mice with low levels of D1 such as C3H would have a change in their T3 clearance rates (9).

One thing that is striking about the C3H-D2KO mice is their additional 20% increase in plasma T4 above the already elevated levels found in C3H mice (Fig. 2 B). Thus, their T4 levels are 2.2-fold that of C57 animals with wild type D1 and D2 activity, changing their T3/T4 ratios from 0.14 to 0.8. This increase in T4, in conjunction with their increased, albeit still low, hepatic and renal D1, might provide enough T4 to T3 conversion to allow the maintenance of euthyroid serum T3 levels (Table 2). The comparison of C3H-D2KO mouse with mice that have been recently generated that completely lack both the *Dio1* and *Dio2* genes will provide interesting insights into the role of the residual small amount of D1 in the C3H-D2KO in the maintenance of thyroid hormone homeostasis (19).

What is the basis of this substantial increase in T4 in the C3H-D2KO animals? Their elevated TSH relative to C3H suggests that their thyroidal activity should be increased, with more production of T4 (Fig. 2C). Yet, thyroidal ^{125}I uptake is not increased in C3H-D2KO mice relative to C3H (Fig. 2D), indicating that TSH bioactivity may be decreased. However, thyroidal ^{125}I uptake also indicates that C3H have a greater capacity to concentrate iodide than C57 and suggests that their thyroids may be more active for reasons that are currently unknown (Fig. 2D). Additionally, the T4 clearance rate in D2KO mice is decreased, and thus this could also compound the accumulation of T4 (10)

The mechanism by which D1 increased in the C3H-D2KO animals in liver and kidney has also yet to be defined (Table 2). While the *Dio1* gene is a known to be a very T3-responsive gene, expression of the T3-responsive hepatic genes spot 14 and α-glycerol phosphate dehydrogenase were not increased in C3H-D2KO mice suggesting

that either their livers are not thyrotoxic, or else that these other genes are simply not sensitive enough markers to detect a slight alteration in thyroid status (16).

While the tissue-specific thyroid status of the C3H-D2KO mice remains to be investigated in detail, overall our results indicate that few phenotypic consequences not already associated with the D2KO mouse result from a combined deficiency in *Dio1* and loss of *Dio2* gene expression. Our results with the C3H-D2KO mouse further underscore the powerful network of mechanisms that exist to maintain thyroid hormone at appropriate levels.

Acknowledgements:

We would like to acknowledge Dr. Stephan Huang and Ms. Michelle Mulcahey and Alessandra Crescenzi for their assistance with D3 assays. This work was supported by NIH grants DK06576 (A.M.Z), DK65055 (A.C.B) and DK36256 (P.R.L).

References:

1. **Zhang J, Lazar MA** 2000 The mechanism of action of thyroid hormones. Annu Rev Physiol 62:439-466
2. **Bianco AC, Salvatore D, Gereben B, Berry MJ, Larsen PR** 2002 Biochemistry, cellular and molecular biology and physiological roles of the iodothyronine selenodeiodinases. Endocr Rev 23:38-89

3. **Schoenmakers CHH, Pigmans IGAJ, Poland A, Visser TJ** 1993 Impairement of the selenoenzyme type I iodothyronine deiodinase in C3H/He mice. Endocrinology 132:357-361

4. **Maia AL, Berry MJ, Sabbag R, Harney JW, Larsen PR** 1995 Structural and functional differences in the dio1 gene in mice with inherited type 1 deiodinase deficiency. Mol Endocrinol 9:969-980

5. **Maia AL, Kieffer JD, Harney JW, Larsen PR** 1995 Effect of 3,5,3'-Triiodothyronine (T3) administration on dio1 gene expression and T3 metabolism in normal and type 1 deiodinase-deficient mice. Endocrinology 136:4842-4849

6. **Berry MJ, Grieco D, Taylor BA, Maia AL, Kieffer JD, Beamer W, Glover E, Poland A, Larsen PR** 1993 Physiological and genetic analyses of inbred mouse strains with a type I iodothyronine 5' deiodinase deficiency. J Clin Invest 92:1517-1528

7. **Steinsapir J, Bianco AC, Buettner C, Harney J, Larsen PR** 2000 Substrate-induced down-regulation of human type 2 deiodinase (hD2) is mediated through proteasomal degradation and requires interaction with the enzyme's active center. Endocrinology 141:1127-1135

8. **Christoffolete MA, Ribeiro R, Singru P, Fekete C, da Silva WS, Gordon DF, Huang SA, Crescenzi A, Harney JW, Ridgway EC, Larsen PR, Lechan RM, Bianco AC** 2006 Atypical expression of type 2 iodothyronine deiodinase in thyrotrophs explains the thyroxine-mediated pituitary TSH feedback mechanism. Endocrinology 147:1735-1743

9. **Schneider MJ, Fiering SN, Thai B, Wu SY, St Germain E, Parlow AF, St Germain DL, Galton VA** 2006 Targeted disruption of the type 1 selenodeiodinase gene (dio1) results in marked changes in thyroid hormone economy in mice. Endocrinology 147:580-9

10. **Schneider MJ, Fiering SN, Pallud SE, Parlow AF, St. Germain DL, Galton VA** 2001 Targeted disruption of the type 2 selenodeiodinase gene (Dio2) results in a phenotype of pituitary resistance to T4. Mol Endocrinol 15:2137-2148

11. **de Jesus LA, Carvalho SD, Ribeiro MO, Schneider M, Kim S-W, Harney JW, Larsen PR, Bianco AC** 2001 The type 2 iodothyronine deiodinase is essential for adaptive thermogenesis in brown adipose tissue. J Clin Invest 108:1379-1385

12. **Ng L, Goodyear RJ, Woods CA, Schneider MJ, Diamond E, Richardson GP, Kelley MW, Germain DL, Galton VA, Forrest D** 2004 Hearing loss and retarded cochlear development in mice lacking type 2 iodothyronine deiodinase. Proc Natl Acad Sci U S A 101:3474-9

13. **Jackson Laboratories** 2001 Production of congenic strains using marker-assisted ("Speed") technologies. Jax Communication. The Jackson Laboratory, Bar Harbor, ME

14. **Christoffolete MA, Linardi CCG, de Jesus LA, Ebina KN, Carvalho SD, Ribeiro MO, Rabelo R, Curcio C, Martins L, Kimura ET, Bianco AC** 2004 Mice with targeted disruption of the Dio2 gene have cold-induced overexpression of uncoupling protein 1 gene but fail to increase brown adiose tissue lipogenesis and adaptive thermogenesis. Diabetes 53:577-584

15. **Larsen PR** 1972 Direct immunoassay of triiodothyronine in human serum. J Clin Invest 51:1939-49

16. **Zavacki AM, Ying H, Christoffolete MA, Aerts G, So E, Harney JW, Cheng SY, Larsen PR, Bianco AC** 2005 Type 1 iodothyronine deiodinase is a sensitive marker of peripheral thyroid status in the mouse. Endocrinology 146:1568-75

17. **Pohlenz J, Maqueem A, Cua K, Weiss RE, Van Sande J, Refetoff S** 1999 Improved radioimmunoassay for measurement of mouse thyrotropin in serum: strain differences in thyrotropin concentration and thyrotroph sensitivity to thyroid hormone. Thyroid 9:1265-71.

18. **Callebaut I, Curcio-Morelli C, Mornon JP, Gereben B, Buettner C, Huang S, Castro B, Fonseca TL, Harney JW, Larsen PR, Bianco AC** 2003 The iodothyronine selenodeiodinases are thioredoxin-fold family proteins containing a glycoside hydrolase-clan GH-A-like structure. J Biol Chem 278:36887-36896

19. **St Germain DL, Hernandez A, Schneider MJ, Galton VA** 2005 Insights into the role of deiodinases from studies of genetically modified animals. Thyroid 15:905-16

Fig. 1

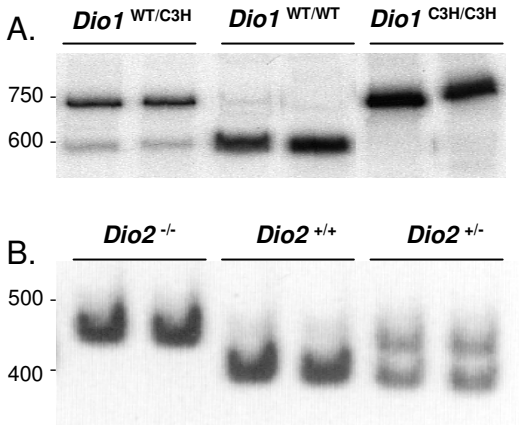
A.
Dio1 WT/C3H
Dio1 WT/WT
Dio1 C3H/C3H
750
600
B.
Dio2 -/-
Dio2 +/+
Dio2 +/-
500
400

Fig. 2

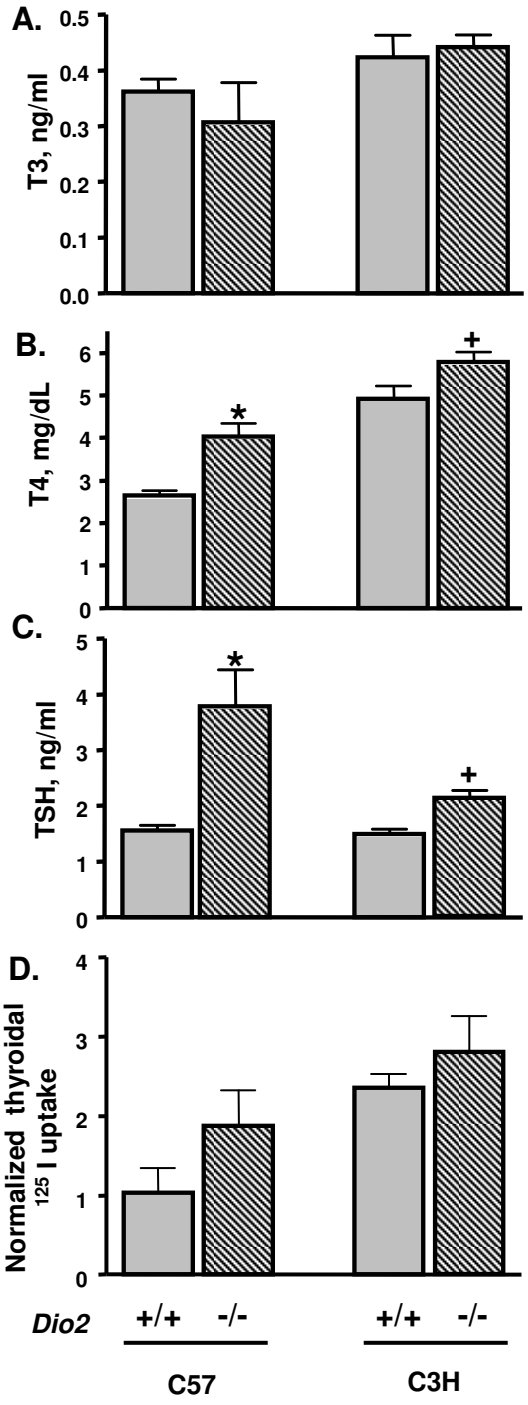
A.
T3, ng/ml
0.5
0.4
0.3
0.2
0.1
0.0
B.
T4, mg/dL
6
5
4
3
2
1
0
*
+
C.
TSH, ng/ml
5
4
3
2
1
0
*
+
D.
Normalized thyroidal 125I uptake
4
3
2
1
0
Dio2
+/+
-/-
+/+
-/-
C57
C3H

TABLE 1. Serum T3, T4, and TSH values of mice generated by crossing *Dio1* $^{WT/C3H}$ and *Dio2* $^{+/-}$ mice.

Geneotype (n)	T3, ng/ml	T4, ug/dl	TSH, ng/ml
Dio1 $^{WT/WT}$ *Dio2* $^{+/+}$(8)	0.76 ± 0.07	1.61 ± 0.17	5.47 ± 0.28
Dio1 $^{WT/WT}$ *Dio2* $^{-/-}$(7)	0.77 ± 0.06	2.79 ± 0.32[a]	7.32 ± 0.83
Dio1 $^{C3H/C3H}$ *Dio2* $^{+/+}$(8)	0.69 ± 0.06	2.61 ± 0.28[a]	5.17 ± 0.45
Dio1 $^{C3H/C3H}$ *Dio2* $^{-/-}$(17)	0.72 ± 0.05	3.20 ± 0.20[b]	8.34 ± 0.54[b]

Values indicated are the mean ± SEM. Mice were sacrificed at 8 weeks of age with n= indicating the number of mice in each group. Mice are both male and female due to the low number progeny produced of the homozygous genotypes. [a]$P < 0.05$ or [b]$P < 0.01$ when compared to wild type siblings by ANOVA.

TABLE 2. Deiodinase activities in C57, D2KO, C3H, and C3H-D2KO mice.

	C57	D2KO	C3H	C3H-D2KO
D1 activity, pmol/min/mg				
Liver	2526 ± 451	3340 ± 1505	34 ± 12	287 ± 67[a]
Kidney	782 ± 254	304 ± 15	48 ± 8	98 ± 13[a]
Pituitary	378	552	6.7	6.7
Thyroid	189 ± 21	204 ± 40	97 ± 16	120 ± 14
D2 activity, fmol/hr/mg				
Cerebral cortex	34 ± 7	*	11 ± 2	*
Pituitary	158	*	33	*
D3 activity, fmol/min/mg				
Cerebral cortex	14.4 ± 2.8	15.0 ± 2.8	11.2 ± 2.8	8.0 ± 1.2

Deiodinase activities were measured as described previously (18) using rT3 as a substrate for D1, T4 for D2, and T3 for D3. Values indicated are the mean ± SEM for 6-11 male mice 8 weeks of age in each group, except for pituitary where tissues from 5-9 animals were pooled, and thyroid, where activity from 4-5 animals/group were measured. [a]$P < 0.01$ when compared to C3H by Student's t-test. *=not detectable.

Figure Legends:

FIG. 1. Genotyping of mice for the C3H allele of the *Dio1* gene and the targeted disruption of the *Dio2* gene. Mice were genotyped using primers that flank a ~150 bp insertion in exon 2 of the C3H *Dio1* gene (A) or primers that either amplify a 396 bp fragment from the wild type *Dio2* gene or a 450 bp fragment from the neomycin-disrupted *Dio2* gene (B).

FIG. 2. Serum T3, T4 and TSH concentrations, and ^{125}I thyroidal uptake. The mean serum concentrations ± standard error for T3 (A), T4 (B), and TSH (C) for the indicated strain of mice is shown. For T4 and TSH measurements n= 6, 11, 9 and 9 mice, while for T3 n= 6, 3, 9 and 9 mice respectively. (D) Thyroidal uptake of ^{125}I (cpm) normalized by the ^{125}I content (cpm) of 1ml of serum for 3-5 mice in each group is shown. *= $p < 0.05$ when compared to C57 by student's t-test. += $p < 0.01$ when compared to C3H by Student's t-test.

IV – Segundo Artigo

Resumo

T4, o principal produto da secreção tiroideana, é um sinal crítico no plasma e media o mecanismo de retroalimentação negativa do TSH. Como um pró-hormônio, T4 deve ser convertido a T3 para adquirir atividade biológica; desta forma, é esperado que a desiodase do tipo 2 (D2) desempenhe um papel crítico neste mecanismo de retroalimentação.

Entretanto, os detalhes dos mecanismos desta via ainda não foram elucidados porque, contra-intuitivamente, a atividade da D2 é perdida rapidamente na presença do T4 por um mecanismo de ubiquitinação-proteassomal. Neste estudo, nós demonstramos que a D2 e o TSH são co-expressos nos tirotrofos da pituitária de ratos e que hipotiroidismo promove o aumento da expressão de D2 nestas células. Estudos usando duas linhagens celulares derivadas de tirotrofos de camundongos, TtT-97 e TαT1, demonstram alta expressão de D2 no tirotrofo e confirma sensibilidade desta enzima a degradação proteassomal induzida pelo T4. Apesar disso, a expressão do gene da D2 em células TαT1 é maior do que a capacidade de ubiqüitinar a D2, induzida pelo T4. Como resultado, a atividade de D2 e produção de T3 nestas células é sustentada, mesmo a concentrações livre de T4 muito acima da faixa fisiológica. Neste sistema, a concentração livre de T4 e a produção de T3 mediada pela D2 correlacionam-se negativamente com a expressão do gene do TSH. Estes resultados esclarecem o paradoxo aparente entre a regulação homeostática da D2 e seu papel mediando o mecanismo crítico pelo qual o T4 promove a retroalimentação negativa do TSH.

0013-7227/06/$15.00/0
Printed in U.S.A.

Endocrinology 147(4):1735–1743

doi: 10.1210/en.2005-1300

Atypical Expression of Type 2 Iodothyronine Deiodinase in Thyrotrophs Explains the Thyroxine-Mediated Pituitary Thyrotropin Feedback Mechanism

Marcelo A. Christoffolete, Rogério Ribeiro, Praful Singru, Csaba Fekete, Wagner S. da Silva, David F. Gordon, Stephen A. Huang, Alessandra Crescenzi, John W. Harney, E. Chester Ridgway, P. Reed Larsen, Ronald M. Lechan, and Antonio C. Bianco

Thyroid Section (M.A.C., R.R., W.S.d.S., J.W.H., P.R.L., A.C.B.), Division of Endocrinology, Diabetes, and Hypertension, Brigham and Women's Hospital and Harvard Medical School, and Division of Endocrinology (S.A.H., A.C.), Children's Hospital Boston, Boston, Massachusetts 02115; Tupper Research Institute and Department of Medicine (P.S., C.F., R.M.L.), Division of Endocrinology, Diabetes, and Metabolism, New England Medical Center, Boston, Massachusetts 02111; Department of Endocrine Neurobiology (C.F.), Institute of Experimental Medicine, Hungarian Academy of Sciences, H-1083 Budapest, Hungary; and Department of Medicine/Endocrinology (D.F.G., E.C.R.), University of Colorado Health Sciences Center at Fitzsimons, Aurora, Colorado 80045

T_4, the main product of thyroid secretion, is a critical signal in plasma that mediates the TSH-negative feedback mechanism. As a prohormone, T_4 must be converted to T_3 to acquire biological activity; thus, type 2 iodothyronine deiodinase (D2) is expected to play a critical role in this feedback mechanism. However, the mechanistic details of this pathway are still missing because, counterintuitively, D2 activity is rapidly lost in the presence of T_4 by a ubiquitin-proteasomal mechanism. In the present study, we demonstrate that D2 and TSH are coexpressed in rat pituitary thyrotrophs and that hypothyroidism increases D2 expression in these cells. Studies using two murine-derived thyrotroph cells, TtT-97 and TαT1, demonstrate high expression of D2 in thyrotrophs and confirm its sensitivity to negative regulation by T_4-induced proteasomal degradation of this enzyme. Despite this, expression of the *Dio2* gene in TαT1 cells is higher than their T_4-induced D2 ubiquitinating capacity. As a result, D2 activity and net T_3 production in these cells are sustained, even at free T_4 concentrations that are severalfold above the physiological range. In this system, free T_4 concentrations and net D2-mediated T_3 production correlated negatively with TSHβ gene expression. These results resolve the apparent paradox between the homeostatic regulation of D2 and its role in mediating the critical mechanism by which T_4 triggers the TSH-negative feedback. (*Endocrinology* 147: 1735–1743, 2006)

TSH STIMULATES virtually every aspect of thyroid hormone biosynthesis and secretion. In the absence of TSH, thyroidal activity falls to very low levels, eventually resulting in secondary hypothyroidism. TSH is regulated by a negative-feedback mechanism triggered by thyroid hormone at the pituitary and hypothalamic levels, the latter involving suppression of TRH by paraventricular neurons. As a result of this well-orchestrated mechanism, measurement of serum TSH is the single most sensitive laboratory test for diagnosis of primary hyper- and hypothyroidism (reviewed in Ref. 1).

The free T_4 concentration in serum is a key player mediating the TSH feedback mechanism (2). This assumption is derived from data obtained during iodine deficiency or mild primary hypothyroidism (3). In both conditions, a declining serum T_4 concentration, in the presence of normal serum T_3, promotes dramatic increases in TSH secretion. The effects of T_4 on TSH secretion are possible only because of the presence of type 2 iodothyronine deiodinase (D2) in the pituitary, which rapidly converts T_4 to the biologically active T_3. Although serum T_3 can also reach pituitary thyroid hormone receptors (TRs) and by itself plays a significant role in repressing TSHβ gene transcription (4), most TR-bound T_3 present in the pituitary gland originates from the local conversion of T_4 to T_3 (5–8). In fact, both serum T_4 and TSH levels were found to be significantly elevated in mice with targeted disruption of the *Dio2* gene, confirming that in the absence of D2, the thyrotrophic cell is relatively resistant to the feedback effect of plasma T_4 (9). Furthermore, whereas serum TSH levels in wild-type mice are suppressed by administration of either T_4 or T_3, only T_3 was effective in the mouse with targeted disruption of the *Dio2* gene (9).

Nonetheless, the intrinsic homeostatic nature of D2 weakens the argument for its proposed major role in the TSH feedback mechanism (10). It is well known that low-serum T_4 increases D2 activity and that high T_4 concentrations do the opposite (11). This has been understood as an adaptive mechanism in brain and other D2-expressing tissues to minimize changes in the intracellular concentration of T_3 during iodine deficiency and hypothyroidism (12). However, such homeo-

First Published Online January 5, 2006

Abbreviations: aFGF, Acidic fibroblast growth factor; bFGF, basic fibroblast growth factor; D2, type 2 iodothyronine deiodinase; D3, type 3 deiodinase; DTT, dithiothreitol; EGF, epidermal growth factor; FBS, fetal bovine serum; PTU, 6-*n*-propyl-2-thiouracil; RT-PCR, real-time PCR; SSC, standard sodium citrate; Se, sodium selenite; TPA, 12-*O*-tetradecanoylphorbol 13-acetate; TR, thyroid hormone receptor.

***Endocrinology* is published monthly by The Endocrine Society (http://www.endo-society.org), the foremost professional society serving the endocrine community.**

static behavior at the thyrotroph, if operational, would impair the efficient transduction of changes in serum T_4, leaving TSH levels unchanged. This rationale raises questions about the role played by D2 in the TSH feedback mechanism. In fact, T_4-to-T_3 production has never been demonstrated in pure thyrotrophic cell lines, and data obtained from studies of human TSH-producing tumors are controversial, with one study (13) suggesting that the inactivating type 3 deiodinase (D3) is the predominant deiodinase in TSH-secreting tumor cells and another study (14) finding both type 1 iodothyronine deiodinase and D2.

The present study was undertaken to test the paradigm that D2 is a major player in the TSH feedback mechanism in light of the substantial progress that has been made in our understanding of posttranslational regulation of D2 (15). Here we show that D2 is highly expressed in rat thyrotrophs and is up-regulated during hypothyroidism. This is the result of posttranslational mechanisms, as demonstrated in two mouse thyrotroph-derived cells, TtT-97, a transplantable thyrotrophic tumor, and TαT1, an immortalized simian virus-40 T-antigen-expressing pituitary cell line. However, using the TαT1 mouse tumor cell line, we find that the absolute rate of T_4-induced loss of D2 activity in these cells is offset by the combined effect of D2 reactivation and a high rate of D2 synthesis. As a result, an increase in T_4 rapidly translates into an increase in thyrotrophic D2-mediated T_3 production and suppression of TSHβ gene expression, thus explaining the T_4-mediated TSH feedback mechanism.

Materials and Methods

Chemicals and drugs

Recombinant TGFβ1 and IL-1β were purchased from R&D Systems (Minneapolis, MN); 12-*O*-tetradecanoylphorbol 13-acetate (TPA), from Alexis Biochemicals (Lausane, Switzerland); epidermal growth factor (EGF), acidic fibroblast growth factor (aFGF), and basic fibroblast growth factor (bFGF), from Chemicon International (Temecula, CA); T_4, T_3, rT_3, methimazole, sodium perchlorate, and sodium selenite (Se) from Sigma-Aldrich (St. Louis, MO); 6-*n*-propyl-2-thiouracil (PTU) from United States Biochemical Corp. (Cleveland, OH); and MG132 and dithiothreitol (DTT) from Calbiochem (San Diego, CA). A stock solution of TGFβ was prepared in 4 mM HCl with 0.1% BSA; IL-1β in 1 × PBS with 0.1% BSA; EGF in distilled water; aFGF in 5 mM sodium phosphate (pH 7.2); bFGF in 5 mM Tris (pH 7.6); TPA and MG132 in dimethyl sulfoxide; T_4, T_3, and rT_3 in 0.04 N NaOH; and sodium selenite in 70% ethanol. Working solutions of T_4, T_3, and rT_3 were prepared in 70% ethanol; methimazole and sodium perchlorate were in drinking water.

Animals

Adult, male Sprague Dawley rats weighing between 150 and 200 g were acclimated to a 12-h light, 12-h dark cycle (lights between 0600 and 1800 h) and controlled temperature (22 ± 1 C). The studies were approved by the Institutional Animal Care and Use Committee at Tufts-New England Medical Center and Tufts University School of Medicine. Rat chow and tap water were provided *ad libitum*. Animals were made hypothyroid by the addition of 0.05% methimazole and 0.5% sodium perchlorate to their drinking water for 3 wk. Nontreated euthyroid animals of the same age were used as controls.

Studies on LAF1 mice bearing TtT-97 thyrotropic tumors were conducted with the highest standards of humane animal care in accordance with the National Institutes of Health (NIH) Guide for the Care and Use of Laboratory Animals. The animal protocols were approved by the Committee on Animal Care and Use of the University of Colorado Health Sciences Center (Denver/Aurora, CO). LAF1 mice were radiothyroidectomized 2 months before being injected with a mince of TtT-97 thyrotrophic tumor, and the resulting tumors were allowed to propagate *in vivo* for 5 months (16). One tumor-bearing mouse received T_4 (Sigma, St. Louis, MO), 5 mg/liter, in 0.75% ethanol in the drinking water for 3 wk, whereas a control hypothyroid mouse received the ethanol vehicle. The T_4 treatment resulted in a serum level of 573 nmol/liter in the treated mouse, as compared with a level of 3 nmol/liter in the hypothyroid control. Tumors were excised and homogenized in 10 volumes of 4 M guanidinium thiocyanate solution supplemented with 5% 2-mercaptoethanol.

Animal and tissue preparation for in situ hybridization histochemistry

Thyroid hormone production was inhibited by treating adult, male Sprague Dawley rats with 0.02% methimazole in the drinking water for 3 wk. Control rats received regular drinking water. At the end of the treatments, the animals were anesthetized with sodium pentobarbital (50 mg/kg body weight ip); blood was taken from the inferior vena cava, and the animals were immediately perfused transcardially with 20 ml of 0.01 M PBS (pH 7.4), containing 15,000 U/liter heparin sulfate followed by 150 ml of 4% paraformaldehyde in PBS. The pituitary glands were removed, postfixed by immersion in the same fixative for 2 h at room temperature and then cryoprotected in 20% sucrose in PBS at 4 C overnight. The pituitaries were then placed in a cryo mold, covered with OCT (Tissue-Tek, Torrance, CA), and snap frozen on dry ice. Serial 14-μm-thick coronal sections were cut on a cryostat (Leica CM3050 S, Leica Microsystems GmbH, Nussloch, Germany) and adhered to SuperFrost/Plus glass slides (Fisher Scientific, Pittsburgh, PA). The tissue sections were desiccated overnight at 42 C and stored at −80 C until prepared for *in situ* hybridization histochemistry.

Cell culture

TαT1 cells, kindly provided by Dr. Pamela L. Mellon (University of California, San Diego, San Diego, CA), were grown till confluence in DMEM supplemented with L-glutamine (2 mM), antibiotics, and 10% fetal bovine serum (FBS) (growth medium) as detailed described previously (17). GH4C1, MSTO-211, and HEK cells were cultivated as described previously (18, 19). Experiments were carried out in experimental medium: DMEM with 0.1% BSA (T_4 experiments) or 0.5% BSA (T_3 experiments). The free T_4 fraction in 0.1% BSA is 2.7% of total T_4, and the free T_3 fraction is 3% of total T_3 in 0.5% BSA (20).

RNA isolation, Northern blot, and real-time PCR (RT-PCR)

For all samples used in RT-PCR, the total RNA was isolated with Trizol reagent (Invitrogen, Carlsbad, CA) according to manufacturer's protocol. For the Northern blot analysis of Dio2 mRNA in mouse TtT-97 thyrotrophic tumors, total RNA was isolated by sedimentation through a 5.7 M cesium chloride cushion and polyA+ RNA purified on oligo-(dT) cellulose as described (21). Five micrograms of polyA+ mRNA were separated by electrophoresis through a 0.8% agarose/6% formaldehyde denaturing gel and transferred to a nylon membrane (Schleicher and Schuell, Keene, NH). The mRNA separated on the filters was hybridized at 42 C with a cDNA probe for rat D2 (22) and subsequently probed with a nearly full-length cDNA for mouse TSHβ or β-actin (21).

RT-PCR was performed as described elsewhere using cyclophilin A as a housekeeping internal control (23, 24). For the reverse transcriptase reaction, 2–4 μg total RNA were used in the SuperScript first-strand synthesis system for RT-PCR (Invitrogen) on a Robocycler thermocycler (Stratagene, La Jolla, CA). RT-PCR was performed using IQ SYBR Green PCR kit (Bio-Rad, Hercules, CA). The cycle conditions were 5 min at 94 C (Hot Start); 30 sec at 94 C, 30 sec at 58 C, and 45 sec at 72 C for 40 cycles followed by the melting curve protocol to verify the specificity of amplicon generation. Standard curves consisting of four points serial dilution (factor of 5) of mixed experimental and control groups cDNA were performed in each assay and used as calibrators. Comparable efficiency was observed presenting r^2 greater than 0.99. The following primers were used: TSHβ (sense, 5′-CTCGGGTTGTTCAAAGCATGAGTG-3′, antisense, 5′-TGGTGTTGATGGTCAGGCAGTAG-3′); and cyclophilin A (sense, 5′-GCCGATGACGAGCCCTTG-3′, antisense 5′-TGCCGCCAGTGCCATTATG-3′).

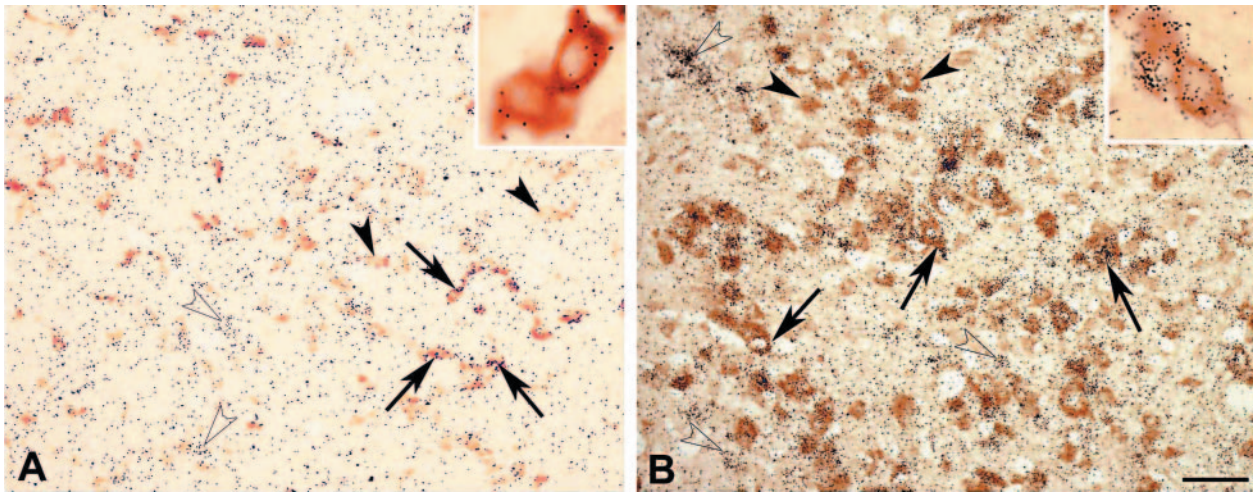

FIG. 1. Transverse sections through the pars distalis of the pituitary gland in euthyroid (A) and hypothyroid (B) rats, double labeled for TSH immunoreactivity (*brown cytoplasmic stain*) and D2 mRNA (*silver grains*). *Insets* show high-magnification fields and *bar* represents 50 μm. The percentage of TSH cells containing D2 mRNA (*arrows*) and the number of silver grains per cell are substantially increased in the hypothyroid animals. *Closed arrowheads* denote TSH-immunoreactive cells that do not contain silver grains. *Open arrowheads* denote pars distalis cells that do not show TSH immunolabeling. Original magnification, ×120 and ×630 in *inset*.

Double-labeling in situ hybridization and immunocytochemistry

Methods for double-labeling *in situ* hybridization and immunocytochemistry have been described in detail (25–28). Pituitary sections were hybridized with an 800-bp single-stranded [^{35}S]UTP-labeled cRNA probe complementary to the entire coding region of the rat D2 gene (29). Briefly, the hybridizations were performed under plastic coverslips in a buffer containing 50% formamide, 2× standard sodium citrate (SSC), 10% dextran sulfate, 0.5% sodium dodecyl sulfate, 250 μg/ml denatured salmon sperm DNA, and 6×10^5 cpm of radiolabeled probe for 16 h at 56 C. The slides were washed in 1× SSC for 15 min and then treated with RNase (25 μg/ml) for 1 h at 37 C. After additional washes in 0.1× SSC (2×30 min) at 65 C, the slides were washed in PBS and treated in 0.5% Triton X-100 and 0.5% H_2O_2 for 15 min and with 1% BSA in PBS. Then the sections were incubated with a rabbit antiserum to rat TSH (NIH, National Pituitary Hormone Program, Torrance, CA) diluted at 1:900 in PBS containing 1% BSA in a humidified chamber for 2 d at 4 C. After several rinses in PBS, the sections were incubated in biotinylated donkey antirabbit IgG (1:200; Jackson ImmunoResearch, West Grove, PA) for 2 h, followed by ABC Elite (1:100; Vector Laboratories, Burlingame, CA) in PBS for 2 h at room temperature. The immunoreaction product was developed with 0.025% 3,3 diamino benzidine/0.0036% H_2O_2 in 0.05 M Tris buffer (pH 7.6). Slides were dehydrated in a graded series of ethanol containing 0.3 M ammonium acetate and were dipped into NTB2 autoradiography emulsion (Eastman Kodak, Rochester, NY). The autoradiograms were developed after 3 d of exposure at 4 C.

Quantitative analysis

Bright-field and dark-field microscopy were used to determine the percentage of immunostained thyrotrophs containing D2 mRNA and the mean number of silver grains denoting D2 mRNA per thyrotroph. Sections were visualized at ×200 magnification, pictures taken at ×120 and ×630 magnification. All cells immunolabeled for TSH lying within a 1 mm × 1 mm area were counted from three different regions of the pituitary with the use of an ocular reticule. Cells that contained 2 or more times the number of silver grains per unit area were considered positive. A total of five to seven sections through the pituitary and an average of 70–80 cells were counted in each animal.

The number of silver grains per TSH cell were counted at ×400 magnification under dark-field microscopy and adjusted for background grain counts. An average of approximately 30 TSH cells were counted from each pituitary section for a total of three sections per animal.

T_4-to-T_3 conversion in cultured cells

The production of ^{125}I from outer ring-labeled T4 (NEN Life Science Products, Boston, MA), specific activity of 5692 μCi/μg, in intact cells can be analyzed by measuring the level of ^{125}I in the medium as described and validated elsewhere (30, 31) with the following modifications: at the end of experiment, 300 μl of medium were removed, 200 μl of horse serum was added, and protein was precipitated by the addition of 100 μl 50% trichloroacetic acid followed by centrifugation at 12,000 × *g* for 3 min; 360 μl of the supernatant containing $^{125}I^-$ generated were counted in a γ-counter (Cobra II; Packard, Meriden CT) and expressed as the fraction of the total T_4 counts minus the nonspecific deiodination in HEK cell lysate (<5% of the total $^{125}I^-$ T_4 counts) and corrected for the volume counted (60%) and the 50% reduction in the specific activity relative to T_4. The remaining medium was discarded, the cell pellet was sonicated in 0.1 M potassium phosphate-1 mM EDTA (pH 6.9) (PE buffer), and total protein was assayed for activity normalization. Net T_3 production is calculated by multiplying the fractional conversion by the free T_4 concentration in the media and expressed as fmol/h/mg protein.

Outer ring (5′) deiodinase activity assay in cell sonicates

At the end of each experiment, cells were harvested in PBS and centrifuged at 10,000 *g* for 3 min; the pellet was sonicated briefly in PE buffer containing 10 mM DTT and 0.25 M sucrose. Protein determinations were by the Bradford method using BSA as standard. The assay was performed in the presence of 0.1–2 nM [^{125}I]5′-T_4, 20 mM DTT, in the presence and absence of 1 mM PTU, during different incubation periods, depending on cell type. Specific T_4-to-T_3 conversion was calculated by subtracting nonspecific deiodination using either a saturating concentration of T_4 (100 nM) or the same amount of protein obtained from a HEK cell lysate. Deiodinase activity was expressed as femtomoles T_4 per minute per milligram protein. The assays consumed less than 70% of the substrate.

Inner ring (5) deiodinase activity assay in cell sonicates

D3 activity was assayed by incubating 100–150 μg cellular protein, about 200,000 cpm of 3,5,[^{125}I]3′-triiodothyronine (NEN Life Science Products), specific activity of 3390 μCi/μg, 1 mM (PTU), 10 mM DTT, and 0.1 nM unlabeled T_3 for variable times. Reactions were stopped by the addition of methanol, and the products of deiodination were resolved and quantified by reverse-phase HPLC as described earlier (32). D3

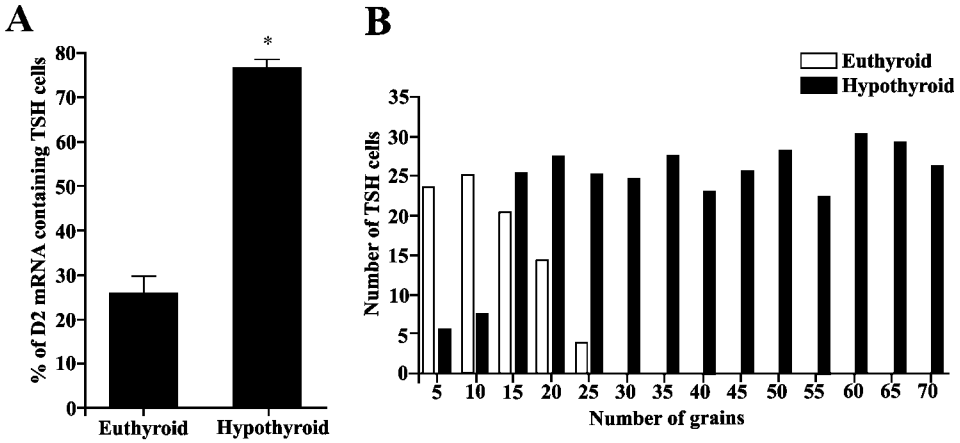

FIG. 2. A, Semiquantitative morphometric analysis of the percentage of D2-containing thyrotrophs in the pituitary of the euthyroid and hypothyroid rat. The pooled mean of the percentage of D2-containing thyrotrophs of the euthyroid rats differ significantly (*, $P < 0.05$) from that of hypothyroid rats. B, Histogram showing the distribution of silver grains denoting the accumulation of D2 mRNA in thyrotrophs of euthyroid and hypothyroid animals. The means of the numbers of D2 mRNA grains per cell for each of the euthyroid rats differs significantly from that of hypothyroid rats ($P < 0.05$).

velocities are expressed as fmol of T_3 inner-ring deiodinated per milligram of sonicate protein per minute (fmol/min/mg protein).

Statistical analysis

All data were analyzed using PRISM software (GraphPad Software, Inc., San Diego, CA) and are expressed as mean ± SEM. ANOVA followed by Newman-Keuls multiple comparison test were used for statistical analysis in all experiments, except for *in situ* hybridization and immunocytochemistry studies, in which the mean percentage and SEs of positive and negative TSH cells and the means and medians of the total number of silver grains per TSH cell were calculated for each animal and for each group and compared using the Student's *t* test. $P < 0.05$ was considered statistically significant.

Results

In situ hybridization of D2 mRNA and TSH immunocytochemistry

Thyrotrophs were distributed throughout the pars distalis of the pituitary gland of both euthyroid and hypothyroid rats (Fig. 1). TSH cells in euthyroid animals were small and angulated and contained a small nucleus. In contrast, TSH cells in hypothyroid rats were larger, less angulated, and had a larger nucleus. Accumulation of silver grains over TSH cells, denoting the presence of D2 mRNA, was seen in both euthyroid and hypothyroid animals. However, the percentage

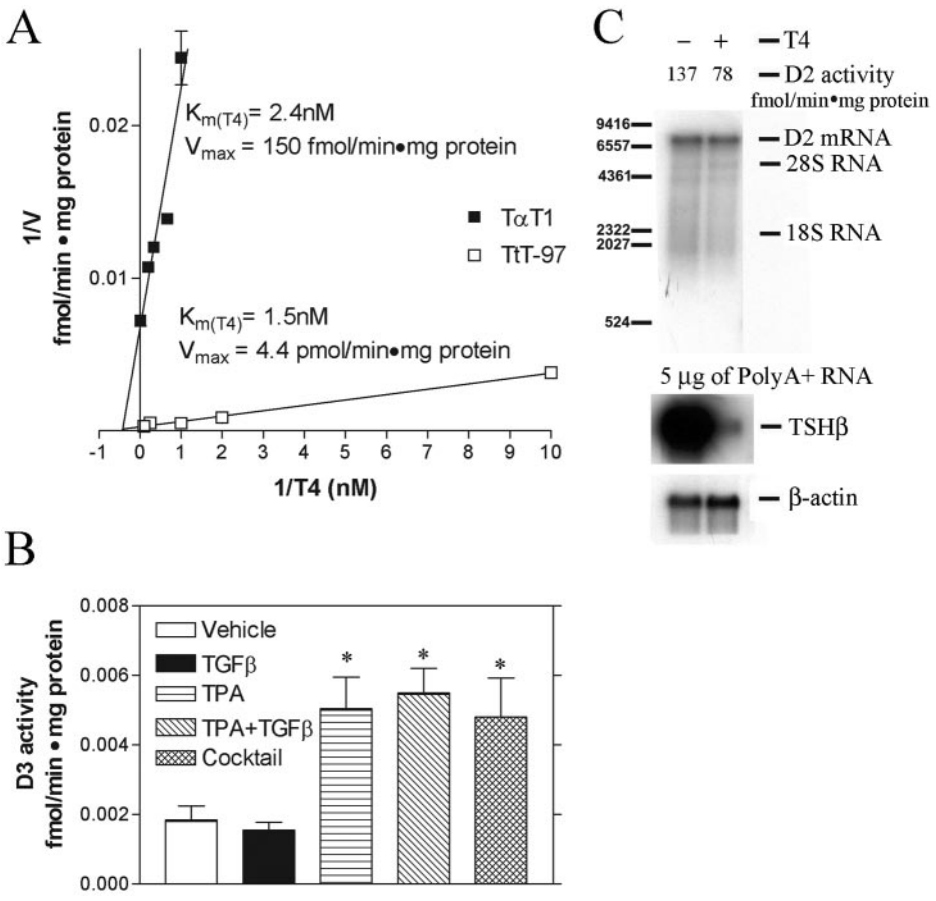

FIG. 3. A, Double-reciprocal plot of D2 activity in TtT-97 and TαT1 cells. TtT-97 cells were grown in a LAF1 host and then harvested and processed for protein activity. TαT1 cells were grown in growth medium, harvested, and processed for D2 activity. B, D3 activity in TαT1 cells. Cells were kept in growth medium supplemented with 10^{-7} M Se. After reaching confluence, cells were incubated with vehicle, TGFβ1 (5 ng/ml), TPA (10^{-7} M), TGFβ1 + TPA, or a cocktail containing aFGF (50 ng/ml), bFGF (20 ng/ml), EGF (25 ng/ml), TGFβ1 (5 ng/ml), TPA (10^{-7} M), and IL-1β (10 ng/ml) for 10 h. At the end of experiment, cells were harvested and processed for D3 activity (n = 3–4, *, $P < 0.05$ *vs.* vehicle). C, D2 activity and mRNA, TSHβ, and β-actin mRNA. TtT-97 cells were grown in an LAF1 host treated with T_4 or vehicle in the drinking water for 21 d. At the end of experiment, tumor was harvested and processed for D2 activity and RNA analysis. Five micrograms of polyA-RNA were submitted to electrophoresis in 0.8% denaturating agarose gel and transferred to a nylon membrane. After hybridization, film was exposed for 18 h at −80 C. *Numbers on the left* of the image indicate size markers. Km, Michaelis constant; Vmax, maximum velocity.

of TSH cells containing D2 mRNA was significantly greater in the hypothyroid animals (Fig. 2A). In addition, the number of silver grains accumulating over TSH-immunoreactive cells was significantly greater in the hypothyroid animals, with grain density ranging from 1 to 70 above background in the hypothyroid animals and from 1 to 25 in euthyroid animals. (Fig. 2B). Silver grains also accumulated over anterior pituitary cells that were not immunoreactive for TSH.

D2 is highly expressed in two TSH-producing murine tumor cell lines

Because of the low abundance and intrinsic difficulties in isolating primary thyrotrophs, TSH-producing thyrotrophic tumor cells (TtT-97) and an immortalized cell line (TαT1) constitute the only experimental models available for the study of D2 regulation in thyrotrophs. TtT-97 cells have the highest endogenous D2 activity reported to date, 4.4 pmol/min·mg protein, and an apparent Michaelis constant (T_4) of 1.5 nM, whereas TαT1 cells have a lower endogenous activity, 150 fmol/min·mg protein and an apparent michaelis constant (T_4) of 2.4 nM (Fig. 3A), but still higher than most D2-expressing cells (19). No type 1 iodothyronine deiodinase activity was detected in TtT-97 or TαT1 cells (data not shown). However, by supplementing growth medium with 10^{-7} M selenium and using extrasensitive D3 activity assay conditions (low substrate concentration and extended incubation times), we detected some D3 activity in the TαT1 cell line (Fig. 3B). Although significantly stimulated by TPA or the combination of TPA and TGFβ or a cocktail containing aFGF, bFGF, EGF, TGFβ1, TPA, and IL-1β ($P < 0.05$), D3 activity remained at very low levels (Fig. 3B).

Posttranscriptional mechanisms are the primary determinant of D2 activity in thyrotrophic cell lines

Treatment of animals that were bearing TtT-97 tumors with T_4 for 21 d resulted in a dramatic decrease in levels of TSHβ mRNA and about a 50% loss of D2 activity but no change in levels of D2 mRNA (Fig. 3C). Despite this loss in D2, the remaining D2-mediated outer ring deiodinase capacity is still by far higher than in any other tissue. In similar studies, treatment of TαT1 cells with T_4 resulted in 65–80% loss of D2 activity but only a 20–35% decrease in D2 mRNA levels (Fig. 4A). Poor *Dio2* gene responsiveness to thyroid hormone was further confirmed by treating TαT1 cells with T_3. Whereas incubation with T_3 barely changed D2 mRNA levels, TSHβ mRNA levels decreased by more than 50% (Fig. 4B). This confirms that posttranscriptional mechanisms are the major determinants of D2 activity in these two thyrotrophic cell models.

To determine the apparent D2 activity half-life in TαT1 cells, we used 100 μM cycloheximide and observed a loss of approximately 50% D2 activity in the first 60 min (Fig. 4C). Next, we used different concentrations of the proteasome inhibitor MG132 to test how efficiently these cells degrade D2. GH4C1 cells, originally used to describe the effects of

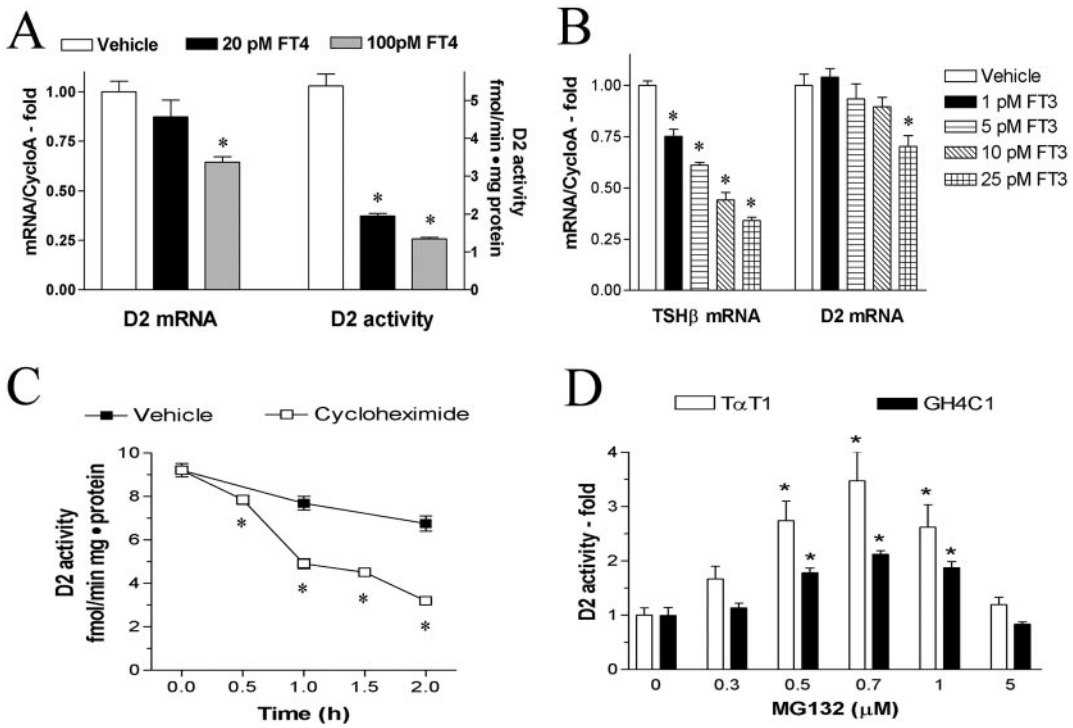

FIG. 4. A, TαT1 cells were kept in growth medium until confluence and then placed in hypothyroid medium for 24 h; medium was then replaced by 0.1% BSA-containing vehicle or 20 or 100 pM of free T_4 (FT_4), and cells were incubated for 16 h and processed for protein and RNA (*, $P < 0.01$ *vs.* vehicle). B, TαT1 cells were kept in growth medium until confluence and placed in hypothyroid medium for 24 h; medium was then replaced by 0.5% BSA-containing vehicle or increasing concentrations of free T_3 (FT_3), incubated for 16 h, and processed for RNA analysis (*, $P < 0.05$ *vs.* vehicle). C, TαT1 cells were kept in growth medium until confluence, placed in hypothyroid medium for 24 h, and medium replaced by 0.1% BSA-containing cycloheximide (100 μM) for 30, 60, 90, or 120 min and processed for D2 activity (*, $P < 0.05$ *vs.* vehicle). D, TαT1 and GH4C1 cells were kept in growth medium until confluence and then incubated with increasing concentration of MG132 for 5 h then processed for D2 activity (n = 4–7) (*, $P < 0.05$ *vs.* 0 μM of MG132).

MG132 on D2 activity (18), were used as reference. Whereas a 5-h incubation of GH4C1 cells with MG132 resulted in an approximately 2-fold increase in D2 activity, in similarly treated TαT1 cells D2 activity increased by almost 4-fold (Fig. 4D). These results indicate that TαT1 cells actively process D2 in a fashion similar to that used by many other D2-expressing cells characterized to date (33). Thus, the remainder of the experiments was performed in TαT1 cells.

To understand the relationship between T_4 concentration and D2 activity in thyrotrophs, we exposed TαT-1 cells overnight to variable free T_4 concentrations and compared the results with those of two other D2-expressing cell lines, *ie* a rat pituitary tumor cell line (GH4C1) and a human mesothelioma cell line (MSTO-211H). Before the experiment, all cells were preincubated for 24 h in medium containing charcoal-stripped FBS. The next day, cells were exposed for 12 h to medium containing 0.1% BSA and known amounts of T_4 to generate a defined range of free T_4 concentrations of 0–400 pM (the physiological free T_4 concentration in serum is ~20 pM). This resulted in a sharp drop in D2 activity in all three cell lines, with most of the loss occurring over the 0–50 pM T_4 range (Fig. 5A). It is notable that the fall in D2 activity varied according to the initial D2 level. In GH4C1 cells, which had the lowest starting point, D2 activity dropped to undetectable levels at 40 pM T_4, whereas the decrease was less pronounced in MSTO-211H and TαT1 cells. In MSTO-211H cells, D2 activity continued to fall as the free T_4 concentration increased, eventually disappearing at approximately 350 pM T_4. Remarkably, D2 activity in TαT1 cells stabilized at approximately 50 pM T_4, despite increasing free T_4 concentrations to 400 pM (Fig. 5A).

D2 ubiquitination seems to be in order in these cells because of the partial T_4-induced loss of D2 activity and presence of the mRNA of key proteins involved in D2 inactivation via ubiquitination such as WD40 containing SOCS box protein (WSB)-1 and Von Hippel-Lindau interacting deubiquitinating protein (VDU)-1/2 in these cells (data not shown). Thus, to explore further the mechanisms underlying the maintenance of D2 activity in T_4-treated TαT1 cells, we repeated the T_4-induced loss of D2 activity experiment exposing cells to zero or 100 pM T_4 for 16 h, except that 2 h before harvesting, we treated cells with cycloheximide to stop protein synthesis. Such treatment resulted in a sharp drop in D2 activity, at a fractional rate that was independent of the T_4 content in the medium (Fig. 5, B and C). This indicates that the D2 turnover in TαT1 cells remains high, despite a relatively constant level of D2 activity.

D2-mediated T_3 production suppresses TSHβ gene expression in TαT1 cells

Next we wished to test the hypothesis that maintenance of D2 activity in the presence of increasing free T_4 concentra-

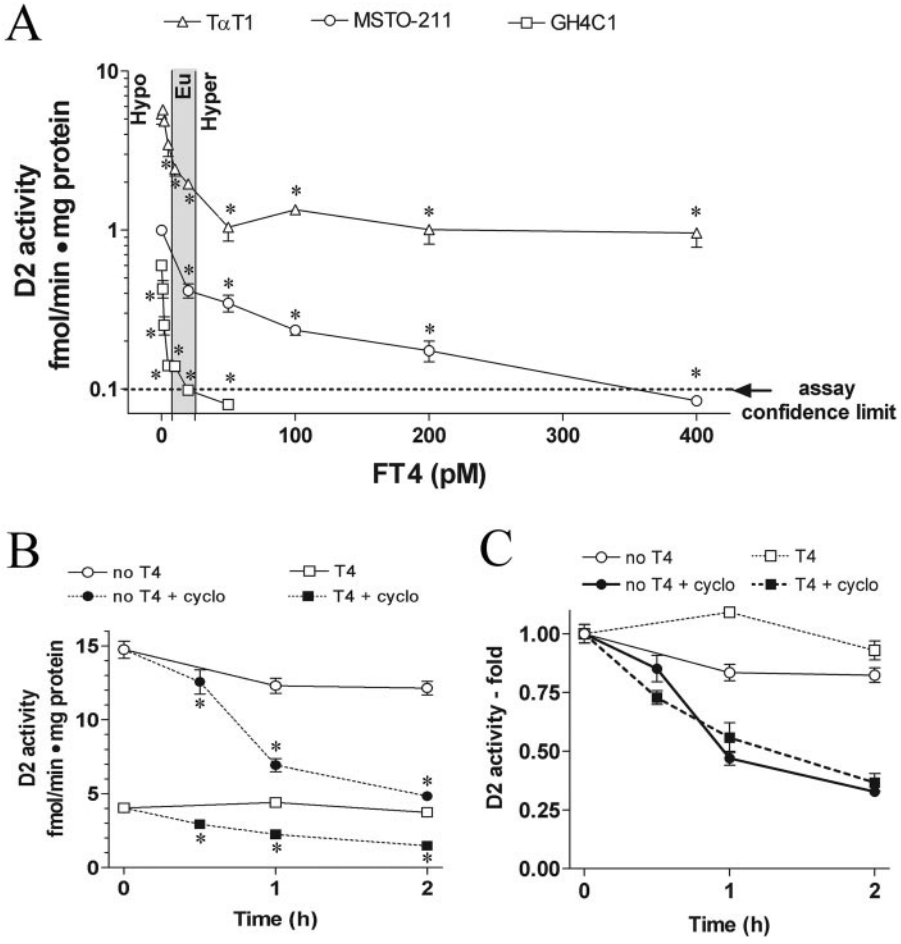

FIG. 5. Response of D2 activity to T_4 in TαT1, GH4C1, and MSTO-211 cells. A, GH4C1 and MSTO-211 cells were kept in growth medium supplemented with 10^{-7} M Se, whereas TαT1 were grown in growth medium. Cells were made hypothyroid by 24 h of incubation in DMEM + 10% charcoal-stripped FBS. Medium was replaced by DMEM + 0.1% BSA-containing vehicle or doses of free T_4 (FT4), ranging from 0 to 8 pM hypothyroid (hypo), 8–25 pM euthyroid (Eu), and 25–400 pM (hyperthyroid -hyper) for 20 h. Cells were then processed for D2 activity (*, $P < 0.001$ *vs.* 0 pM of FT4). B, TαT1 cells were kept in growth medium until confluence and placed in hypothyroid medium for 24 h; medium was then replaced by 0.1% BSA-containing vehicle (*circle*) or 100 pM of free T_4 (*square*) for 16 h. After that, vehicle (*open symbols*) or 100 μM cycloheximide (*solid symbols*) was added to medium, and cells were harvested at 0, 0.5, 1, or 2 h (*, $P < 0.05$ *vs.* time 0 h). C, The data presented in B were normalized by the time point 0 h and plotted as fold difference (n = 2–6).

tions, as evidenced in Fig. 5A, would increase net T_3 production and suppress TSH expression. To test this, we monitored TαT1 whole-cell deiodination measuring the 12-h integrated T_3 production (from added T_4) and also processed cells for measurement of TSHβ mRNA levels. T_3 production was calculated by multiplying the T_4-to-T_3 conversion rate (^{125}I-T_3/^{125}I-T_4) by the gravimetric amounts of added T_4 as described in detail elsewhere (34). As predicted, incubation of TαT1 cells with increasing concentrations of T_4 resulted in a progressive decrease in the fractional conversion of T_4 to T_3 (Fig. 6A, *inset*) but, because of the increasing free T_4 concentration in the media, this results in a reciprocal increase in D2-mediated T_3 production (Fig. 6A) and suppression of TSHβ gene expression (Fig. 6B). This decrease in the fractional conversion (Fig. 6A, *inset*) also indicates that increasing T_4 amounts are entering the cells, and thus, D2 stabilization is not likely to be due to decreased T_4 transport.

To verify that suppression of the TSHβ gene is mediated by D2-mediated T_4-to-T_3 conversion, we treated TαT1 cells with 50 nM rT_3, a relatively high concentration of rT_3 that not only will induce D2 inactivation but also will compete with T_4 for binding to the residual active D2 molecules. Treatment with rT_3 stopped T_4-to-T_3 conversion and prevented D2-mediated suppression of TSHβ (Fig. 7A) but did not interfere with TSHβ suppression mediated by exogenously added T_3 (Fig. 7B).

Discussion

Thyrotrophs lend themselves to understanding how intracellular thyroid hormone activation controls occupation of nuclear T_3 receptor and thyroid hormone action. Such cells are equipped with a highly T_3-responsive gene, *ie* TSHβ, express very high levels of D2 (Fig. 3A), the key deiodinase that activates thyroid hormone and mediates the signal transduction between serum T_4 and binding of T_3 to TR. In fact, this mechanism is possible only because of the typical homeostatic behavior of D2 (inactivation by catalysis) is offset in the thyrotrophs by the high rate at which this enzyme is synthesized in these cells. This allows for sustained T_3 production, even in the presence of elevated T_4 concentrations, restraining and eventually turning off the expression of the TSHβ gene, the basis for the TSH feedback mechanism.

The presence of D2 in the pituitary gland is generally

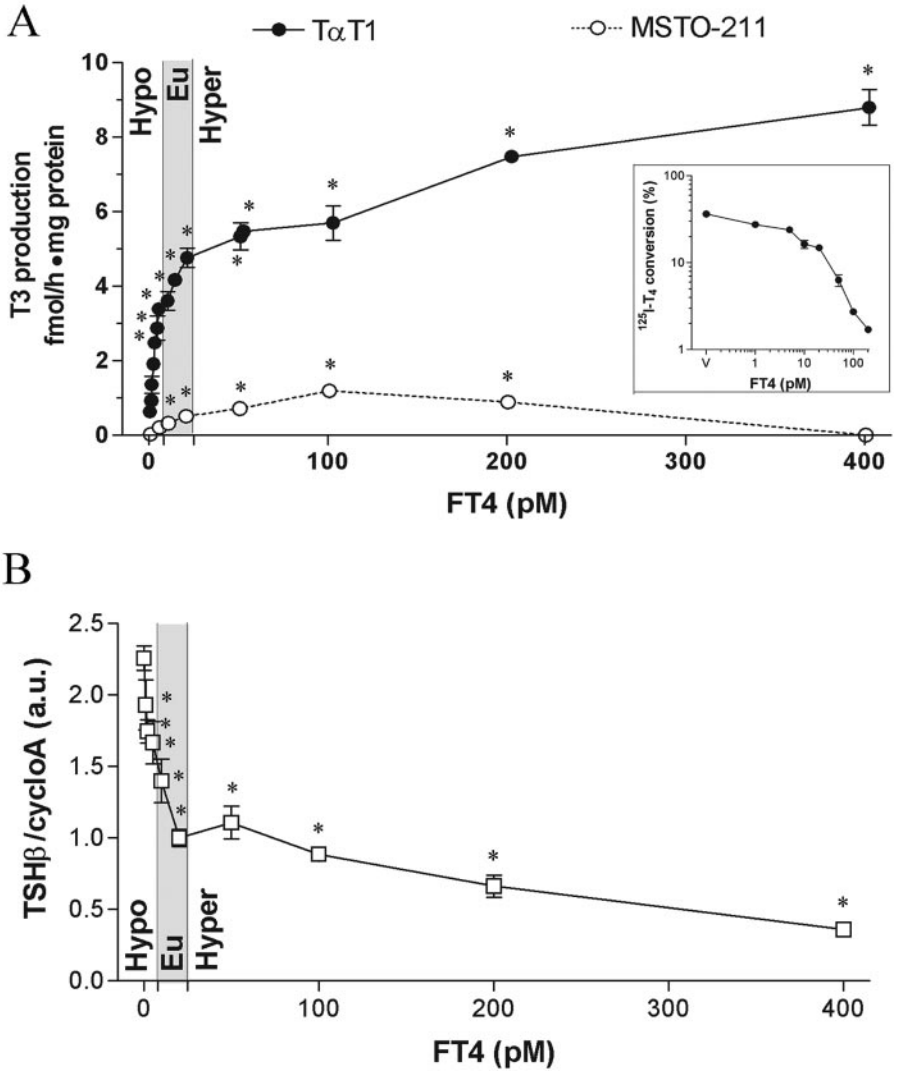

FIG. 6. T_3 production and TSHβ gene regulation. TαT1 and Msto-211 cells were grown in growth medium and rendered hypothyroid in DMEM + 10% charcoal-stripped FBS for 24 h; medium was then replaced by DMEM + 0.1% BSA. (For MSTO-211 cells 10^{-7} M Se was added to medium.) A, Cells were incubated for 18–20 h with vehicle or doses of free T_4 (FT4), ranging from 0 to 8 pM hypothyroid (hypo), 8 to 25 pM euthyroid (Eu), and 25 to 400 pM hyperthyroid (hyper) state and ^{125}I-T_4 (100,000–250,000 cpm/ml). At the end of experiment, medium was collected and cells were harvested and processed for determination of T_3 production (see *Materials and Methods*). The *inset* shows the fractional conversion of tracer T_4 in response to increasing concentration of FT_4 in the media. B, Cells were incubated for 20 h with vehicle or concentrations of free T_4 ranging from 0 to 8 pM hypothyroid (hypo), 8 to 25 pM euthyroid (Eu), and 25 to 400 pM hyperthyroid (hyper), harvested, and processed for RNA analysis. For normalization, the ratio TSHβ/CycloA at 20 pM T_4 was considered 1 (n = 2–6). *, $P < 0.01$ *vs.* 0 pM of FT_4.

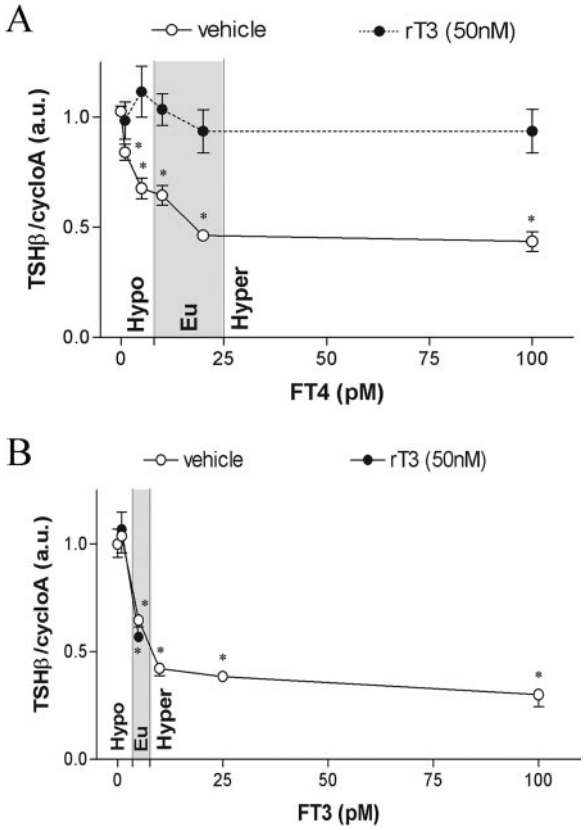

FIG. 7. TαT1 cells were kept in growth medium until confluence, rendered hypothyroid for 24 h in DMEM + 10% charcoal-stripped FBS, and then incubated in DMEM + 0.1% BSA and treated with vehicle (open circle) or 50 nM of rT_3 (solid circle), receiving doses of free T_4 (FT4), ranging from 0 to 8 pM hypothyroid (hypo), 8 to 25 pM euthyroid (Eu), and 25 to 100 pM hyperthyroid (hyper) state for 16 h (A) or in DMEM + 0.5% BSA treated with vehicle (*open circle*) or 50 nM of rT_3 (*solid circle*), receiving doses of free T_3 (FT3), ranging from 0 to 3.5 pM hypothyroid (hypo), 3.5 to 7.7 pM euthyroid (Eu), and 7.7 to 100 pM hyperthyroid (hyper) state for 16 h (B). Cells were harvested and processed for RNA analysis (n = 4–6). *, $P < 0.01$ *vs.* 0 pM of FT4 (A) and *, $P < 0.01$ *vs.* 0 pM of FT3 (B).

accepted, but its presence in thyrotrophs is not well established. Based on the intrinsic role of serum T_4 in the TSH feedback mechanism (2), D2 is expected to be present in thyrotrophs. However, this has been difficult to prove because of the lack of abundance of TSH-producing cells in the pituitary gland (35). One alternative strategy has been to screen pituitary tumors for the presence of D2. At least two reports (14, 36) indicate that D2 is present in TSH-secreting adenomas, but another (13) has found D3 as the predominant deiodinase in TSH-producing tumors. In the present investigation, the presence of D2 in thyrotrophs was clearly demonstrated in rat pituitary sections by *in situ* hybridization histochemistry (Figs. 1 and 2) and in two rodent thyrotrophic cell models (Fig. 3A). In the rat pituitary sections, the fact that only approximately 30% of the thyrotrophs are positive for D2 under euthyroid conditions (Fig. 2A) probably reflects the low abundance of D2 mRNA, which is below the detection level of this technique. This is supported by the increase in the presence of D2 mRNA to almost 80% of the thyrotrophs during hypothyroidism (Fig. 2B). However, it is not possible to exclude at this time the existence of a thyrotrophic subpopulation that does not express D2 in which TSH secretion would be controlled primarily by serum T_3.

TαT1 cells express WSB-1, the D2-specific ubiquitin ligase adaptor, and VDU-1 and VDU-2, two deubiquitinases involved in rescuing and reactivation of inactive ubiquitinated D2 (data not shown). The presence of these proteins involved in D2 ubiquitination and degradation explains the relatively short half-life of D2 in these cells (Fig. 4C) as well as its sensitivity to T_4 (Fig. 4, A and B) and MG132 (Fig. 4D). However, when a range of concentrations of T_4 is used, it is notable that at T_4 concentrations greater than 50 pM the loss of D2 activity is impaired in TαT1 cells as compared with that of two other D2-expressing cells under identical treatment conditions (Fig. 5A). This could indicate that the ubiquitinating/proteolytic machinery is exhausted at high T_4 concentrations or that it has reached its maximal capacity. The experiment with cycloheximide strongly favors the second possibility because D2 activity was rapidly lost after D2 synthesis was stopped (Fig. 5, B and C). This indicates that the ubiquitinating/proteolytic machinery is not exhausted at high T_4 concentrations. Rather, it supports the idea that the rate of D2 synthesis in these cells equals the maximal rate of T_4-induced D2 ubiquitination. This is likely to explain the persistence of D2 activity in the presence of high T_4 concentrations. A high rate of reactivation of inactive ubiquitinated D2 via VDU-1/2-mediated deubiquitination could also contribute to this phenomenon, given the high expression of VDU-1 in the pituitary gland, although levels in TαT1 cells are not particularly high (data not shown).

The expression of D2 in thyrotrophs is at the core of the T_4-mediated TSH feedback mechanism. D2-mediated net T_3 production is low at lower T_4 concentrations and high at high T_4 concentrations (Fig. 6A), demonstrating that fluctuations in D2 activity caused by ubiquitination do not compensate for changes in T_4. This, however, is not the case in GH4C1 and MSTO-211 cells, which express D2 at lower levels (Fig. 5A). In these cell lines, D2 activity decreases with the increase in T_4 concentration so that T_3 production eventually halts at a minimal level. Such a scenario would not be desirable in thyrotrophs because a major decline in D2 activity resulting from an increase in serum T_4 would disrupt the transduction mechanism by which T_4 controls TSHβ gene expression. As a result, the feedback mechanism would lose its exquisite sensitivity to minor elevations in serum T4 concentrations that can normally result in profound TSH suppression.

Acknowledgments

Received October 12, 2005. Accepted December 22, 2005.

Address all correspondence and requests for reprints to: Antonio C. Bianco, M.D., Ph.D., Brigham and Women's Hospital, 77 Avenue Louis Pasteur, HIM Building 643, Boston, Massachusetts 02115. E-mail: abianco@partners.org.

This work was supported by National Institutes of Health Grants DK-37021, DK36843, CA47411, DK36256, and DK58538. W.S.S. is a fellow of the Pew Charitable Trusts Foundation.

The authors have no conflict of interest.

References

1. **Larsen PR, Davies TF, Schlumberger M, Hay ID** 2003 Thyroid physiology and diagnostic evaluation of patients with thyroid disorders. In: Larsen PR, Kro-

nenberg HM, Melmed S, Polonsky KS, eds. Williams textbook of endocrinology. 10th ed. Philadelphia: W. B. Saunders Co.; 331–456
2. **Larsen PR** 1982 Thyroid-pituitary interaction: feedback regulation of thyrotropin secretion by thyroid hormones. N Engl J Med 306:23–32
3. **Riesco G, Taurog A, Larsen R, Krulich L** 1977 Acute and chronic responses to iodine deficiency in rats. Endocrinology 100:303–313
4. **Escobar-Morreale HF, Rey F, Obregon MJ, Escobar GM** 1996 Only the combined treatment with thyroxine and triiodothyronine ensures euthyroidism in all tissues of the thyroidectomized rat. Endocrinology 137:2490–2502
5. **Silva JE, Larsen PR** 1977 Pituitary nuclear 3,5,3′-triiodothyronine and thyrotropin secretion: an explanation for the effect of thyroxine. Science 198:617–620
6. **Silva JE, Dick TE, Larsen PR** 1978 Contribution of local tissue thyroxine monodeiodination to the nuclear 3,5,3′-triiodothyronine in pituitary, liver, and kidney of euthyroid rats. Endocrinology 103:1196–1207
7. **Silva JE, Kaplan MM, Cheron RG, Dick TE, Larsen PR** 1978 Thyroxine to 3,5,3′-triiodothyronine conversion by rat anterior pituitary and liver. Metabolism 27:1601–1607
8. **Silva JE, Larsen PR** 1978 Contributions of plasma triiodothyronine and local thyroxine monodeiodination to triiodothyronine to nuclear triiodothyronine receptor saturation in pituitary, liver, and kidney of hypothyroid rats. Further evidence relating saturation of pituitary nuclear triiodothyronine receptors and the acute inhibition of thyroid-stimulating hormone release. J Clin Invest 61:1247–1259
9. **Schneider MJ, Fiering SN, Pallud SE, Parlow AF, St. Germain DL, Galton VA** 2001 Targeted disruption of the type 2 selenodeiodinase gene (Dio2) results in a phenotype of pituitary resistance to T_4. Mol Endocrinol 15:2137–2148
10. **Abend SL, Fang SL, Alex S, Braverman LE, Leonard JL** 1991 Rapid alteration in circulating free thyroxine modulates pituitary type II 5′ deiodinase and basal thyrotropin secretion in the rat. J Clin Invest 88:898–903
11. **Visser TJ, Kaplan MM, Leonard JL, Larsen PR** 1983 Evidence for two pathways of iodothyronine 5′-deiodination in rat pituitary that differ in kinetics, propylthiouracil sensitivity, and response to hypothyroidism. J Clin Invest 71:992–1002
12. **Silva JE, Larsen PR** 1982 Comparison of iodothyronine 5′-deiodinase and other thyroid-hormone-dependent enzyme activities in the cerebral cortex of hypothyroid neonatal rat. Evidence for adaptation to hypothyroidism. J Clin Invest 70:1110–1123
13. **Tannahill LA, Visser TJ, McCabe CJ, Kachilele S, Boelaert K, Sheppard MC, Franklyn JA, Gittoes NJ** 2002 Dysregulation of iodothyronine deiodinase enzyme expression and function in human pituitary tumours. Clin Endocrinol (Oxf) 56:735–743
14. **Baur A, Buchfelder M, Kohrle J** 2002 Expression of 5′-deiodinase enzymes in normal pituitaries and in various human pituitary adenomas. Eur J Endocrinol 147:263–268
15. **Dentice M, Bandyopadhyay A, Gereben B, Callebaut I, Christoffolete MA, Kim BW, Nissim S, Mornon JP, Zavacki AM, Zeold A, Capelo LP, Curcio-Morelli C, Ribeiro R, Harney JW, Tabin CJ, Bianco AC** 2005 The Hedgehog-inducible ubiquitin ligase subunit WSB-1 modulates thyroid hormone activation and PTHrP secretion in the developing growth plate. Nat Cell Biol 7:698–705
16. **Ross DS, Downing MF, Chin WW, Kieffer JD, Ridgway EC** 1983 Changes in tissue concentrations of thyrotropin, free thyrotropin α, and α-subunits after thyroxine administration: comparison of mouse hypothyroid pituitary and thyrotropic tumors. Endocrinology 112:2050–2053
17. **Yusta B, Alarid ET, Gordon DF, Ridgway EC, Mellon PL** 1998 The thyrotropin β-subunit gene is repressed by thyroid hormone in a novel thyrotrope cell line, mouse TαT1 cells. Endocrinology 139:4476–4482
18. **Steinsapir J, Harney J, Larsen PR** 1998 Type 2 iodothyronine deiodinase in rat pituitary tumor cells is inactivated in proteasomes. J Clin Invest 102:1895–1899
19. **Curcio C, Baqui MMA, Salvatore D, Rihn BH, Mohr S, Harney JW, Larsen PR, Bianco AC** 2001 The human type 2 iodothyronine deiodinase is a selenoprotein highly expressed in a mesothelioma cell line. J Biol Chem 276:30183–30187
20. **Everts M, Verhoeven F, Bezstarosti K, Moerings EP, Hennemann G, Visser TJ, Lamers JM** 1996 Uptake of thyroid hormones in neonatal rat cardiac myocytes. Endocrinology 137:4235–4242
21. **Wood WM, Ocran KW, Gordon DF, Ridgway EC** 1991 Isolation and characterization of mouse complementary DNAs encoding α and β thyroid hormone receptors from thyrotrope cells: the mouse pituitary-specific β2 isoform differs at the amino terminus from the corresponding species from rat pituitary tumor cells. Mol Endocrinol 5:1049–1061
22. **Croteau W, Davey JC, Galton VA, St. Germain DL** 1996 Cloning of the mammalian type II iodothyronine deiodinase. A selenoprotein differentially expressed and regulated in human and rat brain and other tissues. J Clin Invest 98:405–417
23. 1997 Relative quantitation of gene expression: user bulletin no. 2. Norwalk, CT: PerkinElmer Co.; 1–36
24. **Ginzinger DG** 2002 Gene quantification using real-time quantitative PCR: an emerging technology hits the mainstream. Exp Hematol 30:503–512
25. **Kakucska I, Rand W, Lechan RM** 1992 Thyrotropin-releasing hormone gene expression in the hypothalamic paraventricular nucleus is dependent upon feedback regulation by both triiodothyronine and thyroxine. Endocrinology 130:2845–2850
26. **Dyess EM, Segerson TP, Liposits Z, Paull WK, Kaplan MM, Wu P, Jackson IM, Lechan RM** 1988 Triiodothyronine exerts direct cell-specific regulation of thyrotropin-releasing hormone gene expression in the hypothalamic paraventricular nucleus. Endocrinology 123:2291–2297
27. **Fekete C, Kelly J, Mihály E, Sarkar S, Rand WM, Legradi G, Emerson CH, Lechan RM** 2001 Neuropeptide Y has a central inhibitory action on the hypothalamic-pituitary-thyroid axis. Endocrinology 142:2606–2613
28. **Fekete C, Mihály M, Luo LG, Kelly J, Clausen JT, Mao Q, Rand WM, Moss LG, Kuhar M, Emerson CH, Jackson IM, Lechan RM** 2000 Association of CART-immunoreactive elements with thyrotropin-releasing hormone-synthesizing neurons in the hypothalamic paraventricular nucleus and its role in the regulation of the hypothalamic-pituitary-thyroid axis during fasting. J Neurosci 20:9224–9234
29. **Fekete C, Gereben B, Doleschall M, Harney JW, Dora JM, Bianco AC, Sarkar S, Liposits Z, Rand W, Emerson C, Kacskovics I, Larsen PR, Lechan RM** 2004 Lipopolysaccharide induces type 2 iodothyronine deiodinase in the mediobasal hypothalamus: implications for the nonthyroidal illness syndrome. Endocrinology 145:1649–1655
30. **Buettner C, Harney JW, Larsen PR** 2000 The role of selenocysteine 133 in catalysis by the human type 2 iodothyronine deiodinase. Endocrinology 141:4606–4612
31. **Croteau W, Bodwell JE, Richardson JM, St. Germain DL** 1998 Conserved cysteines in the type 1 deiodinase selenoprotein are not essential for catalytic activity. J Biol Chem 273:25230–25236
32. **Richard K, Hume R, Kaptein E, Sanders JP, van Toor H, De Herder WW, den Hollander JC, Krenning EP, Visser TJ** 1998 Ontogeny of iodothyronine deiodinases in human liver. J Clin Endocrinol Metab 83:2868–2874
33. **Bianco AC, Salvatore D, Gereben B, Berry MJ, Larsen PR** 2002 Biochemistry, cellular and molecular biology and physiological roles of the iodothyronine selenodeiodinases. Endocr Rev 23:38–89
34. **Maia AL, Kim BW, Huang SA, Harney JW, Larsen PR** 2005 Type 2 iodothyronine deiodinase is the major source of plasma T_3 in euthyroid humans. J Clin Invest 115:2524–2533
35. **Koenig RJ, Leonard JL, Senator D, Rappaport N, Watson AY, Larsen PR** 1984 Regulation of thyroxine 5′-deiodinase activity by 3,5,3′-triiodothyronine in cultured rat anterior pituitary cells. Endocrinology 115:324–329
36. **Itagaki Y, Yoshida K, Ikede H, Kaise K, Kaise N, Yamamoto M, Sakurada T, Yoshinaga K** 1990 Thyroxine 5′-deiodinase in human anterior pituitary tumors. J Clin Endocrinol Metab 71:340–344

***Endocrinology* is published monthly by The Endocrine Society (http://www.endo-society.org), the foremost professional society serving the endocrine community.**

V – Terceiro Artigo

Resumo

O gene *Dio2* codifica a desiodase do tipo 2 (D2) que ativa a tiroxina (T4) à 3,3',5-triiodotironina (T3), e cuja disrupção (*Dio2*$^{-/-}$) resulta em hipotiroidismo específico do tecido adiposo marrom (BAT). No presente estudo, exposição ao frio aumenta a estimulação simpática no BAT em ~10 vezes (normal ~4 vezes), como resultado, lipólise, bem como os níveis de mRNA da proteína desacopladora 1, guanosina monofosfato redutase e receptor ativado de proliferaçao de peroxissomo γ- co-ativador 1, aumentam bem acima dos níveis detectados em animais selvagens expostos ao frio. A hiper-resposta adrenérgica sustentada no BAT *Dio2*$^{-/-}$ suprime a estimulação de 3 a 4 vezes da lipogênese do BAT, normalmente observada após 24-48 horas no frio. Supressão farmacológica da lipogênese com ββ'-metil-substituído α-ω-acido dicaborxilíco de C14-C18 em animais selvagens também prejudicou a termogênese facultativa no BAT. Estes dados constituem a primeira evidência de que a responsividade adrenérgica diminuída não limita a termogênese facultativa induzida pelo frio. Ao invés disso, a estimulação hiperadrenergética compensatória previne a estimulação normal da lipogênese no BAT durante à exposição ao frio, exaurindo rapidamente a disponibilidade de ácidos graxos. A última é a determinante preponderante da termogênese facultativa prejudicada e hipotermia de camundongos *Dio2*$^{-/-}$ expostos ao frio.

Mice with Targeted Disruption of the Dio2 Gene Have Cold-Induced Overexpression of the Uncoupling Protein 1 Gene but Fail to Increase Brown Adipose Tissue Lipogenesis and Adaptive Thermogenesis

Marcelo A. Christoffolete,[1] Camila C.G. Linardi,[2] Lucia de Jesus,[1] Katia Naomi Ebina,[3] Suzy D. Carvalho,[2] Miriam O. Ribeiro,[4] Rogerio Rabelo,[2] Cyntia Curcio,[1] Luciane Martins,[3] Edna T. Kimura,[3] and Antonio C. Bianco[1]

The Dio2 gene encodes the type 2 deiodinase (D2) that activates thyroxine (T4) to 3,3′,5-triiodothyronine (T3), the disruption of which (Dio2$^{-/-}$) results in brown adipose tissue (BAT)-specific hypothyroidism in an otherwise euthyroid animal. In the present studies, cold exposure increased Dio2$^{-/-}$ BAT sympathetic stimulation ~10-fold (normal ~4-fold); as a result, lipolysis, as well as the mRNA levels of uncoupling protein 1, guanosine monophosphate reductase, and peroxisome proliferator–activated receptor γ coactivator 1, increased well above the levels detected in the cold-exposed wild-type animals. The sustained Dio2$^{-/-}$ BAT adrenergic hyperresponse suppressed the three- to fourfold stimulation of BAT lipogenesis normally seen after 24–48 h in the cold. Pharmacological suppression of lipogenesis with ββ′-methyl-substituted α-ω-dicarboxylic acids of C14–C18 in wild-type animals also impaired adaptive thermogenesis in the BAT. These data constitute the first evidence that reduced adrenergic responsiveness does not limit cold-induced adaptive thermogenesis. Instead, the resulting compensatory hyperadrenergic stimulation prevents the otherwise normal stimulation in BAT lipogenesis during cold exposure, rapidly exhausting the availability of fatty acids. The latter is the preponderant determinant of the impaired adaptive thermogenesis and hypothermia in cold-exposed Dio2$^{-/-}$ mice. *Diabetes* 53:577–584, 2004

From the [1]Department of Medicine, Thyroid Section, Division of Endocrinology, Diabetes and Hypertension, Brigham and Women's Hospital and Harvard Medical School, Boston, Massachusetts; the [2]Department of Physiology & Biophysics, Institute of Biomedical Sciences, University of São Paulo, São Paulo, Brazil; the [3]Department of Histology & Embryology, Institute of Biomedical Sciences, University of São Paulo, São Paulo, Brazil; and the [4]Department of Biosciences, School of Biological, Exact and Experimental Sciences, Mackenzie University, São Paulo, Brazil.

Address correspondence and reprint requests to Antonio C. Bianco, MD, PhD, Brigham and Women's Hospital; HIM Building, Room 643, 77 Ave. Louis Pasteur, Boston, MA 02115. E-mail: abianco@partners.org.

Received for publication 11 September 2003 and accepted in revised form 21 November 2003.

M.A.C. and C.C.G.L. contributed equally to this work.

ACC, acetyl CoA carboxylase; α-MT, α-methyl parathyrosine; BAT, brown adipose tissue; D2, type 2 iodothyronine deiodinase; GMPr, guanine monophosphate reductase; HSL, hormone-sensitive lipase; IBAT, interscapular BAT; NE, norepinephrine; PGC-1α, peroxisome proliferator–activated receptor γ coactivator 1-α; SNS, sympathetic nervous system; T3, 3,3′,5-triiodothyronine; T4, thyroxine; TG, triglyceride; TR, thyroid hormone receptor; UCP-1, uncoupling protein 1; WT, wild-type.

Adequate quantities of thyroid hormone are required for the maintenance of basal energy expenditure (1,2) and are also critical for adjustments in energy homeostasis during acute exposure to cold, without which survival is not possible (3). These adjustments in nonshivering adaptive thermogenesis are initiated by an increase in the activity of the sympathetic nervous system (SNS). In human newborns and other small mammals, brown adipose tissue (BAT) is the main site of the sympathetic-mediated adaptive thermogenesis. During cold exposure, there is an acute ~50-fold increase in type 2 iodothyronine deiodinase (D2) activity in BAT that accelerates thyroxine (T4) to 3,3′,5-triiodothyronine (T3) conversion (4). This increases thyroid hormone receptor (TR) saturation and leads to intracellular thyrotoxicosis specifically in this tissue (5), which in turn increases adrenergic responsiveness (6–8) in a feed-forward mechanism that allows BAT to produce heat in a sustainable manner.

The current paradigm of thyroid-adrenergic synergism is based on the principle that hypothyroidism causes a generalized decrease in adrenergic responsiveness and, therefore, frustrates the homeostatic role of the SNS, including the stimulation of BAT (9,10). However, these studies are largely based on the hypothyroid animal as a model, which has serious limitations for this purpose. The reduced obligatory energy expenditure caused by systemic hypothyroidism leads to a generalized and gradual increase in sympathetic activity that, in the BAT, activates adaptive energy expenditure to sustain normal core temperature, even at room temperature (11). However, chronic norepinephrine (NE) stimulation typically sets off a series of desensitization mechanisms designed to limit adrenergic responsiveness, decreasing the capacity for further increase in the adrenergic signal transduction as required during an acute exposure to cold. Thus, it is difficult to differentiate the primary effects of hypothyroidism in BAT from those caused by the compensatory increase in sympathetic activity.

Conversely, the recently created mouse with targeted disruption of the D2 gene (Dio2$^{-/-}$) constitutes an improved system to study thyroid-adrenergic interactions.

These animals are systemically euthyroid, as their serum T3 is normal and serum T4 is only slightly elevated. Thus, they do not develop homeostatic adaptations at room temperature (12,13). However, the absence of D2 impairs BAT thermogenesis by precluding the adaptive increase in T4 to T3 conversion. As a result, cold-exposed Dio2$^{-/-}$ mice activate shivering, a less efficient thermogenic pathway that ensures survival but does not prevent mild hypothermia (13).

It is not entirely clear why the D2-mediated high T3 receptor saturation is critical for BAT thermogenesis. On the basis of studies performed in hypothyroid rat and mouse models, the Dio2$^{-/-}$ mouse would have been expected to have impaired uncoupling protein 1 (UCP-1) expression (14–16) and decreased adrenergic responsiveness (7,8). However, our previous studies indicate that the nonstimulated Dio2$^{-/-}$ BAT has normal amounts of mitochondria and normal UCP-1 concentration (13). At the same time, Dio2$^{-/-}$ brown adipocytes do have decreased cAMP generation capacity in response to different adrenergic stimulants (13), indicating that the latter is the mechanism of impaired thermogenesis. Unexpectedly, the present studies reveal that cold-exposed Dio2$^{-/-}$ mice have a compensatory approximately ninefold increase in BAT SNS stimulation that bypasses the relative adrenergic insensitivity. At the same time, we now report that the compensatory supernormal sympathetic stimulation causes intense lipolysis and suppresses the otherwise normal lipogenic surge observed during cold exposure, thus rapidly depleting the brown adipocytes of its source of fatty acids, resulting in impaired adaptive thermogenesis.

RESEARCH DESIGN AND METHODS

Chemicals and drugs. Unless otherwise specified, all drugs and reagents were purchased from Sigma Chemical Co. (St. Louis, MO). The ββ′-methyl-substituted α-ω-dicarboxylic acids of C14–C18 chain length (MEDICA-16), a dead-end inhibitor of acetyl CoA carboxylase (ACC) and a competitive inhibitor of citrate lyase (17), was a gift from Dr. Jacob Bar-Tana (Department of Nutrition and Metabolism, Hebrew University Medical School, Jerusalem, Israel).

Animals and treatments. All studies were performed under a protocol approved by the Standing Committee on Animal Research. Some experiments were performed on male Wistar rats that weighed 200–260 g, obtained from our breeding colony as described (18). Surgical thyroidectomy was performed under light ether anesthesia and was followed by administration of 0.05% methimazole in the drinking water. Other studies were performed in C57BL/6J or B6129SF2/J mice that weighed 20–30 g and were either purchased from The Jackson Laboratories (Bar Harbor, MA) or bred in our laboratory as described (13). Dio2 genotyping was by PCR using a wild-type (WT) sense primer (5′-GTTTAGTCATGGAAGCAGCACTATG-3′), a Dio2$^{-/-}$ sense primer (5′-CGTGGGATCATTGTTTTTCTCTTG-3′), and a common antisense primer (5′-CATGGCGTTAGCCAAAACTCATC-3′), which generates an ~400-bp and an ~450-bp fragment corresponding to WT and Dio2$^{-/-}$, respectively.

Interscapular BAT pad thermal response and NE turnover. The interscapular (IBAT) thermal response to NE was performed as described (16,19) in mice anesthetized with urethane (1.2 g/kg i.p.). Raw data were plotted over time and expressed in terms of maximum ΔIBAT temperature (°C). NE turnover was measured in mice acclimated at room temperature or during cold exposure by blocking NE synthesis with 300 mg/kg α-methyl parathyrosine (α-MT) as previously described (20). Mice were killed at 0, 1, 2, 3, or 4 h after the α-MT injection, and the IBAT was processed for NE measurement by radioimmunoassay (Alpco Diagnostics, Windham, NH).

IBAT processing for histologic studies. Animals were killed by perfusion with ice-cold 0.9% NaCl over a period of 15 min, under chloral hydrate anesthesia (33%; 0.1 ml/100 g body wt i.p.), followed by perfusion with 4% paraformaldehyde in 0.05 mol/l phosphate buffer (pH 7.4). The IBAT was rapidly removed and processed for light microscopy or electron microscopy as described (21). Sections were analyzed under a Nikon Eclipse E600 light microscope or at 80 KV with JEOL 100CXII or JEOL 1010 transmission electron microscopes.

Biochemical determinations and IBAT enzymatic activities. The IBAT was processed by homogenization and isolation of the cytosolic fraction as described (18). Malic enzyme and glucose 6-P-dehydrogenase were assayed using 50–100 μg of cytosolic protein (18,22,23). ACC was assayed as described (24,25), and the results are expressed as units per minute per milligram of protein; 1 unit of ACC activity is equal to 1 mmol of [^{14}C]malonyl CoA formed in 1 min at 37°C. Hormone-sensitive lipase (HSL) activity was measured as described (26,27), and the results are expressed as nanomoles of free fatty acid released per minute per milligram of protein. For measuring in vivo BAT lipogenesis, $^{3}H_2O$ (5 mCi; New England Nuclear, Boston, MA) dissolved in 0.5 ml of saline was injected intravenously (jugular vein) into fed mice, which were killed 1 h later. The IBAT was weighed and processed for lipid extraction as described (25). Rates of lipid synthesis were calculated assuming that the specific activity of intracellular water was identical to that of plasma water; each glycerol and each fatty acid incorporated into triglycerides (TG) contained 3.3 and 13.3 atoms of tritium, respectively. TG content was measured by enzyme-linked immunosorbent assay (L-Type TG H; Wako Chemicals USA, Richmond, VA) after extraction with chloroform/methanol (2:1).

IBAT mRNA analysis. Total RNA was isolated by the acid guanidinium thiocyanate-phenol-chloroform method (28) or using TRIzol (Invitrogen, Carlsbad, CA). Northern blots were performed using current standard techniques (29) and specific mouse UCP-1 or peroxisome proliferator–activated receptor γ coactivator 1-α (PGC-1α) cDNA probes provided by Dr. Brad Lowell (Division of Endocrinology, Beth Israel Deaconess Medical Center) or rat guanine monophosphate reductase (GMPr) (30) cDNA probe. RT-PCR was performed as previously described (31,32). PCR cDNA was synthesized using 2.5 μg of total RNA, the SuperScript First-Strand Synthesis System for RT-PCR (Invitrogen), and the Robocycler thermocycler (Stratagene, La Jolla, CA). The cDNA product was used in an RT-PCR reaction using the QuantiTect SYBR Green PCR kit (Qiagen, Valencia, CA). The cycle conditions were 15 min at 94°C (Hot Start), 30–50 s at 94°C, 30–50 s at 55–60°C, and 45–60 s at 72°C for 40 cycles. A final extension at 72°C for 5 min was performed as well as the melting curve protocol to verify the specificity of the amplicon generation. Standard curves consisting of five points of serial dilution (factor of 5) of mixed experimental and control groups cDNA were performed in each assay and used as calibrators. β-actin was used to correct for the loaded amount of cDNA. r^2 was >0.99 for all standard curves, and the amplification efficiency varied between 80 and 100%.

Statistical analysis. One-way ANOVA was used to compare more than two groups, followed by the Student-Newman-Keuls test to detect differences between groups. The Student's t test was used to compare the differences between two groups. $P < 0.05$ was used to reject the null hypothesis.

RESULTS

Exaggerated sympathetic responsiveness in cold-exposed hypothyroid and Dio2$^{-/-}$ animals. Brown adipocytes are typically multilocular, with the bulk of the cell being occupied by numerous round-shaped TG inclusions of various sizes permeated by a profusion of mitochondria separated by a cytoplasmic matrix (Fig. 1) (33,34). Acute cold exposure causes a reduction in the size and number of lipid inclusions (Fig. 1). By 6 h, the round inclusions have developed indentations, and by 12 h, virtually all lipid inclusions have disappeared and the mitochondria have become larger and less dense. By 24 h of cold exposure, however, the cytoplasm is once more filled with small lipid inclusions that permeate the space between the mitochondria (Fig. 1). As these lipid inclusions fuse (48 h), their sizes increase, and by 7 days of cold exposure, they almost have returned to that observed at thermoneutrality.

The typical multilocular aspect is preserved in the hypothyroid brown adipocytes (Fig. 1). Remarkably, after only 6 h of cold exposure, the size and number of the lipid inclusions are decreased, and the nuclei can now be seen at the center of the brown adipocytes (Fig. 1). It is notable that this lipolytic response is greater than in control cells. However, hypothyroid animals die of hypothermia if exposed for >6 h to cold, precluding longer studies of

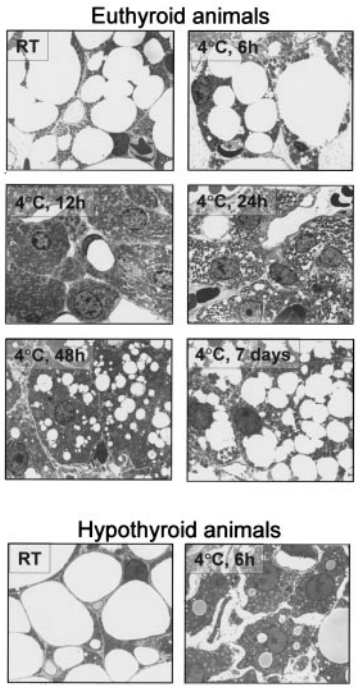

FIG. 1. Cold-induced ultrastructural changes in IBAT of euthyroid and hypothyroid rats. Electron microscopy of brown adipocytes during 0–7 days of cold exposure. Ambient temperature and times in the cold are indicated in the upper left corner of each slide. Pictures are representative of 12–20 images obtained per animal in groups of three to four animals. This experiment was performed two to three times. Magnification ×2,000.

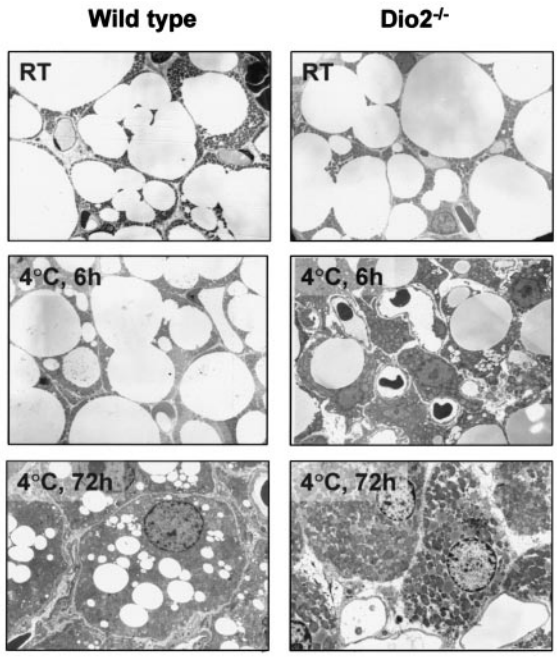

FIG. 2. Cold-induced ultrastructural changes in IBAT of WT and Dio2$^{-/-}$ mice. Electron microscopy of brown adipocytes during 0–72 h of cold exposure. Ambient temperature and times in the cold are indicated in the upper left corner of each slide. Mouse strains are indicated. Pictures are representative of 18–32 images obtained per animal in groups of four animals. This experiment was performed two times. Magnification ×2,000.

the role of thyroid hormone in sustaining BAT adaptive thermogenesis.

To bypass this limitation, we turned to the Dio2$^{-/-}$ mouse model (12,13). Whereas the BAT of WT mice undergoes a similar pattern of ultrastructural changes during cold exposure, the BAT of Dio2$^{-/-}$ mice presents a much more intense lipolytic phase in the first 6–12 h of cold exposure, similar to the hypothyroid BAT (Fig. 2, Table 1). This hyperresponse is characterized by higher HSL activity, lower TG content (Table 1), and marked reduction in the number and size of the lipid inclusions (Fig. 2). Remarkably, even after 72 h of cold exposure, there was no reorganization of the lipid inclusions in the Dio2$^{-/-}$ brown adipocytes (Fig. 2).

Because sympathetic responsiveness in isolated Dio2$^{-/-}$ brown adipocytes is decreased two- to threefold (13), we hypothesized that this super-normal lipolysis might be due to a compensatory increase in the SNS stimulation. In WT animals, basal NE disappearance was ~5%/h (Fig. 3*A*). During cold exposure, NE turnover rate peaked at 12 h (~25%/h) and decreased progressively to ~18% by 48 h. Although the BAT of Dio2$^{-/-}$ mice had a similar basal NE turnover, measurements performed during cold exposure revealed that NE turnover increased to 45–50%/h by 6–8 h and remained at approximately these high levels throughout the time at 4°C (Fig. 3*A*). Hypothyroid mice not only had an increased basal BAT NE turnover but also developed a hyperresponse when exposed to cold (Fig. 3*A*).

Next, we looked for other well-known cAMP-responsive markers in brown adipocytes as additional surrogates of adrenergic signal transduction, namely the gene expression of UCP-1 (35), GMPr (30), and PGC-1α (36). In WT animals, the UCP-1 mRNA levels increased 2- to 2.5-fold by 6 h of cold exposure and remained at these levels until 24 h. Although basal UCP-1 mRNA levels were not different in the Dio2$^{-/-}$ mice (Fig. 3*B*, Table 2), these animals had a super UCP-1 response to cold exposure. UCP-1 mRNA levels were up to ~4-fold higher already at 6 h of cold exposure and kept increasing to ~5.2-fold by 24 h (Fig. 3*B*, Table 2). This translated into significantly more mitochondrial UCP-1 after the 24 h of cold exposure (up 1.4 ± 0.23-fold in WT vs. 2.2 ± 0.37-fold in Dio2$^{-/-}$ mice; $P < 0.05$). Likewise, basal levels of GMPr mRNA were not

TABLE 1
HSL activity and TG content in BAT of cold-exposed mice

Mouse	Hours at 4°C	HSL (nmol FFA · min^{-1} · mg protein^{-1})	TG (mg/IBAT × 10^{-1})
WT			
	0	5.0 ± 0.9	2.5 ± 0.5
	6	9.4 ± 1.2	3.0 ± 0.3
	24	7.8 ± 1.1	1.0 ± 0.2*
Dio2$^{-/-}$			
	0	4.8 ± 0.6	3.5 ± 1.0
	6	13.9 ± 2.0*	1.3 ± 0.4*†
	24	15.2 ± 2.6*	0.5 ± 0.2*†
Hypothyroid			
	0	6.3 ± 1.3	2.0 ± 0.8
	6	12.4 ± 1.9†	0.3 ± 0.3*†

Data are means ± SD of four to five animals. *$P < 0.001$ vs. the same time in WT animals; †$P < 0.01$ vs. the same time in WT animals by ANOVA. Hypothyroid mice are WT. This experiment was performed twice.

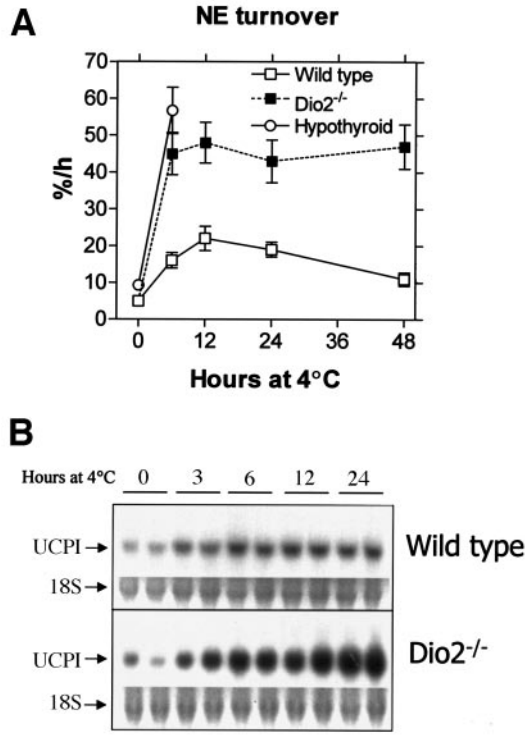

FIG. 3. IBAT NE turnover mRNA levels of cAMP-responsive genes of WT and Dio2$^{-/-}$ mice during cold exposure. *A*: Animals received α-MT and were killed at the indicated times. Values are the mean ± SD of four to five animals. *B*: Northern blot analysis of UCP-1 mRNA levels. The signal was quantified using a phosphoimager (Molecular Dynamics). The average of the relative intensity of each pair is, in the WT animals, 1 (room temperature), 2.2 (3 h at 4°C), 2.5 (6 h at 4°C), 2.6 (12 h at 4°C), and 2.3 (24 h at 4°C), and in the Dio2$^{-/-}$ animals, 1.1 (room temperature), 2.3 (3 h at 4°C), 4.0 (6 h at 4°C), 4.0 (12 h at 4°C), and 5.2 (24 h at 4°C). The ethidium bromide–stained image of the 18S RNA is shown for each gel. Mouse strains and times in the cold are indicated. The experiments were performed two to three times.

different between WT and Dio2$^{-/-}$ mice (Table 2). However, the cold stimulation of GMPr mRNA levels was also significantly higher in Dio2$^{-/-}$ mice (Table 2). When analyzed at 6 and 24 h in the cold, WT animals presented an ~13-fold and ~16-fold increase in GMPr mRNA, respectively, whereas the stimulation in Dio2$^{-/-}$ mice reached ~18-fold by 6 h and remained at this level for up to 24 h of cold exposure. Similar results were obtained in the analysis of the PGC-1α mRNA levels (36) (Table 2), confirming the increased NE stimulation of the BAT of cold-exposed Dio2$^{-/-}$ mice.

BAT lipogenesis during cold exposure. The reorganization of the lipid inclusions in the normal brown adipocytes that follows the initial 12 h of cold exposure indicates a shift from a predominant lipolytic phase to a situation in which lipogenesis and esterification of fatty acids progressively increase and predominate. It is interesting that this takes place despite continued increased β-oxidation and energy expenditure (37). Because cold exposure and T3 stimulate BAT lipogenesis (18,38), we tested whether changes in BAT lipogenesis paralleled the ultrastructural modifications in brown adipocytes. BAT lipogenesis in WT and Dio2$^{-/-}$ mice, measured as the rate of incorporation of ^3H_2O into lipids, decreased during the first 12 h of acute cold exposure, reaching values as low as ~50% of controls after 6–12 h at 4°C (Fig. 4*A*). This was accompanied by a reduction in the activity of the two key NADPH-generating enzymes, malic enzyme (Fig. 4*B*) and glucose 6-P-dehydrogenase (data not shown), and activity and mRNA levels of ACC, the rate-limiting enzyme of the lipogenic pathway (Fig. 4*C* and *D*). It is interesting that the inhibition in lipogenesis was transient. The incorporation of ^3H_2O into lipids and the activity and mRNA of those key enzymes increased from a nadir at 6–12 h to values three- to fourfold higher than in controls after 72 h of continued cold exposure (Fig. 4*A*–*C*).

Remarkably, Dio2$^{-/-}$ BAT lipogenesis, as studied by all four parameters discussed above, was inhibited in the first hours of cold exposure and remained low throughout the 72 h of cold exposure (Fig. 4). A similar decrease in BAT ACC mRNA levels was also observed in the hypothyroid mice after 6 h of cold exposure (Table 2).

To assess the roles that T3 and NE play in regulating ACC and Spot-14 mRNA levels, we treated WT mice with T3 and/or NE as follows: a single T3 injection (15 μg i.p.) at −24 h; five NE injections (3 μg/10 g body wt i.p.) at −7 h, −6 h, −5 h, −3 h, and −1 h; control animals received an injection of saline; all animals were killed at 0 h. T3 treatment doubled ACC and Spot-14 mRNA levels, whereas NE significantly decreased this by ~30% (Table 3). Most important, when both treatments were combined, NE antagonized the effects of T3, blunting the T3-induced increase in ACC and Spot-14 mRNA levels (Table 3). Note that D2 mRNA levels, a gene that is positively regulated by NE, changes in the opposite direction (Table 3). Thus,

TABLE 2
mRNA levels of positively or negatively adrenergic-regulated genes in BAT of cold-exposed mice

Mouse	Hours at 4°C	ACC	UCP-1	GMPr	PGC-1α
WT	0	1.0 ± 0.1	1.0 ± 0.1	1.0 ± 0.3	1.0 ± 0.1
	6	0.5 ± 0.2	2.4 ± 0.2	13.2 ± 2.2	1.2 ± 0.1
	24	1.1 ± 0.2	2.4 ± 0.1	16.5 ± 1.5	3.9 ± 0.6
Dio2$^{-/-}$	0	1.0 ± 0.3	0.8 ± 0.1	1.2 ± 0.3	0.9 ± 0.2
	6	0.3 ± 0.2	3.8 ± 0.4*	17.9 ± 1.8*	3.4 ± 0.5*
	24	0.5 ± 0.2*	5.2 ± 0.6*	18.2 ± 2.9	2.9 ± 0.3
Hypothyroid	0	1.0 ± 0.3	0.6 ± 0.2*	ND	ND
	6	0.3 ± 0.1*	1.2 ± 0.3*	ND	ND

Data are means ± SD of four animals. ACC mRNA levels were determined by RT-PCR. UCP-1, GMPr, and PGC-1α mRNA levels were determined by Northern blot, and the bands of interest were cut from the RNA-containing filter and counted in a liquid scintillation counter. The signal in each lane was corrected for RNA loading by the intensity of the 28S ribosomal RNA band. *$P < 0.05$ vs. the same time in WT animals by ANOVA. Hypothyroid mice are WT. This experiment was performed twice.

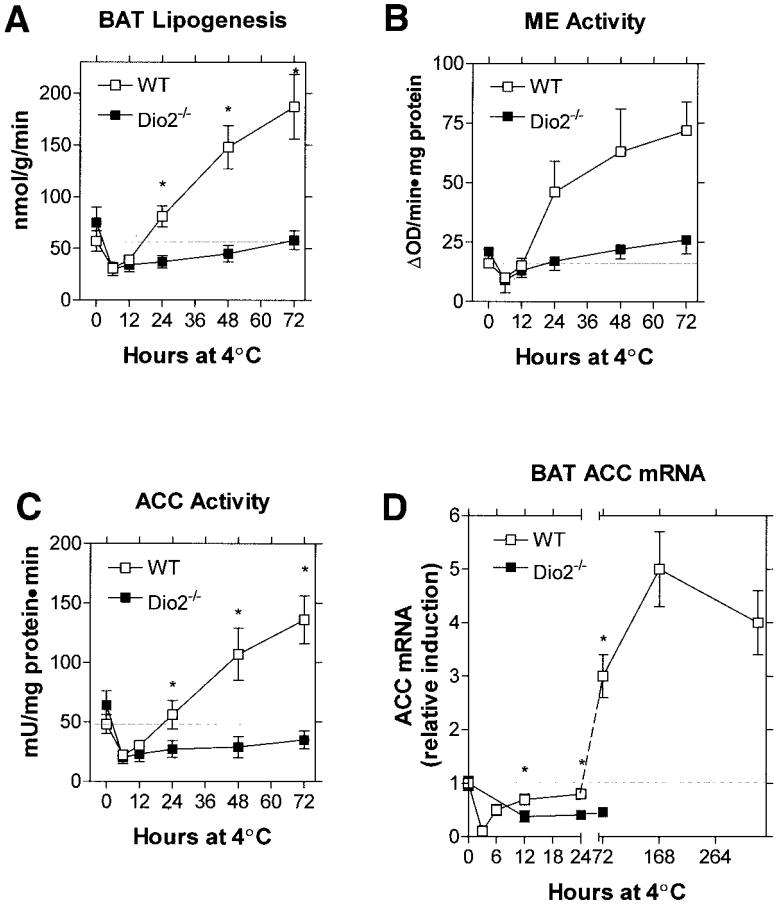

FIG. 4. Lipogenesis and lipogenic enzymes in the BAT of cold-exposed WT and Dio2$^{-/-}$ mice. *A*: Rates of BAT lipogenesis, as measured by incorporation of ^3H_2O into lipids. This experiment was performed twice. *B*: Activity of malic enzyme. *C*: Activity of ACC. *D*: ACC mRNA was measured by real-time PCR and expressed as changes in the ratio ACC/β-actin; values are the mean ± SD of three to four animals assayed twice in triplicate; **P* < 0.05 vs. WT animals at the same time point by ANOVA. The experiments were performed three to four times.

sustained NE stimulation prevents the otherwise potent T3 induction of ACC and Spot-14 mRNA in BAT.

De novo fatty acid synthesis is critical for thermal homeostasis. To test whether cold-induced lipogenesis is vital for sustained adaptive thermogenesis, WT mice were fed 0.25% (wt/wt) MEDICA-16 (or standard diet) for 5 days and then exposed to 4°C for 48 h. This regimen was previously shown to inhibit lipogenesis in liver and adipose tissue (17) and blocked >90% incorporation of ^3H_2O into IBAT lipids in our animals. Whereas standard diet–fed animals sustained their core temperature well throughout the experimental period in the cold, MEDICA-16–fed mice did so only during the first 24 h (Fig. 5*A*). By 48 h, a time at which lipogenesis is highly stimulated in cold-exposed animals (Fig. 4), MEDICA-16–fed mice presented hypothermia, with a core temperature ~1°C lower than WT animals (Fig. 5*A*). The perirenal white adipose tissue depot was dissected and weighed, and no differences were found between standard diet– and MEDICA-16–fed groups (data not shown), indicating that the length of the treatment was not sufficient to significantly decrease adiposity. Also, calorie intake was not affected by MEDICA-16 treatment (data not shown).

For testing the role of lipogenesis in BAT thermogenesis, this was assessed directly in MEDICA-16–fed normal mice by measuring changes in the IBAT temperature during infusion of NE in anesthetized mice, as described (19). Because the unstimulated BAT contains a substantial TG depot, all animals were first exposed to cold during 12 h to deplete the brown adipocytes of multilocular fat depots (Fig. 1). They were then moved to room temperature for 24 h to allow restoration of intracellular fat by de novo synthesis of fatty acids, a mechanism that is >90% suppressed in MEDICA-16–fed mice. The IBAT temperature of mice that were fed standard diet increased ~5°C, indicating a normal BAT thermal response (Fig. 5*B*). However, despite normal mitochondrial UCP-1 levels, the IBAT thermal response of mice that were fed MEDICA-16 was lower at every time point, remaining ~50% below the response observed in the control animals (Fig. 5*B*).

TABLE 3
ACC, Spot-14, and D2 mRNA levels in BAT of WT mice treated with T3 and/or NE

Enzyme mRNA	Saline	T3	NE	T3+NE
ACC	1.0 ± 0.3	1.8 ± 0.3*	0.7 ± 0.1*	1.2 ± 0.3
Spot-14	1.0 ± 0.4	2.3 ± 0.3*	0.7 ± 0.1*	1.3 ± 0.1
D2	1.0 ± 0.3	0.1 ± 0.1*	3.3 ± 0.4*	1.0 ± 0.4

Data are means ± SD of four animals. mRNA levels were determined by RT-PCR and corrected by β-actin mRNA. **P* < 0.05 vs. saline-treated animals by ANOVA. This experiment was performed twice.

DISCUSSION

The present investigation provides three new findings that shift the current paradigm about thyroid-adrenergic synergism and adaptive thermogenesis. First, brown adipocytes of Dio2$^{-/-}$ mice respond to sympathetic stimulation with respect to lipolysis and the activation of three cAMP-responsive genes (Figs. 1–3, Tables 1 and 2). Second, the D2-mediated adaptive increase in T3 production is not

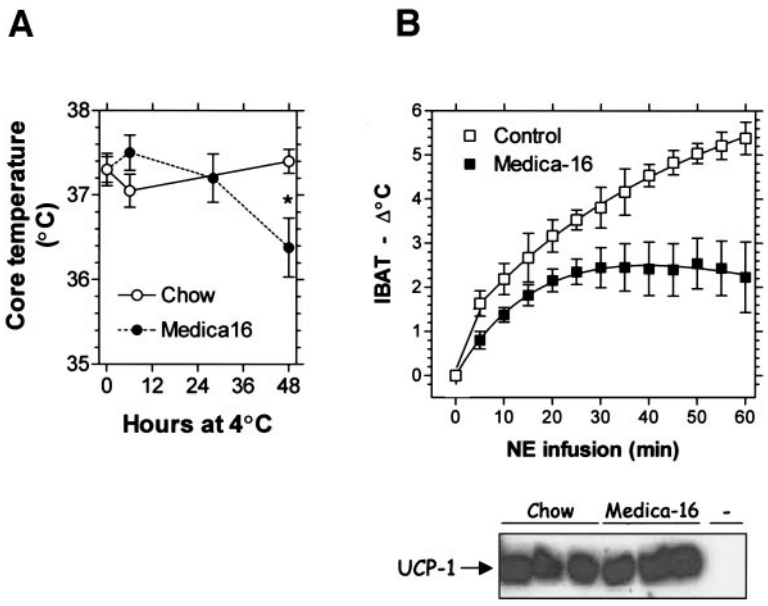

FIG. 5. Core temperature and IBAT thermal response to NE in MEDICA-16–fed WT mice. MEDICA-16 was added to the diet (0.25%), and after 5 days, animals were moved to 4°C; control animals were fed regular diet. *A*: Colonic temperatures were measured at the indicated times. *B*: IBAT temperatures were measured in anesthetized animals during infusion with NE; before NE infusion, all animals were cold-exposed for 12 h and moved to room temperature for the next 24 h. Values are the mean ± SD of four to five animals; *$P < 0.01$. Below is the Western analysis (performed as in ref. 13) of mitochondrial UCP-1 in the BAT of representative animals studied in *B*. −, a negative control. The experiments were performed twice.

critical for NE-induced increase UCP-1 gene expression (Fig. 3, Table 2). Third, the compensatory increase in adrenergic stimulation of Dio2$^{-/-}$ brown adipocytes causes intense lipolysis and prevents the normal increase in BAT lipogenesis observed during cold exposure, rapidly exhausting the availability of fatty acids (Fig. 4). Data obtained in animals that were fed an inhibitor of two key lipogenic enzymes (MEDICA-16) indicate that the de novo synthesis of fatty acids is a critical determinant of BAT thermogenesis (Fig. 5). Its suppression by increased NE stimulation (Fig. 3) explains the impaired adaptive thermogenesis and hypothermia in cold-exposed hypothyroid or Dio2$^{-/-}$ mice (13).

There is no question that hypothyroidism decreases sympathetic responsiveness in a number of tissues and cells, including heart and white and brown adipocytes, all of which produce less cAMP when incubated with a variety of adrenergic stimulators (7,8). Hypothyroid brown adipocytes, for example, produce ~10-fold less cAMP in response to NE or forskolin, supporting the connection between adrenergic insensitivity and cold-induced hypothermia (39). However, using electron microscopy and measuring the TG content and the activity of HSL, UCP-1, and other cAMP-dependent genes, we found that the poor adrenergic responsiveness is easily bypassed and even overcompensated by an increase in sympathetic activity in hypothyroid or Dio2$^{-/-}$ brown adipocytes (Figs. 1–3, Tables 1 and 2). Remarkably, despite reduced in vitro responsiveness to adrenergic stimulators (13), UCP-1 mRNA levels are three- to fourfold higher in the BAT of cold-exposed Dio2$^{-/-}$ animals than in the BAT of cold-exposed WT animals (Fig. 3). This is unexpected, particularly in light of previous observations that the normal increase in UCP-1 gene transcription and mRNA levels observed during acute cold exposure is blunted in hypothyroid rats (14,15) and mice (16) or by treatment with the D2 inhibitor iopanoic acid (40), and is restored by T3 in a dose-dependent manner until full occupation of TR is attained (14,41). These data indicate that the basal TR saturation of ~50% provided by serum T3 is sufficient to confer even super-normal adrenergic responsiveness to the UCP-1 gene. This minimizes the role of adaptive D2 activation in the control of UCP-1 activation in euthyroid mice. In addition, these data constitute the first evidence that decreased sympathetic responsiveness does not cause impaired adaptive thermogenesis in hypothyroid or Dio2$^{-/-}$ animals, indicating that other, as-yet-unrecognized T3-dependent mechanisms must play a pivotal role. This may also apply to other systems, e.g., heart and white adipose tissue, where there is thyroid-adrenergic synergism.

BAT lipogenesis is upregulated during cold acclimatization (38). The present studies show that this is preceded by an acute lipolytic phase during which lipogenesis is markedly inhibited (Fig. 4). The electron microscopy studies as well as the activity of key rate-limiting enzymes indicate that, in normal animals, lipolysis peaks at 12 h of cold exposure, a time at which lipogenesis is minimal and intracellular lipid droplets are not detectable. These events are rapidly followed by the surge in the activity of key lipogenic enzymes and the overall rate of lipogenesis, reaching levels three- to fourfold above normal between 72 and 96 h of continued cold exposure (Fig. 4). This is also illustrated by the reorganization of the lipid inclusions in the cytoplasm of the brown adipocytes (Fig. 1).

Two important physiological events explain the shift in predominance from lipolysis to lipogenesis, namely *1*) a reduction (although not to normal) in the BAT sympathetic stimulation (Fig. 3) and *2*) an increase in the BAT T3 as a result of D2-mediated local conversion of T4 to T3 (5).

That Dio2$^{-/-}$ brown adipocytes of cold-exposed animals enter and remain in the acute lipolytic phase without ever presenting the lipogenic surge (Figs. 2 and 4) indicates that an optimal balance between lipolysis and lipogenesis can be achieved successfully only as a result of the adaptive D2-catalyzed T3 production in these cells. Both the fall in sympathetic activity (Fig. 3) and the stimulation of lipogenesis (Fig. 4) are absent in the Dio2$^{-/-}$ BAT and therefore depend on the D2-mediated development of tissue-specific thyrotoxicosis during cold exposure. As a result, the brown adipocytes of these animals remain locked in the initial high NE-turnover phase in which lipolysis predominates and lipogenesis is suppressed, exhausting the

supply of fatty acids and limiting both the usefulness of β-oxidation as an energy source and the uncoupling process. In fact, the data indicate that sustained NE stimulation suppresses ACC and Spot-14 expression even in animals that had received a bolus injection of T3 to saturate TR.

Support for this hypothesis was obtained in experiments in which MEDICA-16 was used to block lipogenesis. On the basis of the profile of lipogenesis stimulation during cold exposure in normal animals, we anticipated that a blockade in this pathway would impair adaptive thermogenesis between 24 and 48 h. In fact, MEDICA-16–fed mice developed hypothermia after being in the cold for 48 h (Fig. 5*A*). Although MEDICA-16 blocks lipogenesis systemically, our direct measurements of IBAT temperature during NE infusion indicate that the blockade of fatty acid synthesis impairs BAT thermogenesis (Fig. 5*B*).

In conclusion, our data indicate that the decreased adrenergic responsiveness of Dio2$^{-/-}$ brown adipocytes (13) is successfully bypassed and even overcompensated by an increase in the SNS tonus, leading to an exaggerated and sustained lipolytic response, overexpression of cAMP-dependent genes, and suppression of genes encoding key lipogenic enzymes. Exhaustion of fatty acids in brown adipocytes rather than decreased sympathetic responsiveness is the cause of impaired adaptive thermogenesis and hypothermia in cold-exposed hypothyroid and Dio2$^{-/-}$ animals.

ACKNOWLEDGMENTS

This work was supported by research grants (97/13888-5) from the Fundação de Amparo a Pesquisa do Estado de São Paulo (FAPESP), the American Thyroid Association, and the National Institutes of Health (DK36256). C.L and L.M. were the recipients of grants from the Programa Institucional de Bolsas de Iniciação de Pesquisa Conselho Nacional de Pesquisa and K.N.E from FAPESP (98/14692-0). M.O.R. was the recipient of a grant from MackPesquisa.

We thank Dr. Jacob Bar-Tana (MEDICA-16) and Dr. Cary N. Mariash (Spot-14) for providing important reagents used in this study. We thank Gaspar Ferreira de Lima for skillful technical assistance in electron microscopy.

REFERENCES

1. Du Bois EF: Metabolism in exophthalmic goiter. *Arch Intern Med* 6:915–964, 1916
2. Swanson HE: Interrelations between thyroxin and adrenalin in the regulation of oxygen consumption in the albino rat. *Endocrinology* 59:217–225, 1956
3. Ring GC: The importance of the thyroid in maintaining an adequate production of heat during exposure to cold. *Am J Physiol* 137:582–588, 1942
4. Silva JE, Larsen PR: Adrenergic activation of triiodothyronine production in brown adipose tissue. *Nature* 305:712–713, 1983
5. Bianco AC, Silva JE: Cold exposure rapidly induces virtual saturation of brown adipose tissue nuclear T3 receptors. *Am J Physiol* 255:E496–E503, 1988
6. Sundin U, Mills I, Fain JN: Thyroid-catecholamine interactions in isolated rat brown adipocytes. *Metabolism* 33:1028–1033, 1984
7. Rubio A, Raasmaja A, Silva JE: Thyroid hormone and norepinephrine signaling in brown adipose tissue. II: Differential effects of thyroid hormone on beta 3-adrenergic receptors in brown and white adipose tissue. *Endocrinology* 136:3277–3284, 1995
8. Rubio A, Raasmaja A, Maia AL, Kim KR, Silva JE: Effects of thyroid hormone on norepinephrine signaling in brown adipose tissue I: beta 1- and beta 2-adrenergic receptors and cyclic adenosine 3′, 5′-monophosphate generation. *Endocrinology* 136:3267–3276, 1995
9. Bilezekian JP, Loeb JN: The influence of hyperthyroidism and hypothyroidism on the α- and β-adrenergic receptor system and adrenergic responsiveness. *Endocr Rev* 4:378–388, 1983
10. Silva JE: Catecholamines and the sympathoadrenal system in hypothyroidism. In *Werner & Ingbar's The Thyroid: A Fundamental and Clinical Text.* Braverman LE, Utiger RD, Eds. Philadelphia, Lippincott Williams & Wilkins, 2000, p. 820–823
11. Young JB, Saville E, Landsberg L: Effect of thyroid state on norepinephrine (NE) turnover in rat brown adipose tissue (BAT): potential importance of the pituitary (Abstract). *Clin Res* 32:407, 1982
12. Schneider MJ, Fiering SN, Pallud SE, Parlow AF, St. Germain DL, Galton VA: Targeted disruption of the type 2 selenodeiodinase gene (Dio2) results in a phenotype of pituitary resistance to T4. *Mol Endocrinol* 15:2137–2148, 2001
13. de Jesus LA, Carvalho SD, Ribeiro MO, Schneider M, Kim S-W, Harney JW, Larsen PR, Bianco AC: The type 2 iodothyronine deiodinase is essential for adaptive thermogenesis in brown adipose tissue. *J Clin Invest* 108:1379–1385, 2001
14. Bianco AC, Silva JE: Optimal response of key enzymes and uncoupling protein to cold in BAT depends on local T3 generation. *Am J Physiol* 253:E255–E263, 1987
15. Bianco AC, Silva JE: Intracellular conversion of thyroxine to triiodothyronine is required for the optimal thermogenic function of brown adipose tissue. *J Clin Invest* 79:295–300, 1987
16. Ribeiro MO, Carvalho SD, Schultz JJ, Chiellini G, Scanlan TS, Bianco AC, Brent GA: Thyroid hormone-sympathetic interaction and adaptive thermogenesis are thyroid hormone receptor isoform-specific. *J Clin Invest* 108:97–105, 2001
17. Bar-Tana J, Rose-Kahn G, Srebnik M: Inhibition of lipid synthesis by beta beta'-tetramethyl-substituted, C14–C22, alpha, omega-dicarboxylic acids in the rat in vivo. *J Biol Chem* 260:8404–8410, 1985
18. Carvalho SD, Negrao N, Bianco AC: Hormonal regulation of malic enzyme and glucose-6-phosphate dehydrogenase in brown adipose tissue. *Am J Physiol* 264:E874–E881, 1993
19. Ribeiro MO, Lebrun FL, Christoffolete MA, Branco M, Crescenzi A, Carvalho SD, Negrao N, Bianco AC: Evidence of UCP1-independent regulation of norepinephrine-induced thermogenesis in brown fat. *Am J Physiol Endocrinol Metab* 279:E314–E322, 2000
20. Levin BE: Reduced norepinephrine turnover in organs and brains of obesity-prone rats. *Am J Physiol Regul Integr Comp Physiol* 268:R389–R394, 1995
21. Kerr JF, Gobe GC, Winterford CM, Harmon BV: Anatomical methods in cell death. *Methods Cell Biol* 46:1–27, 1995
22. Hsu RY, Lardy HA, Cleland WW: Pigeon liver malic enzyme. V. Kinetic studies. *J Biol Chem* 242:5315–5322, 1967
23. Lee CY: Glucose-6-phosphate dehydrogenase from mouse. *Methods Enzymol* 89:252–257, 1982
24. Inoue H, Lowenstein JM: Acetyl coenzyme A carboxylase from rat liver: EC 6.4.1.2 acetyl-CoA: carbon dioxide ligase (ADP). *Methods Enzymol* 35:3–11, 1975
25. Bianco AC, Carvalho SD, Carvalho CR, Rabelo R, Moriscot AS: Thyroxine 5′-deiodination mediates norepinephrine-induced lipogenesis in dispersed brown adipocytes. *Endocrinology* 139:571–578, 1998
26. Shih MF, Taberner PV: Selective activation of brown adipocyte hormone-sensitive lipase and cAMP production in the mouse by beta 3-adrenoceptor agonists. *Biochem Pharmacol* 50:601–608, 1995
27. Nilsson-Ehle P, Schotz M: A stable, radioactive substrate emulsion for assay of lipoprotein lipase. *J Lipid Res* 17:536–541, 1976
28. Chomczynski P: Single-step isolation of RNA from cultured cells or tissues. In *Current Protocols in Molecular Biology.* 2nd ed. Ausubel FM, Brent R, Kingston RE, Moore DD, Seidman JG, Smith JA, Struhl K, Eds. New York, Wiley Interscience, 1995, p. 4.2.4–4.2.8
29. Kingston RE: Preparation and analysis of RNA. In *Current Protocols in Molecular Biology.* Aususbel FM, Brent R, Kingston RE, Moore DD, Seidman JG, Smith JA, Struhk K, Eds. New York, John Wiley & Sons, 1997, p. 4.9.1–4.9.16
30. Salvatore D, Bartha T, Larsen PR: The guanosine monophosphate reductase gene is conserved in rats and its expression increases rapidly in brown adipose tissue during cold exposure. *J Biol Chem* 273:31092–31096, 1998
31. Ginzinger DG: Gene quantification using real-time quantitative PCR: an emerging technology hits the mainstream. *Exp Hematol* 30:503–512, 2002
32. Relative quantitation of gene expression. In *User Bulletin #2.* Foster City, CA, Applied Biosystems/Perkin-Elmer Co., 1997, p. 1–36
33. Cameron IL, Smith RE: Cytological responses of brown fat tissue in cold-exposed rats. *J Cell Biol* 23:89–100, 1964

34. Suter ER: The fine structure of brown adipose tissue. I. Cold-induced changes in the rat. *J Ultrastruct Res* 26:216–241, 1969
35. Bouillaud F, Ricquier D, Mory G, Thibault J: Increased level of mRNA for the uncoupling protein in brown adipose tissue of rats during thermogenesis induced by cold exposure or norepinephrine infusion. *J Biol Chem* 259:11583–11586, 1984
36. Puigserver P, Wu Z, Park CW, Graves R, Wright M, Spiegelman BM: A cold-inducible coactivator of nuclear receptors linked to adaptive thermogenesis. *Cell* 92:829–839, 1998
37. Yu XX, Lewin DA, Forrest W, Adams SH: Cold elicits the simultaneous induction of fatty acid synthesis and beta-oxidation in murine brown adipose tissue: prediction from differential gene expression and confirmation in vivo. *FASEB J* 16:155–168, 2002
38. McCormack JG: The regulation of fatty acid synthesis in brown adipose tissue by insulin. *Prog Lipid Res* 21:195–223, 1982
39. Silva JE: Thyroid hormone control of thermogenesis and energy balance. *Thyroid* 5:481–492, 1995
40. Reiter RJ, Klaus S, Ebbinghaus C, Heldmaier G, Redlin U, Ricquier D, Vaughan MK, Steinlechner S: Inhibition of 5′-deiodination of thyroxine suppresses the cold-induced increase in brown adipose tissue messenger ribonucleic acid for mitochondrial uncoupling protein without influencing lipoprotein lipase activity. *Endocrinology* 126:2550–2554, 1990
41. Branco M, Ribeiro M, Negrao N, Bianco AC: 3, 5, 3′-Triiodothyronine actively stimulates UCP in brown fat under minimal sympathetic activity. *Am J Physiol* 276:E179–E187, 1999

VI – Quarto Artigo

Title

DIO2 GENE PROMOTES BROWN PRE-ADIPOCYTE TO ADIPOCYTE CONVERSION AND INCREASES OXIDATIVE CAPACITY

Authors:

Marcelo A. Christoffolete[1], Wagner Seixas da Silva[1], Michelle A. Mulcahey[2], Stephen A. Huang[2], Sandra C. Souza[3], Andrew S. Greenberg[3], Mary Elizabeth Patti[4] and Antonio C. Bianco[1]

Institutions:

[1]Thyroid Section, Division of Endocrinology Diabetes and Hypertension, Brigham and Women's Hospital and Harvard Medical School, Boston, MA 02115; [2]Division of Endocrinology, Children's Hospital Boston, Boston, MA 02115; [3]Jean Mayer United States Department of Agriculture Human Nutrition Research Center on Aging, Tufts University, Boston, MA 02111, [4]Research Division, Joslin Diabetes Center, Harvard Medical School, Boston, MA 02215

Running Title: Deiodination and brown adipocytes differentiation

Corresponding author:

Antonio C. Bianco, M.D. Ph.D.

Brigham and Women's Hospital

77 Avenue Louis Pasteur; HIM Bldg. #643; Boston MA 02115

Phone: 617-525-5153

Fax: 617-731 4718

email: abianco@partners.org

Resumo

O hormônio tiroideano é um componente crítico da termogênese adaptativa em adipócitos marrons. Nestas células, a sinalização do hormônio tiroideano é amplificada pela desiodase de iodotironina do tipo 2 (D2), uma enzima que ativa intracelularmente o T4, de baixa atividade, em sua forma completamente ativa, T3. Neste estudo nós usamos o modelo de conversão adiposa de pré-adipócitos marrons para demonstrar que adipócitos marrons *Dio2*$^{-/-}$ em diferenciação não ativam de maneira apropriada a expressão de genes que controlam o programa de diferenciação, PPARγ e C/EBPα. Como resultado, encontramos menos células adipócitas marrons maduras *Dio2*$^{-/-}$, elas acumulam menos gordura e apresentam capacidade oxidativa deficiente, indicando que o gene *Dio2* é um determinante chave da diferenciação de pré-adipócitos marrons.

Dio2 gene promotes brown pre-adipocyte to adipocyte conversion and increases oxidative capacity

Marcelo A. Christoffolete[1], Wagner Seixas da Silva[1], Michelle A. Mulcahey[2], Stephen A. Huang[2], Sandra C. Souza[3], Andrew S. Greenberg[3], Mary Elizabeth Patti[4] and Antonio C. Bianco[1]

[1]Thyroid Section, Division of Endocrinology Diabetes and Hypertension, Brigham and Women's Hospital and Harvard Medical School, Boston, MA 02115; [2]Division of Endocrinology, Children's Hospital Boston, Boston, MA 02115; [3]Jean Mayer United States Department of Agriculture Human Nutrition Research Center on Aging, Tufts University, Boston, MA 02111, [4]Research Division, Joslin Diabetes Center, Harvard Medical School, Boston, MA 02215

Running title: Deiodination and brown adipocytes differentiation

Correspondence:

Antonio C. Bianco, M.D. Ph.D.
Brigham and Women's Hospital
77 Avenue Louis Pasteur; HIM Bldg. #643; Boston MA 02115
Phone: 617-525-5153
fax: 617-731 4718
email: abianco@partners.org

Abstract

Thyroid hormone is a critical component of the adaptive thermogenesis in brown adipocytes. In these cells, thyroid hormone signaling is amplified by the type 2 iodothyronine deiodinase (D2), an enzyme that intracellularly activates the minimally active T4 to its fully active form, T3. Here we used the model of adipose conversion of pre-brown adipocytes to show that differentiating *Dio2*$^{-/-}$ brown adipocytes fail to properly activate the expression of genes that control the adipogenic differentiation program, PPARγ and C/EBPα. As a result, mature *Dio2*$^{-/-}$ brown adipocytes are fewer, accumulate less fat and have impaired oxidative capacity, indicating that *Dio2* is a key determinant of brown pre-adipocyte differentiation.

Introduction

Brown adipose tissue is a major site of adaptive thermogenesis in human newborns and other small mammals. Thermogenesis in this tissue is largely mediated by the uncoupling protein 1 (UCP1), which dissipates the mitochondrial proton-gradient without synthesis of ATP. While this process can be modulated by a number of metabolic signals, it is well accepted that the sympathetic nervous system is the master regulator of thermogenesis in the brown adipose tissue, with cAMP functioning as the key molecule that initiates lypolysis and mitochondrial uncoupling (Cannon and Nedergaard, 2004; Lowell and Spiegelman, 2000).

Thyroid hormone is one of the few truly potent stimulators of the metabolic rate and part of its effects on adaptive thermogenesis is mediated by synergism with the sympathetic nervous system in brown adipose tissue (Silva, 2006). Hypothyroid rodents exhibit severe cold intolerance as their brown adipose tissues fail to respond adequately to norepinephrine stimulation (Ribeiro et al., 2000; Ring, 1942). In fact, a major role for thyroid hormone in brown adipose tissue thermogenesis is explained by the fact that brown adipocytes can activate thyroid hormone by intracellularly converting T_4 to T_3 via the cAMP-inducible type 2 deiodinase (D2) (Bianco and Silva, 1987; Silva and Larsen, 1983). This mechanism, which is also present in the brain, allows for the amplification of the intensity of thyroid hormone signaling on a tissue specific basis. As expected, targeted disruption of the *Dio2* gene (*Dio2*$^{-/-}$) substantially impairs cAMP signaling and thermogenesis in brown adipocytes (de Jesus et al., 2001). As a result, maintenance of thermal homeostasis in cold-exposed *Dio2*$^{-/-}$ mice requires the activation of compensatory mechanisms, such as ~10-fold increase in sympathetic activity as well as shivering, preventing these animals from undergoing more serious hypothermia (Christoffolete et al., 2004).

The brown adipocyte phenotype resulting from *Dio2* inactivation confirms the obligatory requirement of a higher T_3 receptor saturation than that provided by T_3 in serum, via the D2-mediated intracellular activation of T_4. The severity of such phenotype, however, suggests that it could have evolved during differentiation of *Dio2*$^{-/-}$ brown preadipocytes. Here we used the model of adipose conversion of pre-brown adipocytes to show that differentiating *Dio2*$^{-/-}$ brown adipocytes fail to properly activate the expression of genes that control the adipogenic differentiation program, PPARγ and C/EBPα. As a result, mature *Dio2*$^{-/-}$ brown adipocytes are fewer, accumulate less fat and have impaired oxidative capacity, indicating that *Dio2* is a key determinant of brown preadipocyte differentiation.

Results

Dio2$^{-/-}$ brown adipocytes have impaired differentiation and oxidative capacity

Six days after plating in growth media (day 0) the differentiating brown adipocytes are confluent and the majority displays a fibroblast like morphology (pre-adipocyte) (Fig. 1A-a,b). Cells start to differentiate during the following days (Fig. 1A-c-f) and, approximately 10 days later, about half have become rounded and accumulate fat, as evidenced by Oil Red O staining (Fig. 1A-g-h), having acquired the typical multilocular brown adipocyte morphology (mature cells). These cells are also positive for perilipin (Fig. 1A-i-j) and the thyroid hormone inactivating deiodinase, D3, which is found in BODIPY, a neutral lipid fluorescent dye, positive cells (Fig. 1A-k-l). Mature *Dio2*$^{-/-}$ brown adipocytes are ~24 % fewer (Fig. 1B), ~17 % smaller (Fig. 1C) and accumulate ~25 % less Oil Red O per cell plate (Fig. 1D). In cell sonicates, perilipin was found to be reduced by ~40% in *Dio2*$^{-/-}$ brown adipocytes (Fig. 1E). *Dio2*$^{-/-}$ brown adipocytes contain ~40% less mitochondria, as assessed by the Cox1-2/Cox4 DNA ratio (Fig. 1F). Furthermore, when stimulated by forskolin, *Dio2*$^{-/-}$ brown adipocytes fail to increase oxygen (O_2) consumption, which is in contrast to the ~40% increase observed in wild type brown adipocytes (Fig. 1G).

At the end of the 10-day differentiation period, cells were sorted by flow cytometry using BODIPY (Fig. 2A). In each preparation two cell populations were obtained based on the fluorescence intensity: a non-brown adipocyte population in which BODIPY staining was about 30 FL units, close to that obtained in HEK-293 and COS-7 cells (~20 FL units), and a mature brown adipocyte population containing fat droplets in which fluorescence mean was 85-88 FL units (Fig. 2A-insets). Confirming the microscopy studies (Fig. 1), there were about 27% less mature Dio2$^{-/-}$ brown adipocytes than in wild type preparations (Fig. 2A). As expected, the expression of typical brown adipocyte genes by quantitative real time PCR (RT-qPCR) was enriched 2-7 fold as compared to pre-sorted cells, and did not reveal major differences between the two populations of brown adipocytes that had reached maturity (Fig. 2B). However, cell sorting based on fat content excludes brown adipocytes that might have limited capacity to synthesize and/or accumulate lipids, or other associated defects.

Gene expression profile in differentiating *Dio2*$^{-/-}$ brown adipocytes

The underlying mechanisms explaining the observed *Dio2*$^{-/-}$ brown adipocyte phenotype were investigated by studying the expression of key adipogenic genes at different times during differentiation by RT-qPCR (Fig. 3). These genes follow a general profile that is characterized by progressively higher levels of expression during the 10-day dif-

ferentiation period. During the first 4 days of differentiation only minor differences were observed between wild type and *Dio2*$^{-/-}$ brown adipocytes, namely a ~4-10-fold decrease in cytochrome oxidase 8b (COX8b) mRNA, a nuclear encoded gene expressed in heart, skeletal muscle and brown fat (Kadenbach et al., 1990) that is positively regulated by T_3 (Meehan and Kennedy, 1997) and 15-50% in COX4, cytosolic phosphoenolpyruvate dehydrogenase (PEPCKcyt) and Perilipin mRNA levels during days 2-4, and a ~1.5-3.4-fold increase in adiponectin, uncoupling protein 2 (UCP2), fatty acid binding protein 4 (ap2/FABP4), acetyl CoA-oxidase (ACO), CAAT/Enhancer Binding Protein α (C/EBPα), peroxisome proliferator-activated receptor γ2 (PPARγ2) and carnitine-palmytoyl acyltransfarese 1 (CPT-I) mRNA at day 2 (Fig. 3). At days 2-4, the levels of all the other mRNAs analyzed were undistinguishable between wild type and *Dio2*$^{-/-}$ brown adipocytes. Starting from day 6, the expression of several important genes lagged behind in the *Dio2*$^{-/-}$ brown adipocytes, including (i) the key regulators of adipogenesis, PPARγ2, C/EBPα, PPARγ coactivator 1α (PGC1α) and their down-stream targets: ap2/FABP4, perilipin, adiponectin, (ii) thermogenic capacity, PPARα, UCP1, UCP3, ACO, COX4, COX8b, succinate dehydrogenase, subunits b and d (SDHb and SDHd), and (iii) lipogenesis, sterol regulatory element binding protein 1c (SREBP1c), fatty acid synthase (FAS), acetyl CoA carboxylase 1 (ACC1) and PEPCKcyt (Fig. 3).

Gene expression profile in differentiated *Dio2*$^{-/-}$ brown adipocytes

Microarray technology was used to expand the gene expression profile of wild type and *Dio2*$^{-/-}$ brown adipocytes at the 10th day of differentiation. The hybridization signal of 3,593 probes was found to be significantly different ($p<0.05$) between wild type and *Dio2*$^{-/-}$ RNA samples. The analysis also included gene changes that were bellow the typical 0.5 and 2-fold magnitude because they could be grouped in sets of relevant and synergistic genes and their changes were found to be intrinsically coherent, consistent with major alterations in the flux through specific pathways (Subramanian et al., 2005). The use of the gene map annotator and pathway profiler (Genmapp) identified 24 biological pathways that were significantly down regulated in Dio2$^{-/-}$ brown adipocytes (Z scores between 13.1 – 4.6; adjusted $p<0.05$). These pathways were mostly involved in energy homeostasis, and could be grouped under mitochondrial-, electron transport chain- and tri-carboxylic acid (TCA) cycle-related genes (see Supplementary Information, Table 1).

Energy Homeostasis

TCA cycle and OXPHOS pathway: Most genes encoding proteins in these pathways were down-regulated in differentiated *Dio2*$^{-/-}$ brown adipocytes. The expression of at least one representative gene in each TCA cycle step was down-regulated in the Dio2$^{-/-}$

brown adipocytes (Table 1). Starting from the pyruvate conversion to acetyl-CoA, pyruvate dehydrogenase (lipoamide) subunit b (Pdhb) was ~30 % decreased. In the conversion of acetyl-CoA to citrate step, citrate synthase (CS) was ~25 % down-regulated. Aconitases 1 and 2 (Aco1 and Aco2), in the citrate to isocitrate inter-conversion step, were also ~25 % down-regulated. In the inter-conversion of isocitrate-α-ketoglutarate step, a ~15-25 % decrease in the mRNA levels of isocitrate dehydrogenase 2 (Idh2) and isocitrate dehydrogenase 3, subunits α, β and γ (Idh3α, β and γ) was observed. Dihydrolipoamide S-succinyltransferase (Dlt) and oxoglutarate dehydrogenase (Ogdh), in the α-ketoglutarate-succinyl-CoA inter-conversion step, were ~20-30 % down-regulated. The mRNA levels of the subunit α of Succinate-CoA ligase (Suclg 1), in the synthesis of succinate from succinyl-CoA step were ~20 % decreased. In the fumarate-malate inter-conversion step, fumarate hydratase (Fh1) expression was ~25 % down-regulated. In the final step of the cycle, malate dehydrogenase 1 and 2 (Mdh1 and 2) expression, enzymes that catalyse the malate-oxaloacetate inter-conversion, were ~20% down-regulated (Table 1).

There was a 10-30 % decrease in the expression of (i) 15 genes in complex I, (ii) two subunits of succinate dehydrogenase, part of complex II, (iii) four components of ubiquinol-cytochrome c reductase, part of complex III and (iv) ten subunits of cytochrome c oxidase and its assembly factor surfeit gene 1 (Surf1) (Williams et al., 2004), that are present in the complex IV (Table 1). The strongest down-regulated gene in this category is Cox8b, which is ~65 % decreased in Dio2$^{-/-}$ brown adipocytes.. In complex V, ten subunits of ATP synthase complexes FO/ F1 were also 10-30 % down-regulated (Table 1). Combined, these alterations are compatible with a major deficiency in the oxidative capacity in *Dio2*$^{-/-}$ brown adipocytes.

Lipid metabolism: Twenty-six genes in this category were down-regulated, of which 2 are involved in lipid transport and binding, 8 in lipogenesis, 4 in lipolysis and 12 in β-oxidation (Table 2). The ~80 % decrease in FABP3 gene expression (Table 2) combined with the 40 % down-regulation in ap2/FAPB4 (Fig. 2) may be particularly significant in these cells as these proteins have been proposed to affect metabolic resources and inflammatory response (Makowski and Hotamisligil, 2004). Furthermore, the 10-35 % decrease in genes encoding lipogenic proteins (Table 2) correlates well with the decreased levels of SREBP-1c mRNA (Fig. 2). These changes in lipogenic gene expression support the decreased lipid accumulation in *Dio2*$^{-/-}$ brown adipocytes (Fig. 1). At the same time, genes encoding lipoytic proteins were down-regulated by 20-85 % (Table 2), in agreement with the ~55 % down-regulation of PPARα mRNA levels (Fig. 2). The expression of β-oxidation related genes, another process down-stream of PPARα, was also down-regulated by 12-35 % (Table 2). These two process are important to ensure substrate availability during the thermogenic response, and combined to the ~55 % decrease in

UCP1 mRNA levels (Fig. 2) explain the blunted thermogenic response exhibited by *Dio2*$^{-/-}$ brown adipocytes (Fig. 1G).

Carbohydrate metabolism: In this category, genes related to the early steps of glycolysis were up-regulated by as much as 10-30 %, such as phosphoglycerate kinase 1 (Pgk1) and a phosphofructokinase (Pfkp) (Table 3). This is accompanied by a 30-60 % increase in the gene expression of enzymes involved in the early steps of glycogen breakdown, such as glycogen phosphorylase (Pygl) and phosphorylase kinase alpha 1 (Phka1) (Table 3). At the same time, genes encoding enzymes involved in glycogen synthesis, such as glycogenin 1 (Gyg1), glycogen synthase 3 (Gys3) and glucan branching enzyme 1 (Gbe1), were ~20 % down-regulated (Table 3). The expression of the lactate dehydrogenase 2 (Ladh2) gene, as well as that of the regulatory subunit 3c of protein phosphatase 1 (Ppp1r3c/PTG), which favors glycogen storage (Greenberg et al., 2003), were 55-60 % down-regulated in *Dio2*$^{-/-}$ brown adipocytes, respectively (Table 3). mRNA levels of glycerol-3-phosphate transporter 2 (Slc37a2), a glycerol-3-phosphate permease that is associated with increased rate of glycolysis (Bartoloni and Antonarakis, 2004), were ~2-fold up-regulated in *Dio2*$^{-/-}$ brown adipocytes (Table 3). The expression of monocarboxylic acid transporter (Slc16a3/MCT4), which is also associated with increased glycolysis rates, was ~6-fold up-regulated (Table 3). Slc16a3/MCT4 is strongly expressed in glycolytic tissues, regulating the transport across the plasma membrane of lactic acid produced in anaerobic conditions, also promoting glycolysis (Halestrap and Meredith, 2004). In *Dio2*$^{-/-}$ brown adipocytes, the gene expression of another member of the glycolytic pathway, aldolase 3, isoform C (Aldoc), which catalyzes the synthesis of glycerol 3 phosphate and dihydroxiacetone phosphate from fructose 1,6-biphosphate, was ~3.1 fold up-regulated. This pattern of expression suggests increased rate of glycolysis in *Dio2*$^{-/-}$ brown adipocytes.

Cell fate

Although not identified in the Genmapp analysis, examination of the microarray data reveals a pattern of gene expression compatible with changes in proliferation and differentiation in *Dio2*$^{-/-}$ brown adipocytes (Table 4). There was a 2-4 fold up-regulation in the gene expression of tumor necrosis factor receptor 1b (Tnfrs1b) and tumor growth factor β1 (TGFβ1), which repress differentiation in white and brown adipocytes (Porras et al., 1997; Porras et al., 2002; Teruel et al., 1996; Torti et al., 1989; Valladares et al., 2000). mRNA levels of Schlafen (Slfn2), a protein that when overexpressed prevents thymocytes from completing maturation (Schwarz et al., 1998), is up 4-fold in Dio2$^{-/-}$ brown adipocytes (Table 4). On the other hand, preadipocyte factor 1 (Pref-1) gene expression was repressed (~70 %) in *Dio2*$^{-/-}$ brown adipocytes. This gene is highly expressed in pre-adipocytes and functions as a negative modulator of adipogenesis (Harp,

2004). Its expression decreases during differentiation, being undetectable in mature cells.

While the data obtained so far indicate a tendency towards impaired differentiation in the *Dio2*$^{-/-}$ brown adipocytes, a clear up-regulation (2-4.3 fold) of genes that promote proliferation is also observed (Table 4). In the general pro-proliferation category there is retroviral integration site (Ris2/Cdt1), cyclinB2 (Ccnb2), cyclin-dependent kinase 6 (Cdk6), heterogeneous nuclear ribonucleoprotein A1 (Hnrpa1), deoxycytidine kinase (Dck), RAS related protein 1b and 2b (Rap1b and Rap2b), regenerating islet-derived 1 (Reg1) and proliferating cell nuclear antigen (Pcna). Additional genes specifically linked to adipocyte proliferation were also up-regulated in *Dio2*$^{-/-}$ brown adipocytes, such as RAB8B, a member of the RAS oncogene family (Rab8b), and insulin-like growth factor 1 (IGF-1). This increase in IGF-1 expression is likely to be potentiated by the ~50 % decrease in IGF binding proteins 3/5 (IGFBP 3/5), which is likely to increase of IGF-1 free fraction (Table 4).

Responsiveness of *Dio2*$^{-/-}$ brown adipocytes during days 8-10 of differentiation

Adrenergic stimulation

On the 8th day of differentiation brown adipocytes were exposed to the phosphodiasterase inhibitor IBMX for 48 h in order to increase endogenous cAMP signaling. This strategy avoided the reduced uptake of cAMP analogues in brown adipocytes and also bypassed the impaired forskolin-induced cAMP accumulation reported in *Dio2*$^{-/-}$ brown adipocytes (de Jesus et al., 2001). The analysis of key metabolic genes by RT-qPCR revealed that in response to adrenergic stimulation there was a 1.6-3.0-fold increase in ACC1, PGC1α and CPT-I mRNA levels, and a ~110-fold induction in the UCP1 gene expression in wild type brown adipocytes (Fig. 4A), whereas other genes were either unaffected or down-regulated. In general, the positively regulated genes were either unaffected or even down-regulated in stimulated *Dio2*$^{-/-}$ brown adipocytes such as ACC1, PGC1α and CPT-I, while the response of UCP1 was limited to ~30-fold (Fig. 4A). Both SREBP-1c and C/EBPα, which were unaffected by adrenergic stimulation in wild type cells, were 50-70 % down-regulated in *Dio2*$^{-/-}$ brown adipocytes. PPARγ2 was ~70% down-regulated in adrenergic stimulated *Dio2*$^{-/-}$ brown adipocytes, while its expression was ~40% suppressed in wild type brown adipocytes. Furthermore, FAS expression was ~70 % down-regulated in wild type brown adipocytes versus a 45 % down-regulation in *Dio2*$^{-/-}$ brown adipocytes. In contrast, ACO was ~8-fold induced only in the *Dio2*$^{-/-}$ brown adipocytes while COX-8b and ap2/FABP4, which had been suppressed in wild type cells, remained unaffected in *Dio2*$^{-/-}$ brown adipocytes (Fig. 4A).

Stimulation with T_3 and/or PPARs ligands

While all genes included in this profile are down-regulated in the *Dio2*$^{-/-}$ brown adipocytes, with the exception of CPT-I, treatment with T_3 had a positive regulation in the expression of some of these genes, such as ap2/FABP4, SREBP-1c, C/EBPα, PPARγ2, PGC1α, COX-8b and UCP2, although, only PPARγ2 expression was not statistically different from wild type levels. At the same time, treatment with T_3 induced UCP1 expression ~2-fold above the levels in untreated wild type cells (Fig. 4B). Treatment of *Dio2*$^{-/-}$ brown adipocytes with the PPARα selective agonist WY 14,643 resulted in a general increase in the mRNA of genes included in this profile without fully normalizing their expression or substantially affecting their responsiveness to T_3, with the exception of ap2/FABP4, adiponectin, ACC1, FAS, PPARα, C/EBPα, PGC1α, ACO and COX8b, which with WY 14,643 + T_3 treatment had their basal expression comparable to the untreated wild type levels. In contrast, PPARγ2 expression was fully normalized by WY 14,643 alone and the gene became unresponsive to T_3 (Fig. 4C). Treatment of *Dio2*$^{-/-}$ brown adipocytes with the PPARγ selective agonist rosiglitazone resulted in specific but marked changes in gene expression (Fig. 4D). For example, while basal expression of perilipin, adiponectin and COX-8b was normalized, ap2/FABP4, PPARα and ACO expression achieved levels 1.8-3.0-fold above wild type basal levels; basal levels of UCP1 were increased ~30-fold. In general, responsiveness to T_3 was abolished except for the ~90-fold stimulation of UCP1 mRNA levels (Fig. 4D).

Rescuing gene expression in differentiating *Dio2*$^{-/-}$ brown adipocytes

Induction with adipogenic cocktail

Next, we wished to test whether the alterations observed in the gene expression profile of *Dio2*$^{-/-}$ brown adipocytes could be restored by exposure to the potent adipogenic cocktail (IBMX, indomethacin and dexamethasone) during days 2-4 of differentiation. In general, induction with the cocktail substantially up-regulated gene expression in wild type brown adipocytes, except for UCP1, which was unexpectedly suppressed (Fig. 5A). In some cases the induction eliminated the differences between wild type and *Dio2*$^{-/-}$ brown adipocytes, such as for ap2/FABP4, ACC1, COX4 and C/EBPα, while in the remaining genes the differences were maintained. PPARδ was the only gene with a greater induction in the *Dio2*$^{-/-}$ brown adipocytes (Fig. 5A).

Induction with T_3

The attempt to rescue the gene expression profile of *Dio2*$^{-/-}$ brown adipocytes with thyroid hormone consisted of treatment with thyroid hormone receptor-saturating concen-

tration of T_3 during days 0-10 of differentiation. Most genes responded with substantial expression up-regulation that reached or surpassed wild type levels, except for perilipin, ap2/FABP4, FAS, PPARδ, COX-8b, UCP3 and UCP2 (Fig. 5B).

Discussion

Thyroid hormone is an adipogenic factor necessary for the conversion of pre-adipocyte to mature adipocyte (Dani et al., 1990; Darimont et al., 1993; Gharbi-Chihi et al., 1991; Gharbi-Chihi et al., 1993). Culturing Ob17 pre-adipocytes in thyroid hormone-stripped serum disrupts the expression profile of key adipogenic genes, flattening the normal induction of PPARγ, C/EBPδ and C/EBPα seen during differentiation, while mildly up-regulating the induction of PPARδ (Dace et al., 1999). In the present study we found that the additional T3 provided by the perinuclear activating D2 deiodinase is also critically important for brown adipocyte differentiation. In its absence, brown adipocytes are in average fewer (Fig. 1B), smaller (Fig. 1C) and hypometabolic (Fig. 1F-G), even in the presence of physiological amounts of thyroid hormone contained in the media. Using flow cytometry to sort the fully differentiated *Dio2*$^{-/-}$ brown adipocytes based on the fat content of individual cells, we confirmed that these cells were ~30% fewer (Fig. 2A) but had a gene expression profile that was almost normal. This indicates that D2 is mainly required for the conversion of pre-brown adipocyte to mature brown adipocyte, while not being so critical for the unstimulated gene expression in the cells that reach full differentiation. Further studies are necessary to clarify whether D2-generated T3 is critical for clonal expansion or terminal differentiation of pre-brown adipocytes.

In this brown pre-adipocyte conversion model, the critical relevance of D2 is probably heightened by the co-expression of the T3 inactivating deiodinase, D3, in these cells (Fig. 1A). Because D3 is located in the plasma membrane, expressing a perinuclear T3-generating enzyme (D2) is likely to avoid hypothyroidism at critical moments during the differentiation process. This is because D3 has high affinity for T3 but has ten fold less affinity for T4, which allows access to the cytosol and intracellular activation to T3 via D2. In fact, the orchestrated expression of D3 and D2 in these cells during differentiation makes this system an ideal one to study the role of these enzymes in thyroid hormone signaling. At the moment no immortalized brown adipocyte cell line maintained such elaborate system to control thyroid hormone action, directing us to the study of primary cultures of brown adipocytes precursors. One potential problem with such a system is the contamination with non-adipocyte precursor cells, which is difficult to avoid or quantify (Fig. 2). However, because D2 expression is restricted to brown adipocytes, its knock out is not expected to affect other local cell types. In addition, the defects in gene expression observed in mixed populations of *Dio2*$^{-/-}$ brown adipocytes were not present until the forth or sixth day of differentiation (Fig. 3), indicating that cellular composition was not different between wild type and *Dio2*$^{-/-}$ brown adipocytes at the beginning of the differentiation period.

The examination of the expression levels of adipogenic related genes in mixed cultures of mature *Dio2*$^{-/-}$ brown adipocytes revealed progressive impairment in the expression of master genes that control the adipogenic differentiation program, e.g. PPARγ2, C/EBPα, PPARα, PGC1α, as well as many of their down stream targets, e.g. ap2/FABP4, perilipin, adiponectin, UCP1, UCP3, ACO, COX4, COX8b, SDH, SREBP1c, FAS, ACC1 and PEPCKcyt (Fig. 3). This list of downstream genes was expanded in subsequent microarray studies with the identification of thousands of genes with defective expression in the *Dio2*$^{-/-}$, involved in TCA and OXPHOS pathway, glucose homeostasis and lipogenesis (Tables 1-4). While this profile partially resembles that found in Ob17 preadipocytes cultured in thyroid hormone-stripped serum, it does not indicate that the master genes and/or their downstream targets are necessarily responsive to T3 as this expression pattern could be due to a global impairment in the differentiation process. Nevertheless, given that the brown pre-adipocyte conversion model evolves in the presence of 10% FBS, which ensures cell exposure to normal concentrations of thyroid hormones, it is clear that the additional amplification of the thyroid hormone signaling via the D2 pathway is a critical step for the conversion of brown pre-adipocytes to brown adipocytes.

Forskolin-stimulated oxygen consumption is impaired in cultures of mixed mature *Dio2*$^{-/-}$ brown adipocytes (Fig. 1G), indicating that adrenergic-induced adaptive thermogenesis is impaired in these cells. To characterize the underlying mechanisms of this defect and bypass any defect in the cAMP generation that could have resulted from D2 KO, we analyzed the expression of key genes in response to IBMX, which amplifies the unstimulated cAMP signaling. While the response of about 60% of the genes was normal or even slightly increased in the Dio2$^{-/-}$ brown adipocytes, 40% of the genes failed to respond adequately to IBMX exposure (Fig. 4A), revealing that the adrenergic inducibility of a selective group of genes is impaired in these cells. Except for two, all the other genes failed to respond to T3 exposure, remaining well below normal levels of expression (Fig. 4B). This indicates that although the defect in brown pre-adipocyte differentiation is caused by insufficient T3, after the cells have fully differentiated the defective gene expression profile is not correctable by T3 alone. In fact, response to T3 was amplified and the expression of some genes normalized if the mature *Dio2*$^{-/-}$ brown adipocytes were also exposed to the PPARα selective agonist, WY 14,643 (Fig. 4C), or even increased above normal if these mature cells were exposed to the PPARγ selective agonist, rosiglitazone (Fig. 4D).

In an attempt to rescue the *Dio2*$^{-/-}$ brown adipocytes phenotype, *Dio2*$^{-/-}$ brown preadipocytes were treated during differentiation with the adipogenic cocktail or T3, and analyzed after they reached the status of mature cells. Remarkably, while the adipogenic cocktail increased 2-4-fold the expression of a number of key genes, the differ-

ences between the wild type and *Dio2*$^{-/-}$ brown adipocytes remained for most genes (Fig. 5A). Even treatment with T3 during the differentiation period did not fully restore the gene expression profile of *Dio2*$^{-/-}$ brown adipocytes, although it improved substantially. Taken together, these data strongly indicate that exposure to D2-generated T3 must occur at a specific timing during brown pre-adipocyte differentiation without which severe deficiencies in basal and/or stimulated gene expression will result.

The present studies indicate that thyroid hormone signaling as amplified by D2 is critical for brown pre-adipocyte differentiation. *Dio2*$^{-/-}$ brown adipocytes fail to properly activate the expression of genes that control the adipogenic differentiation program, as well as key downstream genes involved in energy homeostasis. As a result, mature *Dio2*$^{-/-}$ brown adipocytes are fewer, accumulate less fat and have impaired oxidative capacity, identifying *Dio2* as a key determinant of the brown pre-adipocyte differentiation program.

Experimental Procedures

Chemicals and Drugs

Rosiglitazone was from GlaxoSmithKline (Research Triangle Park, NC). Ascorbic acid, HEPES, tetracycline, streptomycin, ampycilin, indomethacin, dexametasone, isobutyl-methylxanthine (IBMX), WY 14,643, thyroxine (T4), 3, 5, 3' triiodothyronine (T3), 3, 5', 3' triiodothyronine (rT3) and sodium selenite (Se) were purchased from Sigma-Aldrich (St. Louis, MO). Insulin was purchased from Novo Nordisk (Bagsvaerd, Denmark). Fungizone, D-MEM, Oil Red O, chicken serum and ANTI-FADEGold with DAPI were from Invitrogen (Carlsbad, CA).

Animals

All studies were performed under a protocol approved by the Standing Committee on Animal Research. The original *Dio2*$^{-/-}$ mice were backcrossed with C57BL/6J wild type animals for five generations, yielding a 96.9% C57BL/6J background, being referred as *Dio2*$^{-/-}$. C57BL/6J wild type mice (WT) were purchased from The Jackson Laboratories (Bar Harbor, MA).

Brown pre-adipocytes isolation and cell culture

Fifteen to 20 animals were killed per experiment and interscapular brown fat quickly dissected and processed as previously described (Martinez-deMena et al., 2002). Cells were grown in D-MEM + 10% FBS, supplemented with 10mM HEPES, 10^{-7}M sodium selenite, 3nM insulin, 15 μM ascorbic acid, 25mg/L tetracycline, 25mg/L streptomycin, 25mg/L ampicylin and 1mg/L fungizone. The precursor cells were initially plated in 25 cm^2 flasks, after 3 days transferred to a 75 cm^2 flasks then, 2 days later, plated in 60mm dishes or 35 mm dishes, for RNA or ORO/protein studies, at 15-20,000 cells/cm^2. Cells were let differentiate for additional 10 days. In order to boost differentiation, a potent adipogenic cocktail (Klein et al., 2000) consisting of indomethacin (125 μM), IBMX (0.5 mM) and dexamethasone (0.5 μM), was used in indicated experiments.

OIL Red O staining and analysis

Cells were allowed to differentiate for 10 days. OIL Red O Staining was performed as described (Koopman et al., 2001). Pictures were taken in a CKX41 Culture microscope (Olympus, Melvile, NY) and analyzed in Adobe Photoshop Elements 2.0 (Adobe, San

Jose, CA). Oil Red O in the plates was eluted in DMSO and absorbance performed in smartspec (BioRad, Richmond CA) spectrophotometer at 535nM wavelength.

RT – qPCR

Total RNA was extracted using the Trizol or Trizol-LS (sorted cells) method. For the reverse transcriptase reaction 1.5-3 μg of total RNA was used in the SuperScrit™ First-Strand Synthesis System for RT-PCR (Invitrogen) on Robocycler thermocycler (Stratagene, La Rolla CA). For mitochondrial DNA content, DNA was recovered from the interfase during the Trizol RNA isolation and processed as described in the manufacture's protocol. 18ng of total DNA was used for amplification. Real time PCR was performed using IQ™ SYBR® Green PCR kit (BioRad), using specific primers, based on the literature (Kalaany et al., 2005) or designed using Beacon Designer 3.0 (Premiere Biosoft Intl., Palo Alto, CA), available upon request, having cyclophilin B as the housekeep gene. The cycle conditions were: 5 min at 94°C (Hot Start); 30s at 94°C, 30s at 58°C and 45s at 72°C for 50 cycles followed by the melting curve protocol to verify the specificity of amplicon generation. Gene expression was determined by ΔCT method.

Deiodinase assays

Measurement of D2 and D3 activities were performed as described elsewhere (Christoffolete et al., 2006).

Microarray analysis

Total RNA (8 μg), extracted using the Trizol protocol followed by digestion with DNAseI (Invitrogen) and re-extracted with Trizol, was submitted to microarray analysis at the Dana-Farber Cancer Institute Microarray Core Facility, Boston, MA, using Affimatrix chip MOE430 2.0. Data obtained was entered in the dCHIP software (http://biosun1.harvard.edu/complab/dchip/manual.htm - Dana Farber Group) according to the developer's manual. Comparison between wild type and *Dio2*$^{-/-}$ samples was performed and only genes statically different ($p<0.05$) were selected, regardless the fold difference. This strategy allows a wide approach to spot trends of alterations in different pathways. The total number of genes obtained from our array was loaded into the gene map annotator and pathway profiler – Genmapp (www.genmapp.org) and only genes with statistically different expression where selected, generating the starting point for pathway-based analysis of our gene-expression data.

Immunofluorescence microscopy

After the differentiation period, cells were treated with tripsin and replated at lower confluence in 35 mm bottom glass plates (MatTek Corporation, Ashland, MA). After 24h, fixation was performed with 10% formalin in PBS for 30 minutes, washed in glycine buffer (100 mM glycine, pH 7.4), permeabilized in 0.1% TRITON X-100 in PBS for 10 minutes, incubated for 30 minutes in anti-body buffer (SSC 1x, 2% chicken or goat serum, 1% BSA, 0.05% TRITON X-100, 0.02% sodium azide and 0.1g/L Saponin), incubated overnight with 1st anti-bodies diluted in anti-body buffer at 4ºC, washed 3x with anti-body wash buffer (SSC 1x and 0.05% TRITON X-100) for 5 minutes, incubated with 2nd anti-body diluted in anti-body buffer for 1h at 4°C, washed 3x with washing buffer for 5 minutes. For BODIPY 493/503 (Invitrogen) staining, cells were incubated with anti-body buffer containing BODIPY (1 μg/mL) for 20 min at 4°C and washed 3x with washing buffer for 5 minutes. ANTI-FADEGold with DAPI (Invitrogen) was added to the samples and covered with glass coverslip and mounted using nail polish. Samples were cured for 24 h and then visualized. Images were acquired with ZEISS LSM META 510 (Carl Zeiss, Oberkochen, Germany) confocal microscope at the Harvard Center for Neurodegeneration and Repair (HCNR) Confocal Core Facility, Boston, MA.

Western Blot

Proteins were extracted as described previously (Souza et al., 1998) and quantified using the BCA protein assay from Pierce (Rockford, IL). Total lysates were separated in 10% acrylamide pre-cast gel (BioRad), transferred to nitrocellulose membrane and blotted as described elsewhere (Souza et al., 1998).

Antibodies

Primary antibodies: anti-actin (A5060) was from Sigma-Aldrich, specific polyclonal anti-rabbit Peri A antibody (PREK antibody) was generated using the peptide PREK-PARRVSDSFFRPSVC (Souza et al., 2002), anti-D3 was a gift from Dr. Domenico Salvatore (Università di Napoli, Naples, Italy). Secondary antibodies for immunofluorescence studies: chicken anti-rabbit ALEXA647 (A21443) and goat anti-rabbit ALEXA488 (A11070) were from Invitrogen. Secondary antibody for western blot: donkey anti-rabbit (NA934V) from GE Healthcare (Little Chalfont, Buckinghamshire, England).

Flow cytometry cell sorting

Wild type and *Dio2*$^{-/-}$ cells differentiated for 10 days were treated with trypsin, ressuspended in growth media, centrifuged briefly and both the upper layer of supernatant (2mL) and cell pellet were mixed together with BODIPY493/503 (6 ng/mL) containing PBS for 5 minutes at room temperature, centrifuged briefly and upper layer of super-

natant and cell pellet ressuspended together in PBS (3mL). Cells were sorted in Dako-Cytomation MoFlo (Dako North America, Inc., Carpinteria, CA) using the FL1 channel (488nm excitation and 515nm emission) at the Dana-Farber Cancer Institute Flow Cytometry Core Facility, Boston, MA, and separated as positive and negative for BOPIDY staining. The distinct populations were submitted to total RNA preparation and RT-qPCR analysis.

Cellular O_2 consumption

Ten days differentiated wild type and *Dio2*$^{-/-}$ brown adipocytes were seeded at the same density in 24-well microplates. Cells were assayed in the XF24 instrument from Seahorse Bioscience (Billerica, MA) to perform non-destructive, time-resolved measurements of O_2 consumption rate as described elsewhere (Watanabe et al., 2006). Immediately before measurement, medium was replaced with non-buffered pH 7.4 medium. Three successive 4 min measurements were performed simultaneously at 2-min intervals to obtain baseline respiratory rate followed by increasing concentrations of Forskolin administered in 5 minutes interval and measured for 4 min. The rate of O_2 consumption was then expressed as fold stimulation in comparison to the baseline rate.

Statistical analysis

All data were analyzed using PRISM software (GraphPad Software, Inc, San Diego, CA) and is expressed as mean ± SEM. Student's t-test was used for gene screening comparisons; Gaussian distribution was used to illustrate the cell area distribution.

Acknowledgements

We would like to acknowledge Jack Y. Lee and Christine Knoblauch for assistance in cell preparation for FACS analysis. These studies were supported by DK65055.

References

Bartoloni, L., and Antonarakis, S. E. (2004). The human sugar-phosphate/phosphate exchanger family SLC37. Pflugers Archiv - European Journal of Physiology *447*, 780-783.

Bianco, A. C., and Silva, J. E. (1987). Intracellular conversion of thyroxine to triiodothyronine is required for the optimal thermogenic function of brown adipose tissue. J Clin Invest *79*, 295-300.

Cannon, B., and Nedergaard, J. (2004). Brown adipose tissue: function and physiological significance. Physiol Rev *84*, 277-359.

Christoffolete, M. A., Linardi, C. C. G., de Jesus, L. A., Ebina, K. N., Carvalho, S. D., Ribeiro, M. O., Rabelo, R., Curcio, C., Martins, L., Kimura, E. T., and Bianco, A. C. (2004). Mice with targeted disruption of the Dio2 gene have cold-induced overexpression of uncoupling protein 1 gene but fail to increase brown adiose tissue lipogenesis and adaptive thermogenesis. Diabetes *53*, 577-584.

Christoffolete, M. A., Ribeiro, R., Singru, P., Fekete, C., da Silva, W. S., Gordon, D. F., Huang, S. A., Crescenzi, A., Harney, J. W., Ridgway, E. C., *et al.* (2006). Atypical expression of type 2 iodothyronine deiodinase in thyrotrophs explains the thyroxine-mediated pituitary TSH feedback mechanism. Endocrinology *in press*.

Dace, A., Sarkissian, G., Schneider, L., Martin-El Yazidi, C., Bonne, J., Margotat, A., Planells, R., and Torresani, J. (1999). Transient expression of c-erbAbeta1 messenger ribonucleic acid and beta1 thyroid hormone receptor early in adipogenesis of Ob 17 cells. Endocrinology *140*, 2983-2990.

Dani, C., Amri, E. Z., Bertrand, B., Enerback, S., Bjursell, G., Grimaldi, P., and Ailhaud, G. (1990). Expression and regulation of pOb24 and lipoprotein lipase genes during adipose conversion. J Cell Biochem *43*, 103-110.

Darimont, C., Gaillard, D., Ailhaud, G., and Negrel, R. (1993). Terminal differentiation of mouse preadipocyte cells: adipogenic and antimitogenic role of triiodothyronine. Mol Cell Endocrinol *98*, 67-73.

de Jesus, L. A., Carvalho, S. D., Ribeiro, M. O., Schneider, M., Kim, S.-W., Harney, J. W., Larsen, P. R., and Bianco, A. C. (2001). The type 2 iodothyronine deiodinase is essential for adaptive thermogenesis in brown adipose tissue. J Clin Invest *108*, 1379-1385.

Gharbi-Chihi, J., Facchinetti, T., Berge-Lefranc, J. L., Bonne, J., and Torresani, J. (1991). Triiodothyronine control of ATP-citrate lyase and malic enzyme during differentiation of a murine preadipocyte cell line. Horm Metab Res *23*, 423-427.

Gharbi-Chihi, J., Teboul, M., Bismuth, J., Bonne, J., and Torresani, J. (1993). Increase of adipose differentiation by hypolipidemic fibrate drugs in Ob 17 preadipocytes: requirement for thyroid hormones. Biochim Biophys Acta *1177*, 8-14.

Greenberg, C. C., Meredith, K. N., Yan, L., and Brady, M. J. (2003). Protein targeting to glycogen overexpression results in the specific enhancement of glycogen storage in 3T3-L1 adipocytes. Journal of Biological Chemistry *278*, 30835-30842.

Halestrap, A. P., and Meredith, D. (2004). The SLC16 gene family-from monocarboxylate transporters (MCTs) to aromatic amino acid transporters and beyond. Pflugers Archiv - European Journal of Physiology *447*, 619-628.

Harp, J. B. (2004). New insights into inhibitors of adipogenesis. Current Opinion in Lipidology *15*, 303-307.

Kadenbach, B., Stroh, A., Becker, A., Eckerskorn, C., and Lottspeich, F. (1990). Tissue- and species-specific expression of cytochrome c oxidase isozymes in vertebrates. Biochimica et Biophysica Acta *1015*, 368-372.
Kalaany, N. Y., Gauthier, K. C., Zavacki, A. M., Mammen, P. P., Kitazume, T., Peterson, J. A., Horton, J. D., Garry, D. J., Bianco, A. C., and Mangelsdorf, D. J. (2005). LXRx regulate the balance between fat storage and oxidation. Cell Metabolism *1*, 231-244.
Klein, J., Fasshauer, M., Benito, M., and Kahn, C. R. (2000). Insulin and the beta3-adrenoceptor differentially regulate uncoupling protein-1 expression. ME *14*, 764-773.
Koopman, R., Schaart, G., and Hesselink, M. K. (2001). Optimisation of oil red O staining permits combination with immunofluorescence and automated quantification of lipids. Histochemistry & Cell Biology *116*, 63-68.
Lowell, B. B., and Spiegelman, B. M. (2000). Towards a molecular understanding of adaptive thermogenesis. Nature *404*, 652-660.
Makowski, L., and Hotamisligil, G. S. (2004). Fatty acid binding proteins--the evolutionary crossroads of inflammatory and metabolic responses. Journal of Nutrition *134*, 2464S-2468S.
Martinez-deMena, R., Hernandez, A., and Obregon, M. J. (2002). Triiodothyronine is required for the stimulation of type II 5'-deiodinase mRNA in rat brown adipocytes. American Journal of Physiology - Endocrinology & Metabolism *282*, E1119-1127.
Meehan, J., and Kennedy, J. M. (1997). Influence of thyroid hormone on the tissue-specific expression of cytochrome c oxidase isoforms during cardiac development. Biochemical Journal *327*, 155-160.
Porras, A., Alvarez, A. M., Valladares, A., and Benito, M. (1997). TNF-alpha induces apoptosis in rat fetal brown adipocytes in primary culture. FEBS Letters *416*, 324-328.
Porras, A., Valladares, A., Alvarez, A. M., Roncero, C., and Benito, M. (2002). Differential role of PPAR gamma in the regulation of UCP-1 and adipogenesis by TNF-alpha in brown adipocytes. FEBS Letters *520*, 58-62.
Ribeiro, M. O., Lebrun, F. L., Christoffolete, M. A., Branco, M., Crescenzi, A., Carvalho, S. D., Negrao, N., and Bianco, A. C. (2000). Evidence of UCP1-independent regulation of norepinephrine-induced thermogenesis in brown fat. Am J Physiol Endocrinol Metab *279*, E314-322.
Ring, G. C. (1942). The importance of the thyroid in maintaining an adequate production of heat during exposure to cold. Am J Physiol *137*, 582-588.
Schwarz, D. A., Katayama, C. D., and Hedrick, S. M. (1998). Schlafen, a new family of growth regulatory genes that affect thymocyte development. Immunity *9*, 657-668.
Silva, J. E. (2006). Thermogenic mechanisms and their hormonal regulation. Physiol Rev *86*, 435-464.
Silva, J. E., and Larsen, P. R. (1983). Adrenergic activation of triiodothyronine production in brown adipose tissue. Nature *305*, 712-713.
Souza, S. C., Muliro, K. V., Liscum, L., Lien, P., Yamamoto, M. T., Schaffer, J. E., Dallal, G. E., Wang, X., Kraemer, F. B., Obin, M., and Greenberg, A. S. (2002). Modulation of hormone-sensitive lipase and protein kinase A-mediated lipolysis by perilipin A in an adenoviral reconstituted system. Journal of Biological Chemistry *277*, 8267-8272.
Souza, S. C., Yamamoto, M. T., Franciosa, M. D., Lien, P., and Greenberg, A. S. (1998). BRL 49653 blocks the lipolytic actions of tumor necrosis factor-alpha: a potential new insulin-sensitizing mechanism for thiazolidinediones. Diabetes *47*, 691-695.

Subramanian, A., Tamayo, P., Mootha, V. K., Mukherjee, S., Ebert, B. L., Gillette, M. A., Paulovich, A., Pomeroy, S. L., Golub, T. R., Lander, E. S., and Mesirov, J. P. (2005). Gene set enrichment analysis: a knowledge-based approach for interpreting genome-wide expression profiles.[see comment]. Proceedings of the National Academy of Sciences of the United States of America *102*, 15545-15550.

Teruel, T., Valverde, A. M., Benito, M., and Lorenzo, M. (1996). Transforming growth factor beta 1 induces mitogenesis in fetal rat brown adipocytes. Journal of Cellular Physiology *166*, 577-584.

Torti, F. M., Torti, S. V., Larrick, J. W., and Ringold, G. M. (1989). Modulation of adipocyte differentiation by tumor necrosis factor and transforming growth factor beta. Journal of Cell Biology *108*, 1105-1113.

Valladares, A., Alvarez, A. M., Ventura, J. J., Roncero, C., Benito, M., and Porras, A. (2000). p38 mitogen-activated protein kinase mediates tumor necrosis factor-alpha-induced apoptosis in rat fetal brown adipocytes. Endocrinology *141*, 4383-4395.

Watanabe, M., Houten, S. M., Mataki, C., Christoffolete, M. A., Kim, B. W., Sato, H., Messaddeq, N., Harney, J. W., Ezaki, O., Kodama, T., *et al.* (2006). Bile acids induce energy expenditure by promoting intracellular thyroid hormone activation. Nature *439*, 484-489.

Williams, S. L., Valnot, I., Rustin, P., and Taanman, J. W. (2004). Cytochrome c oxidase subassemblies in fibroblast cultures from patients carrying mutations in COX10, SCO1, or SURF1. Journal of Biological Chemistry *279*, 7462-7469.

Table 1 - Basal mRNA levels of genes involved in energy homeostasis in differentiated wild type and *Dio2*$^{-/-}$ brown adipocytes.

Gene Annotation	Gene symbol	WT mean ± sem	n	*Dio2*$^{-/-}$ mean ± sem	n	Ratio *Dio2*$^{-/-}$/WT	P value
TCA cycle							
dihydrolipoamide S-succinyltransferase (E2 component)	Dlst	1010 ± 16	3	711 ± 33	3	**0.70**	0.004
pyruvate dehydrogenase (lipoamide) beta	Pdhb	3032 ± 51	3	2160 ± 56	3	**0.71**	0.000
isocitrate dehydrogenase 3 (NAD+) alpha	Idh3a	1426 ± 33	3	1086 ± 50	3	**0.76**	0.007
aconitase 2, mitochondrial	Aco2	1949 ± 79	3	1434 ± 79	3	**0.74**	0.010
citrate synthase	Cs	1538 ± 103	3	1135 ± 78	3	**0.74**	0.039
fumarate hydratase 1	Fh1	1071 ± 24	3	799 ± 23	3	**0.75**	0.001
aconitase 1	Aco1	526 ± 17	3	396 ± 18	3	**0.75**	0.006
succinate-CoA ligase, GDP-forming, alpha subunit	Suclg1	1365 ± 42	3	1070 ± 34	3	**0.78**	0.006
oxoglutarate dehydrogenase (lipoamide)	Ogdh	1199 ± 46	3	952 ± 42	3	**0.79**	0.016
malate dehydrogenase 1, NAD (soluble)	Mdh1	2280 ± 64	3	1850 ± 24	3	**0.81**	0.013
malate dehydrogenase 2, NAD (mitochondrial)	Mdh2	3237 ± 56	3	2642 ± 105	3	**0.82**	0.015
isocitrate dehydrogenase 2 (NADP+), mitochondrial	Idh2	694 ± 17	3	578 ± 17	3	**0.83**	0.008
isocitrate dehydrogenase 3 (NAD+) beta	Idh3b	1281 ± 20	3	1072 ± 41	3	**0.84**	0.021
isocitrate dehydrogenase 3 (NAD+), gamma	Idh3g	2079 ± 47	3	1743 ± 54	3	**0.84**	0.010
Complex I							
NADH dehydrogenase (ubiquinone) 1 beta subcomplex, 9	Ndufb9	2898 ± 56	3	2123 ± 87	3	**0.73**	0.003
NADH dehydrogenase (ubiquinone) 1 alpha subcomplex 10	Ndufa10	76 ± 5	3	57 ± 5	3	**0.75**	0.050
NADH dehydrogenase (ubiquinone) 1 alpha subcomplex, 5	Ndufa5	599 ± 20	3	450 ± 15	3	**0.75**	0.005
NADH dehydrogenase (ubiquinone) 1 beta subcomplex, 10	Ndufb10	1630 ± 28	3	1248 ± 40	3	**0.77**	0.002
NADH dehydrogenase (ubiquinone) 1 beta subcomplex, 2	Ndufb2	1093 ± 25	3	843 ± 37	3	**0.77**	0.008
NADH dehydrogenase (ubiquinone) flavoprotein 2	Ndufv2	1186 ± 22	3	919 ± 19	3	**0.77**	0.001
NADH dehydrogenase (ubiquinone) 1, alpha/beta subcomplex, 1	Ndufab1	1480 ± 28	3	1171 ± 53	3	**0.79**	0.013
NADH dehydrogenase (ubiquinone) 1 alpha subcomplex, 4	Ndufa4	1414 ± 63	3	1156 ± 30	3	**0.82**	0.038
NADH dehydrogenase (ubiquinone) Fe-S protein 3	Ndufs3	1547 ± 27	3	1277 ± 24	3	**0.83**	0.002
NADH dehydrogenase (ubiquinone) 1 alpha subcomplex, 9	Ndufa9	1330 ± 36	3	1106 ± 35	3	**0.83**	0.011
NADH dehydrogenase (ubiquinone) 1 beta subcomplex 4	Ndufb4	1498 ± 54	3	1259 ± 47	3	**0.84**	0.030
NADH dehydrogenase (ubiquinone) 1 alpha subcomplex, 8	Ndufa8	1719 ± 37	3	1448 ± 42	3	**0.84**	0.009
NADH dehydrogenase (ubiquinone) 1 alpha subcomplex, 6 (B14)	Ndufa6	1177 ± 30	3	1012 ± 20	3	**0.86**	0.015
NADH dehydrogenase (ubiquinone) 1 alpha subcomplex, 2	Ndufa2	1603 ± 15	3	1439 ± 31	3	**0.90**	0.020
NADH dehydrogenase (ubiquinone) 1 alpha subcomplex, 3	Ndufa3	2053 ± 42	3	1869 ± 33	3	**0.91**	0.028
Complex II							
succinate dehydrogenase complex, subunit B, iron sulfur (Ip)	Sdhb	3036 ± 58	3	2395 ± 94	3	**0.79**	0.008
succinate dehydrogenase complex, subunit D, integral membrane protein	Sdhd	1277 ± 49	3	1061 ± 39	3	**0.83**	0.028
Complex III							
ubiquinol cytochrome c reductase core protein 2	Uqcrc2	1245 ± 17	3	922 ± 29	3	**0.74**	0.002
ubiquinol-cytochrome c reductase hinge protein	Uqcrh	1534 ± 42	3	1231 ± 22	3	**0.80**	0.008
ubiquinol-cytochrome c reductase binding protein	Uqcrb	979 ± 31	3	791 ± 19	3	**0.81**	0.011
ubiquinol-cytochrome c reductase core protein 1	Uqcrc1	2444 ± 95	3	2082 ± 77	3	**0.85**	0.043
Complex IV							
cytochrome c oxidase, subunit VIIIb	Cox8b	711 ± 36	3	245 ± 21	3	**0.34**	0.001
cytochrome c, somatic	Cycs	2269 ± 38	3	1668 ± 59	3	**0.74**	0.002
cytochrome c oxidase, subunit Vb	Cox5b	2504 ± 64	3	1921 ± 46	3	**0.77**	0.003
cytochrome c oxidase, subunit VIIc	Cox7c	2342 ± 61	3	1864 ± 32	3	**0.80**	0.006
cytochrome c oxidase, subunit Va	Cox5a	2843 ± 55	3	2348 ± 99	3	**0.83**	0.020
cytochrome c oxidase, subunit VIIa 2	Cox7a2	3958 ± 104	3	3387 ± 100	3	**0.86**	0.017
cytochrome c oxidase, subunit VIIIa	Cox8a	3251 ± 123	3	2783 ± 83	3	**0.86**	0.041
cytochrome c oxidase, subunit VIb polypeptide 1	Cox6b1	3448 ± 56	3	2981 ± 76	3	**0.86**	0.010
surfeit gene 1	Surf1	665 ± 12	3	583 ± 12	3	**0.88**	0.009
cytochrome c oxidase subunit IV isoform 1	Cox4i1	4535 ± 79	3	3991 ± 83	3	**0.88**	0.009
cytochrome c oxidase, subunit VI a, polypeptide 1	Cox6a1	3297 ± 48	3	2965 ± 51	3	**0.90**	0.009
Complex V							
ATP synthase, H+ transporting, F1 complex, O subunit	Atp5o	1005 ± 35	3	713 ± 23	3	**0.71**	0.004
ATP synthase, H+ transporting, F0 complex, subunit c (subunit 9), isoform 1	Atp5g1	894 ± 44	3	665 ± 20	3	**0.74**	0.021
ATP synthase, H+ transporting, F0 complex, subunit f, isoform 2	Atp5j2	2001 ± 86	3	1641 ± 19	3	**0.82**	0.047
ATP synthase, H+ transporting, F1 complex, delta subunit	Atp5d	3306 ± 104	3	2747 ± 62	3	**0.83**	0.016
ATP synthase, H+ transporting, F1 complex, gamma polypeptide 1	Atp5c1	2345 ± 86	3	1976 ± 38	3	**0.84**	0.035
ATP synthase, H+ transporting, F0 complex, subunit d	Atp5h	2463 ± 61	3	2087 ± 32	3	**0.85**	0.012
ATP synthase, H+ transporting, F1 complex, alpha subunit, isoform 1	Atp5a1	3613 ± 88	3	3066 ± 37	3	**0.85**	0.014
ATP synthase, H+ transporting, F1F0 complex, subunit e	Atp5k	1949 ± 36	3	1693 ± 38	3	**0.87**	0.008
ATP synthase, H+ transporting F1 complex, beta subunit	Atp5b	4427 ± 74	3	3990 ± 80	3	**0.90**	0.016
ATP synthase, H+ transporting, F0 complex, subunit g	Atp5l	2518 ± 55	3	2280 ± 53	3	**0.91**	0.036
ATPase, H+ transporting, lysosomal V0 subunit a isoform 1	Atp6v0a1	460 ± 16	3	535 ± 18	3	**1.16**	0.037
ATPase, Cu++ transporting, alpha polypeptide	Atp7a	41 ± 3	3	54 ± 2.6	3	**1.33**	0.035

Table 2 - Basal mRNA levels of genes involved in lipid metabolism in differentiated wild type and *Dio2*$^{-/-}$ brown adipocytes.

Gene Annotation	Gene symbol	WT mean ± sem	n	*Dio2*$^{-/-}$ mean ± sem	n	Ratio *Dio2*$^{-/-}$/WT	P value
Fatty acid transport and binding							
fatty acid binding protein 3, muscle and heart	Fabp3	428 ± 24	3	88 ± 6	3	**0.21**	0.003
low-density lipoprotein receptor-related protein 10	Lrp10	1725 ± 43	3	1553 ± 28	3	**0.90**	0.036
choline/ethanolaminephosphotransferase 1	Cept1	215 ± 18	3	309 ± 18	3	**1.4**	0.022
Solute carrier family 27 (fatty acid transporter), member 1	Slc27a1	70 ± 6	3	114 ± 11	3	**1.6**	0.038
Lipogenesis							
acetyl-Coenzyme A acyltransferase 2	Acaa2	502 ± 31	3	327 ± 26	3	**0.65**	0.013
diacylglycerol O-acyltransferase 2	Dgat2	3061 ± 102	3	2188 ± 168	3	**0.71**	0.017
abhydrolase domain containing 5	Abhd5	943 ± 22	3	696 ± 35	3	**0.74**	0.007
lipin 1	Lpin1	987 ± 21	3	760 ± 41	3	**0.77**	0.016
fatty acid desaturase 1	Fads1	1169 ± 30	3	1000 ± 33	3	**0.86**	0.020
acetyl-Coenzyme A acyltransferase 1	Acaa1	949 ± 24	3	821 ± 11	3	**0.86**	0.020
Acyl-CoA synthetase long-chain family member 1	Acsl1	1965 ± 52	3	1744 ± 52	3	**0.89**	0.040
SREBP cleavage activating protein	Scap	1014 ± 17	3	913 ± 23	3	**0.90**	0.027
Lipolysis							
cell death-inducing DNA fragmentation factor, alpha subunit-like effector A	Cidea	68 ± 9	3	11 ± 5	3	**0.16**	0.011
glycerol phosphate dehydrogenase 2, mitochondrial	Gpd2	335 ± 19	3	241 ± 12	3	**0.72**	0.019
protein kinase, cAMP dependent regulatory, type II beta	Prkar2b	476 ± 32	3	353 ± 14	3	**0.74**	0.046
protein kinase, AMP-activated, gamma 1 non-catalytic subunit	Prkag1	803 ± 15	3	630 ± 21	3	**0.79**	0.004
glycerol kinase	Gyk	38 ± 4	3	69 ± 3	3	**1.8**	0.006
β-oxidation							
RIKEN cDNA 4632408A20 gene	4632408A20Rik	56 ± 5	3	37 ± 3	3	**0.65**	0.046
nuclear receptor binding factor 1	Nrbf-1	270 ± 8	3	189 ± 16	3	**0.70**	0.023
dodecenoyl-Coenzyme A delta isomerase	Dci	1015 ± 29	3	717 ± 25	3	**0.71**	0.002
acyl-Coenzyme A dehydrogenase, very long chain	Acadvl	1577 ± 54	3	1208 ± 37	3	**0.77**	0.007
mitochondrial acyl-CoA thioesterase 1	Acot2	478 ± 21	3	375 ± 14	3	**0.78**	0.019
carnitine palmitoyltransferase 1c	Cpt1c	610 ± 17	3	479 ± 29	3	**0.79**	0.025
L-3-hydroxyacyl-Coenzyme A dehydrogenase, short chain	Hadhsc	2871 ± 68	3	2306 ± 39	3	**0.80**	0.005
acetyl-Coenzyme A dehydrogenase, long-chain	Acadl	1308 ± 38	3	1054 ± 24	3	**0.81**	0.008
sterol carrier protein 2, liver	Scp2	1855 ± 44	3	1566 ± 17	3	**0.84**	0.013
hydroxyacyl-Coenzyme A dehydrogenase/3-ketoacyl-Coenzyme A thiolase/enoyl	Hadhb	1426 ± 34	3	1214 ± 37	3	**0.85**	0.014
enoyl coenzyme A hydratase 1, peroxisomal	Ech1	1868 ± 69	3	1619 ± 41	3	**0.87**	0.048
carnitine palmitoyltransferase 2	Cpt2	1089 ± 35	3	955 ± 23	3	**0.88**	0.039

Table 3 - Basal mRNA levels of genes involved in carbohydrate metabolism in differentiated wild type and *Dio2*$^{-/-}$ brown adipocytes.

		WT			*Dio2*$^{-/-}$			Ratio	
Gene Annotation	Gene symbol	mean	± sem	n	mean	± sem	n	*Dio2*$^{-/-}$/WT	P value
Carbohydrate Metabolism									
protein phosphatase 1, regulatory (inhibitor) subunit 3C	Ppp1r3c/PTG	225	± 13	3	93	± 13	3	**0.41**	0.002
lactate dehydrogenase 2, B chain	Ldh2	948	± 29	3	415	± 25	3	**0.44**	0.000
argininosuccinate synthase 1	Ass1	1022	± 50	3	451	± 29	3	**0.44**	0.002
phosphomannomutase 1	Pmm1	555	± 33	3	397	± 37	3	**0.72**	0.034
pyruvate dehydrogenase E1 alpha 1	Pdha1	517	± 11	3	393	± 17	3	**0.76**	0.005
glucan (1,4-alpha-), branching enzyme 1	Gbe1	214	± 11	3	167	± 8	3	**0.78**	0.026
glycogen synthase 3, brain	Gys3	543	± 25	3	425	± 15	3	**0.78**	0.022
brain glycogen phosphorylase	Pygb	588	± 16	3	465	± 20	3	**0.79**	0.010
amylo-1,6-glucosidase, 4-alpha-glucanotransferase	Agl	217	± 9	3	175	± 5	3	**0.81**	0.022
glycogenin 1	Gyg1	1795	± 61	3	1450	± 37	3	**0.81**	0.014
phosphofructokinase, muscle	Pfkm	281	± 9	3	230	± 8	3	**0.82**	0.015
ribose 5-phosphate isomerase A	Rpia	316	± 13	3	270	± 10	3	**0.85**	0.048
glucose-6-phosphate dehydrogenase X-linked	G6pdx	2177	± 58	3	1875	± 78	3	**0.86**	0.040
phosphoglucomutase 2	Pgm2	890	± 20	3	768	± 27	3	**0.86**	0.027
3-hydroxyisobutyrate dehydrogenase	Hibadh	1289	± 33	3	1134	± 26	3	**0.88**	0.024
6-phosphogluconolactonase	Pgls	1030	± 26	3	927	± 18	3	**0.90**	0.036
adiponectin, C1Q and collagen domain containing	Adipoq	3328	± 44	3	3077	± 68	3	**0.92**	0.044
phosphoglycerate kinase 1	Pgk1	3253	± 61	3	3623	± 28	3	**1.1**	0.014
pyruvate kinase, muscle	Pkm2	3481	± 63	3	3938	± 70	3	**1.1**	0.009
adiponectin receptor 1	Adipor1	885	± 17	3	1015	± 22	3	**1.2**	0.012
phosphofructokinase, platelet	Pfkp	433	± 14	3	544	± 22	3	**1.3**	0.019
liver glycogen phosphorylase	Pygl	347	± 18	3	436	± 13	3	**1.3**	0.019
Phosphorylase kinase alpha 1	Phka1	93	± 5	3	147	± 11	3	**1.6**	0.026
solute carrier family 37 (glycerol-3-phosphate transporter), member 2	Slc37a2	91.2	± 13	3	202	± 11	3	**2.2**	0.003
aldolase 3, C isoform	Aldoc	76.8	± 16	3	239	± 14	3	**3.1**	0.002
2,3-bisphosphoglycerate mutase	Bpgm	33	± 19	3	173	± 30	3	**5.3**	0.022
solute carrier family 16 (monocarboxylic acid transporters), member 3	Slc16a3/MCT4	119	± 12	3	678	± 43	3	**5.7**	0.003

Table 4 - Basal mRNA levels of genes involved in cell fate in differentiated wild type and *Dio2*$^{-/-}$ brown adipocytes.

Gene Annotation	Gene symbol	WT mean ± sem	n	*Dio2*$^{-/-}$ mean ± sem	n	Ratio *Dio2*$^{-/-}$/WT	P value
Differentiation							
Preadipocyte factor-1	Pref-1	646 ± 71	3	187 ± 13	3	**0.29**	0.020
tumor necrosis factor (ligand) superfamily, member 13	Tnfsf13	70 ± 5	3	141 ± 11	3	**2.0**	0.012
tumor necrosis factor receptor superfamily, member 1b	Tnfrsf1b	158 ± 8	3	336 ± 16	3	**2.1**	0.002
transforming growth factor, beta 1	Tgfb1	389 ± 24	3	1090 ± 40	3	**2.8**	0.000
schlafen 2	Slfn2	122 ± 13	3	484 ± 14	3	**4.0**	0.000
Proliferation							
insulin-like growth factor binding protein 5	Igfbp5	738 ± 22	3	332 ± 14	3	**0.45**	0.000
insulin-like growth factor binding protein 3	Igfbp3	496 ± 16	3	227 ± 11	3	**0.46**	0.000
retroviral integration site 2	Ris2/Cdt1	120 ± 5	3	245 ± 18	3	**2.0**	0.014
cyclin B2	Ccnb2	55 ± 11	3	112 ± 9	3	**2.1**	0.016
proliferating cell nuclear antigen	Pcna	553 ± 24	3	1140 ± 36	3	**2.1**	0.000
regenerating islet-derived 1	Reg1	99 ± 7	3	204 ± 14	3	**2.1**	0.006
RAS related protein 1b	Rap1b	256 ± 24	3	533 ± 23	3	**2.1**	0.001
heterogeneous nuclear ribonucleoprotein A1	Hnrpa1	97 ± 18	3	271 ± 27	3	**2.8**	0.008
RAP2B, member of RAS oncogene family	Rap2b	181 ± 25	3	517 ± 51	3	**2.9**	0.010
cyclin-dependent kinase 6	Cdk6	62 ± 16	3	190 ± 11	3	**3.1**	0.004
RAB8B, member RAS oncogene family	Rab8b	82 ± 15	3	279 ± 14	3	**3.4**	0.001
insulin-like growth factor 1	IGF-1	411 ± 19	3	1483 ± 64	3	**3.6**	0.002
deoxycytidine kinase	Dck	24 ± 7	3	101 ± 7	3	**4.3**	0.002

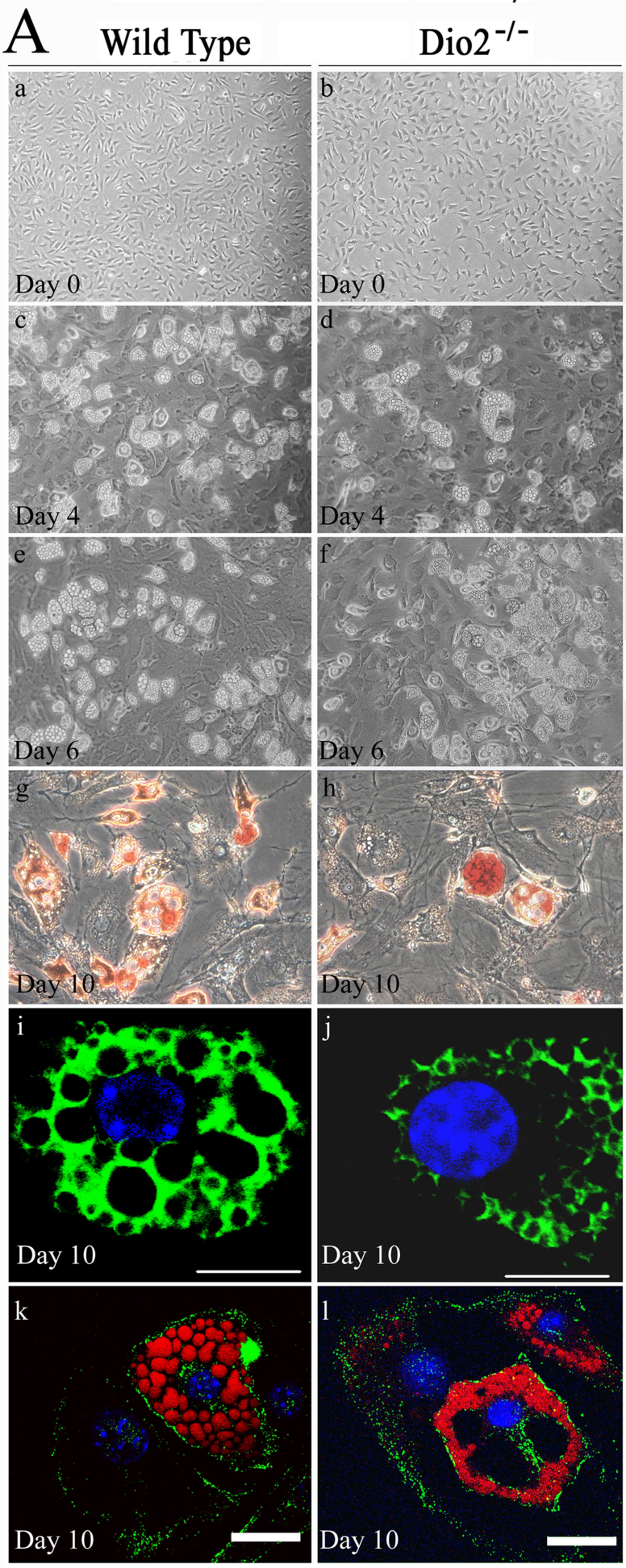
A
Wild Type
Dio2 -/-
a
b
Day 0
Day 0
c
d
Day 4
Day 4
e
f
Day 6
Day 6
g
h
Day 10
Day 10
i
j
Day 10
Day 10
k
l
Day 10
Day 10

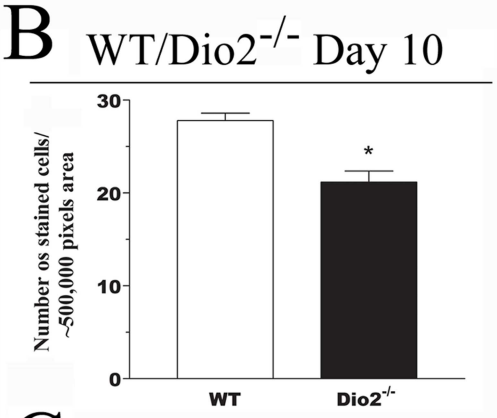
B
WT/Dio2 -/- Day 10
Number os stained cells/ ~500,000 pixels area
30
20
10
0
*
WT
Dio2 -/-

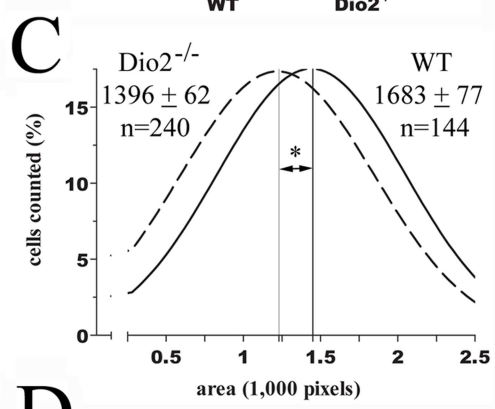
C
Dio2 -/-
1396 ± 62
n=240
WT
1683 ± 77
n=144
*
cells counted (%)
15
10
5
0
0.5
1
1.5
2
2.5
area (1,000 pixels)

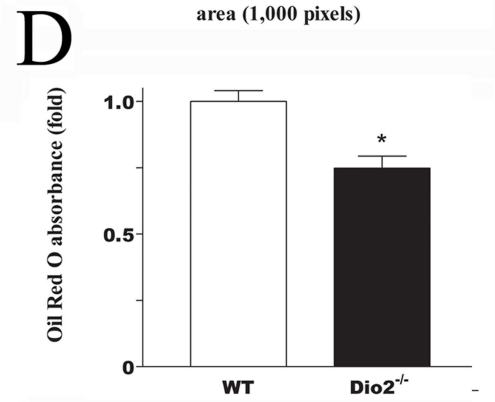
D
Oil Red O absorbance (fold)
1.0
0.5
0
*
WT
Dio2 -/-

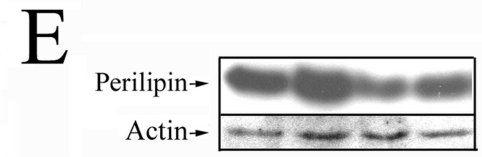
E
Perilipin
Actin

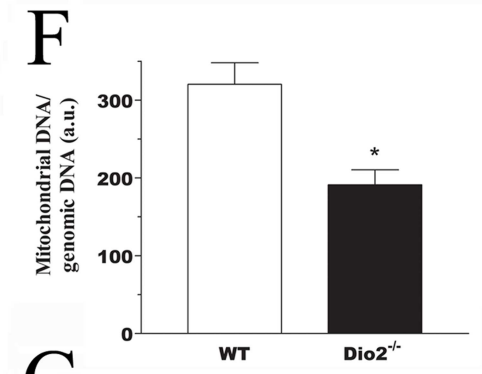
F
Mitochondrial DNA/ genomic DNA (a.u.)
300
200
100
0
*
WT
Dio2 -/-

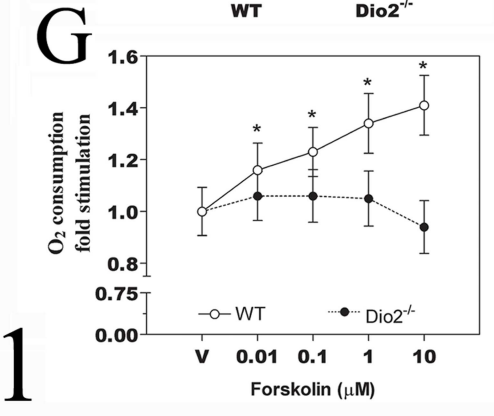
G
O2 consumption fold stimulation
1.6
1.4
1.2
1.0
0.8
0.75
0.00
*
WT
Dio2 -/-
V
0.01
0.1
1
10
Forskolin (μM)

Figure 1

A

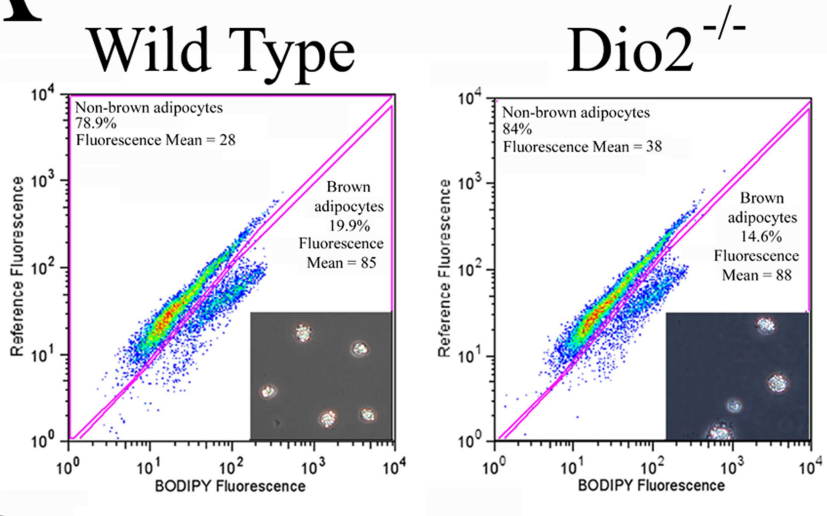
Wild Type
Dio2 -/-
Non-brown adipocytes
78.9%
Fluorescence Mean = 28
Brown
adipocytes
19.9%
Fluorescence
Mean = 85
Non-brown adipocytes
84%
Fluorescence Mean = 38
Brown
adipocytes
14.6%
Fluorescence
Mean = 88
Reference Fluorescence
BODIPY Fluorescence

B

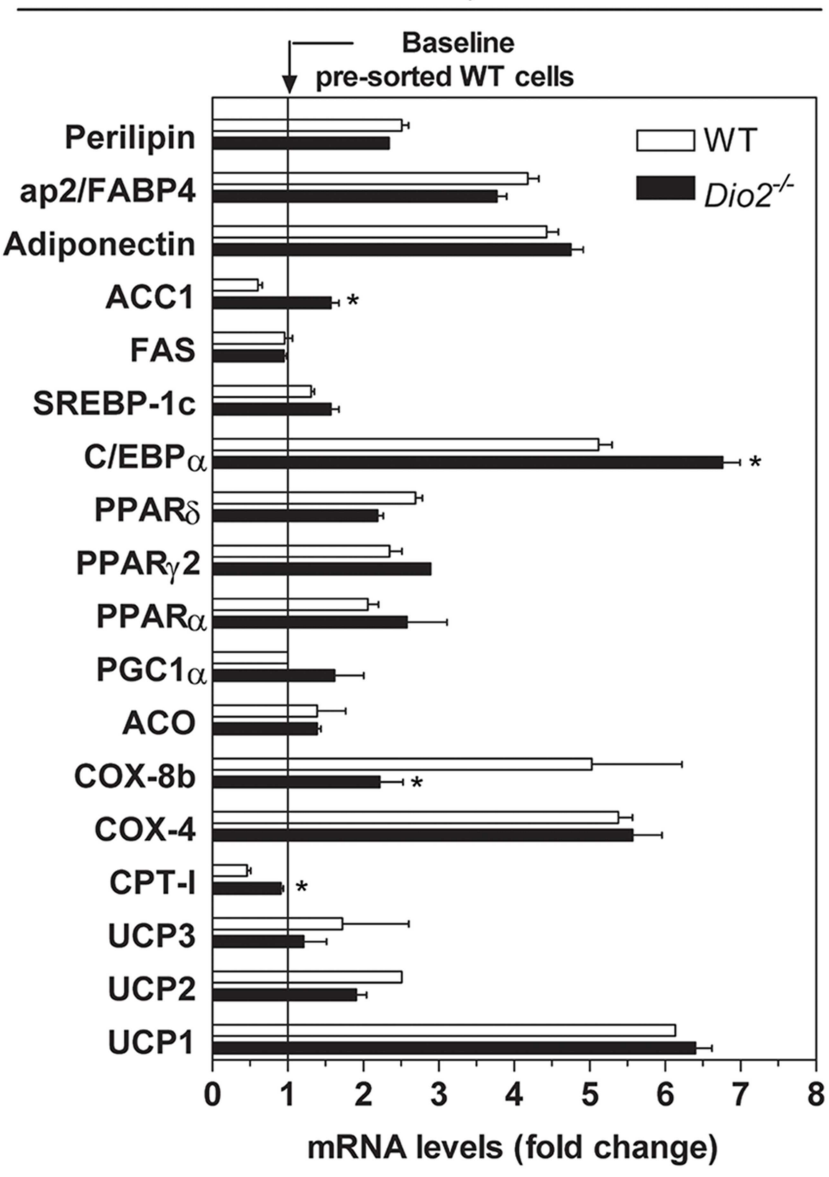
WT and Dio2-/- cell positive for BODIPY staining sorted in flow cytometer
Baseline
pre-sorted WT cells
WT
Dio2-/-
Perilipin
ap2/FABP4
Adiponectin
ACC1
FAS
SREBP-1c
C/EBPα
PPARδ
PPARγ2
PPARα
PGC1α
ACO
COX-8b
COX-4
CPT-I
UCP3
UCP2
UCP1
mRNA levels (fold change)

Figure 2

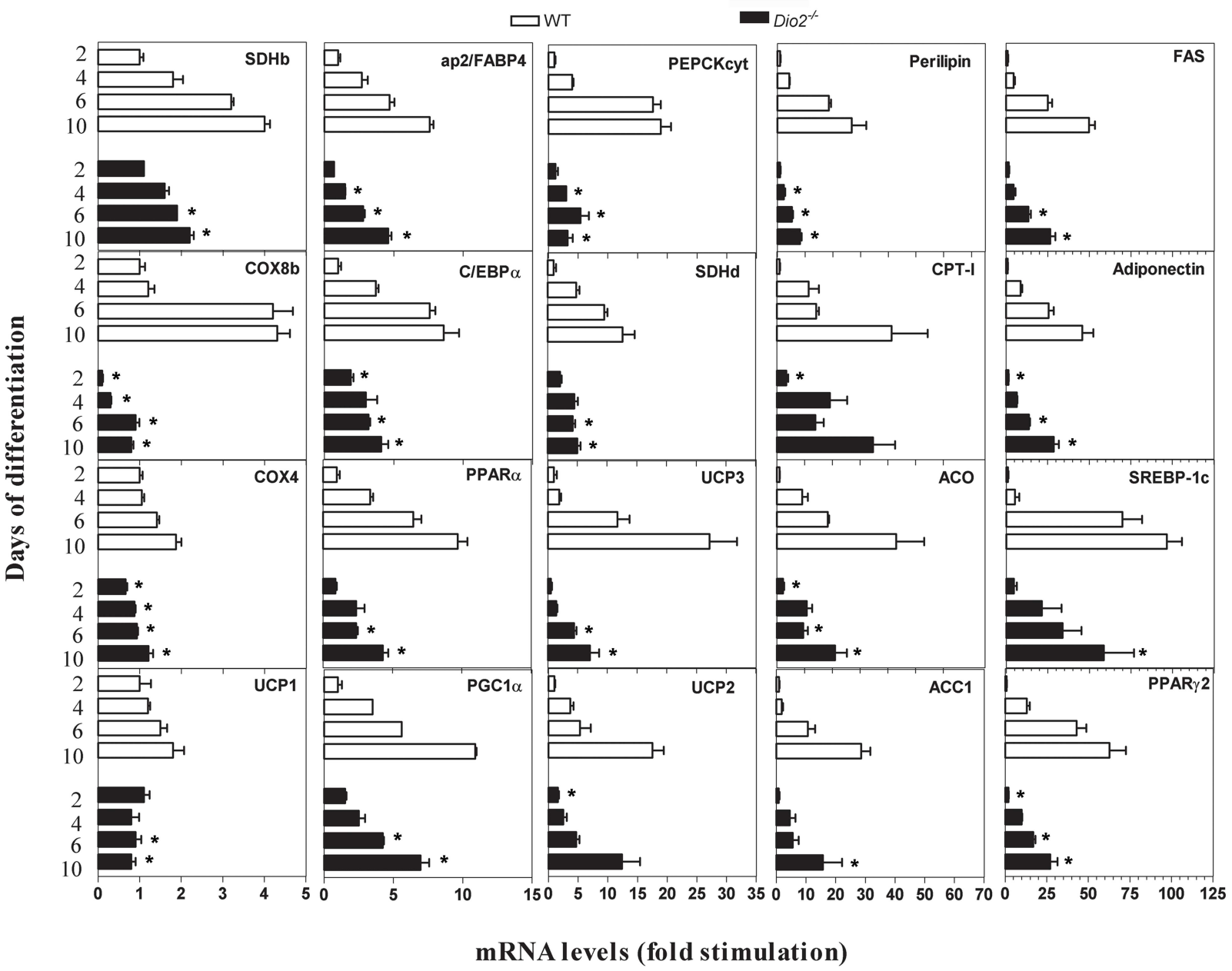
WT
Dio2-/-
SDHb
ap2/FABP4
PEPCKcyt
Perilipin
FAS
COX8b
C/EBPα
SDHd
CPT-I
Adiponectin
COX4
PPARα
UCP3
ACO
SREBP-1c
UCP1
PGC1α
UCP2
ACC1
PPARγ2
Days of differentiation
mRNA levels (fold stimulation)

Figure 3

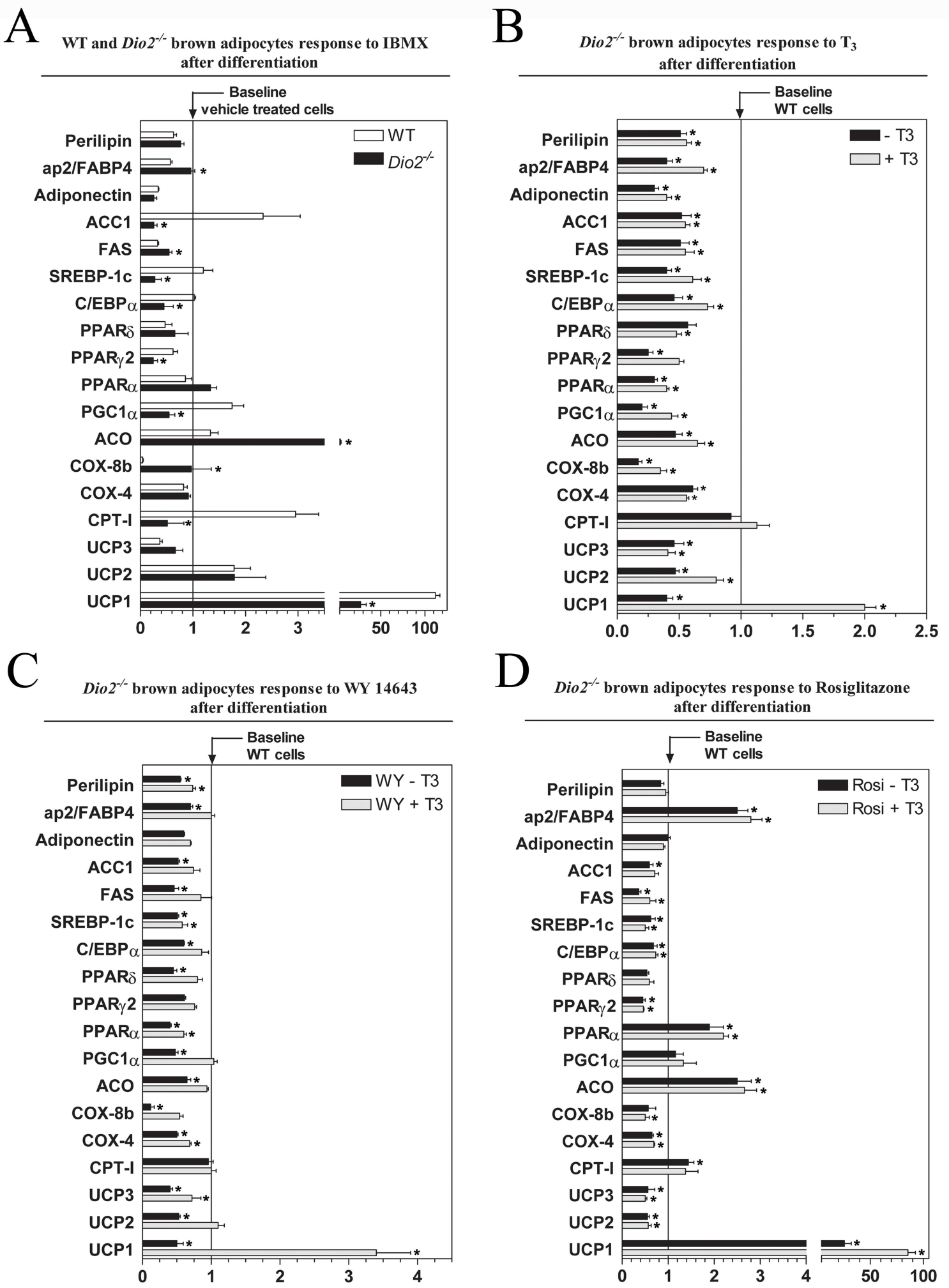
A
WT and Dio2-/- brown adipocytes response to IBMX after differentiation
Baseline vehicle treated cells
WT
Dio2-/-
Perilipin
ap2/FABP4
Adiponectin
ACC1
FAS
SREBP-1c
C/EBPα
PPARδ
PPARγ2
PPARα
PGC1α
ACO
COX-8b
COX-4
CPT-I
UCP3
UCP2
UCP1
0 1 2 3 50 100
B
Dio2-/- brown adipocytes response to T3 after differentiation
Baseline WT cells
- T3
+ T3
0.0 0.5 1.0 1.5 2.0 2.5
C
Dio2-/- brown adipocytes response to WY 14643 after differentiation
Baseline WT cells
WY - T3
WY + T3
0 1 2 3 4
D
Dio2-/- brown adipocytes response to Rosiglitazone after differentiation
Baseline WT cells
Rosi - T3
Rosi + T3
0 1 2 3 4 50 100

Figure 4

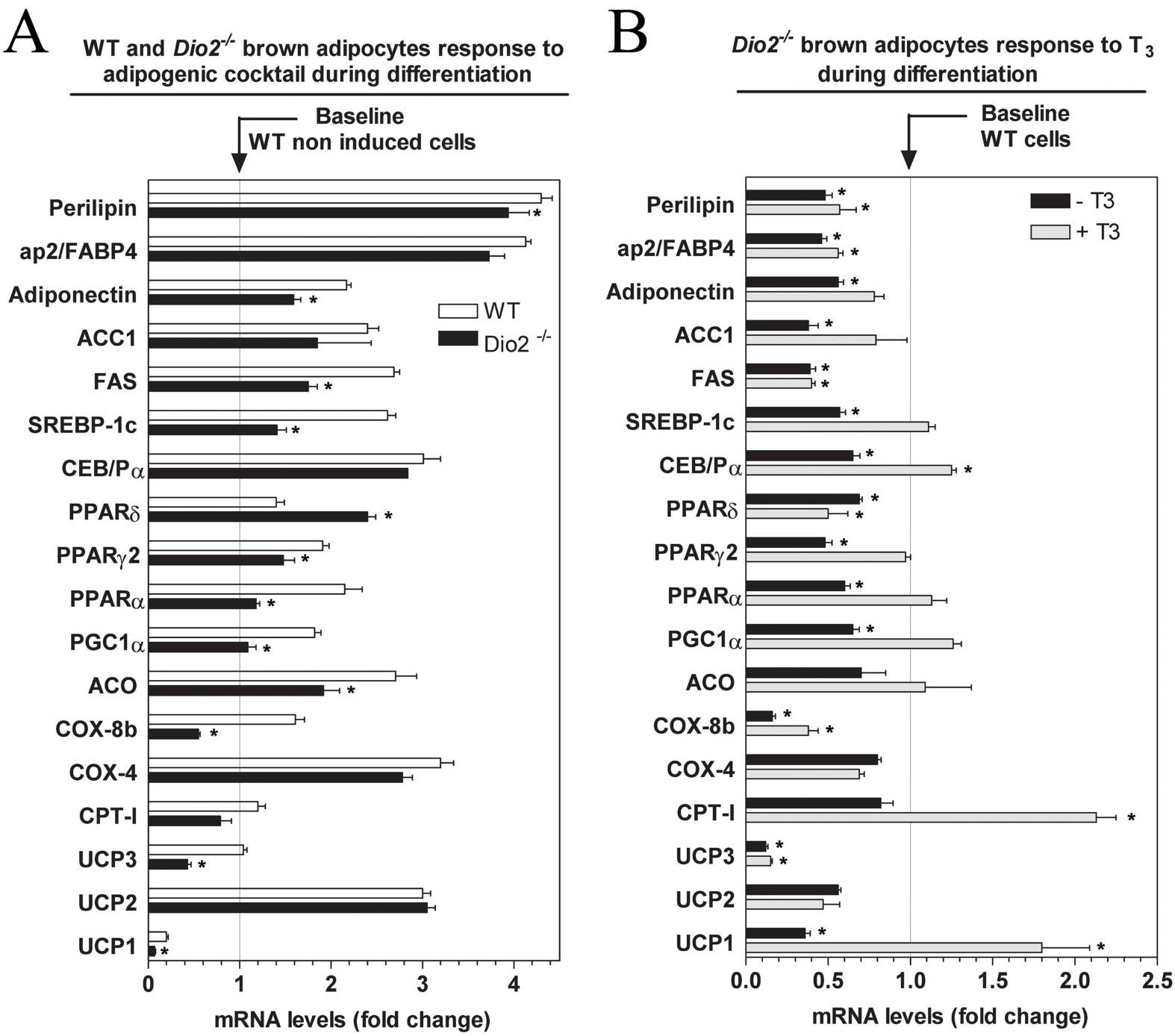
A
WT and Dio2-/- brown adipocytes response to adipogenic cocktail during differentiation
Baseline
WT non induced cells
Perilipin
ap2/FABP4
Adiponectin
ACC1
FAS
SREBP-1c
CEB/Pα
PPARδ
PPARγ2
PPARα
PGC1α
ACO
COX-8b
COX-4
CPT-I
UCP3
UCP2
UCP1
WT
Dio2 -/-
0
1
2
3
4
mRNA levels (fold change)
B
Dio2-/- brown adipocytes response to T3 during differentiation
Baseline
WT cells
- T3
+ T3
0.0
0.5
1.0
1.5
2.0
2.5
mRNA levels (fold change)

Figure 5

Figure 1 – *Dio2*$^{-/-}$ brown adipocyte phenotype. **A**. Wild type (a, c, e, g, i, k) and *Dio2*$^{-/-}$ (b, d, f, h, j, l) brown pre-adipocytes were differentiated in the presence of insulin and ascorbic acid. Cells reached confluence at Day 0 (a, b) and 4-6 days later, brown adipocytes exhibiting lipid droplets are observed in the wild type and *Dio2*$^{-/-}$ populations (c-f). At day 10, mature brown adipocytes stain positive with ORO (g, h). Such cells were also stained with anti-perilipin antibody (green) and DAPI (blue) (i, j) or anti-D3 antibody (green), BODIPY (red) and DAPI (blue) (k, l). **B**. Number of ORO stained adipocytes in 6 random fields from wild type (g) and *Dio2*$^{-/-}$ (h) populations. **C**. Adipocyte size distribution and average cell size ± SEM in wild type (g) and *Dio2*$^{-/-}$ (h) populations. **D**. ORO was eluted from positive adipocytes with DMSO and quantified at 535nm. **E**. Perilipin in wild type and *Dio2*$^{-/-}$ brown adipocytes as quantified by western blot. Actin was used as a control for loading. **F**. Mitochondrial content in wild type and *Dio2*$^{-/-}$ brown adipocytes was estimated from the mitochondrial/genomic DNA ratio in the cell samples. **G**. O_2 consumption of wild type and *Dio2*$^{-/-}$ brown adipoctes in response to increasing concentrations of forskolin. Values are mean ± SEM of 3-30 data points otherwise indicated. *p<0.05 vs. wild type by Student's t-test.

Figure 2 – Brown adipocyte sorting by flow cytometry. **A.** Frequency distribution of approximately $3x10^6$ wild type or *Dio2*$^{-/-}$ brown adipocytes as sorted by fluorescence activated cell sorting (FACS) using BODIPY, a neutral lipid fluorescent dye. Fluorescence intensity is given in arbitrary units. Viability was about 50% for both cell genotypes. **B.** Relative mRNA levels as quantified by RT-qPCR of the indicated genes after 10 days of differentiation in wild type (open bars) and *Dio2*$^{-/-}$ (black bars) brown adipocytes sorted by FACS. All entries were normalized to the respective pre-sorted wild type value. Values are mean ± SEM of 2-4 data points. *p<0.05 vs. sorted wild type value by Student's t-test.

Figure 3 – Gene expression profile in differentiating brown adipocytes. Relative mRNA levels as quantified by RT-qPCR of the indicated genes during the 2nd, 4th, 6th and 10th days of differentiation in wild type (open bars) and *Dio2*$^{-/-}$ (black bars) cells. All entries were normalized to the respective wild type value at day 2. Values are mean ± SEM of 4 data points. *p<0.05 vs. same day wild type value by Student's t-test. Gene profile at day 10 was similar in another 4 independent experiments.

Figure 4 – Gene expression profile in stimulated wild type and *Dio2*$^{-/-}$ brown adipocytes. A. Eight-day wild type (open bars) and *Dio2*$^{-/-}$ (black bars) brown adipocytes were treated with 0.5 mM IBMX for 48 h prior to the differentiation endpoint. Control cells were treated with vehicle. The reference line represents untreated brown adipocytes. **B**. Same as in **A** except that only *Dio2*$^{-/-}$ brown adipocytes were treated with vehicle (black bars) or 50 nM T_3 (gray bars). The reference line corresponds to untreated wild type

cells. **C**. Same as in **B** except that *Dio2*$^{-/-}$ brown adipocytes were treated with 10 μM WY 14643 (black bars) or 10 μM WY 14643 + 50 nM T_3 (gray bars). **D**. Same as in **C** except that *Dio2*$^{-/-}$ brown adipocytes were treated with 10 μM rosiglitazone (black bars) or 10 μM rosiglitazone + 50 nM T_3 (gray bars). Values are mean ± SEM of 3-4 data points. *p<0.05 vs. IBMX-treated wild type values (**A**) or vs. untreated wild type cells (**B-D**) by Student's t-test.

Figure 5 – Rescuing gene expression in differentiating Dio2$^{-/-}$ brown adipocytes. **A**. Wild type (open bars) and *Dio2*$^{-/-}$ (black bars) brown adipocytes treated with adipogenic cocktail (IBMX, indomethacin and dexamethasone) on the 2nd day of differentiation for 48 h and let differentiate until day 10 in comparison to non-induced wild type cells. **B**. Same as **A,** except that only *Dio2*$^{-/-}$ brown adipocytes were used and treatment with 50 nM T_3 (gray bars) lasted 10 days. Values are mean ± SEM of 4 data points. *p<0.05 vs. similarly treated wild type adipocytes (**A**) or vs. untreated wild type cells (**B**) by Student's t-test.

Supplementary Table 1 - Pathways down-regulated in differentiated *Dio2*$^{-/-}$ brown adipocytes according to Genmapp software analysis

MAPP Name	Z Score	PermuteP	AdjustedP
mitochondrion 2	13.1	<0.001	<0.001
mitochondrion	12.6	<0.001	<0.001
Mm_Electron_Transport_Chain	12.4	<0.001	<0.001
hydrogen ion transporter activity	11.0	<0.001	<0.001
monovalent inorganic cation transporter activity	10.8	<0.001	<0.001
primary active transporter activity	10.2	<0.001	<0.001
inner membrane	9.7	<0.001	<0.001
mitochondrial inner membrane	8.9	<0.001	<0.001
mitochondrial membrane	8.9	<0.001	<0.001
cofactor metabolism	8.8	<0.001	<0.001
Mm_Krebs-TCA_Cycle	8.7	<0.001	<0.001
coenzyme metabolism	8.1	<0.001	<0.001
oxidoreductase activity	7.7	<0.001	<0.001
cofactor metabolism 2	7.5	<0.001	<0.001
ribosome	7.1	<0.001	<0.001
electron transporter activity	6.1	<0.001	0.002
structural constituent of ribosome	5.7	<0.001	0.005
nucleotide metabolism 7	5.1	<0.001	0.017
nucleotide metabolism 10	5.0	<0.001	0.018
nucleotide metabolism 11	4.9	<0.001	0.022
Mm_Cholesterol_Biosynthesis	4.7	<0.001	0.027
nucleotide metabolism 12	4.7	<0.001	0.028
nucleotide metabolism 8	4.6	<0.001	0.049
oxidoreductase activity, acting on the CH-OH group of donors, NAD or NADP as acceptor	4.6	<0.001	0.049

Z score, the standard statistical test under the hypergeometric distribution; PermuteP, a non-parametric statistic based on 2000 permutations of the data and AdjustedP, based on Westfall-Young adjustment for multiple testing were calculated by Genmapp software. n=3

VII - Conclusões

1 – Camundongos da linhagem C3H com deficiência da desiodase do tipo 1 portando disrupção do gene da desiodase do tipo 2 (C3H-D2KO) apresentam níveis séricos de T3 eutiroideos e T4 sérico elevado. Estes animais apresentam aumento da atividade da D1 hepática e renal em relação a animais C3H, mas que permanece bem abaixo daquelas observadas em animais C57. Estes fatores podem estar relacionados com a manutenção de T3 sérico na faixa eutiroidea, enquanto que alterações da atividade tiroideana e/ou atividade da D1 tiroideana, bem como alterações da atividade da enzima inativadora do T3 (D3) não foram observadas.

2 – A desiodase do tipo 2 expressa em tirotrofos desempenha papel fundamental na retroalimentação negativa do TSH mediada por T4 e embora sujeita a degradação promovida pela exposição ao substrato, a alta taxa de síntese da enzima nestas células garante produção de T3, mesmo durante a vigência de altos níveis de T4

3 – A exaustão de ácidos graxos, ao invés de resposta diminuída ao sistema simpático, é a causa da termogênese facultativa ineficiente e hipotermia apresentada por animais hipotiroideos ou portando disrupção do gene da desiodase do tipo 2.

4 – A sinalização do hormônio tiroideano, amplificado pela D2 é fundamental para a diferenciação do pré-adipócito marrom. Adipócitos marrons *Dio2*$^{-/-}$ não ativam apropriadamente o programa de diferenciação e, conseqüentemente, genes alvo envolvidos na homeostase energética. Como resultado, encontramos menos adipócitos marrons *Dio2*$^{-/-}$ maduros, que acumulam menos gordura e apresentam capacidade oxidativa defeituosa, apontando a D2 como componente chave do programa de diferenciação de pré-adipócitos marrons.

VIII – Anexo

Produção científica durante o doutorado

1. **Christoffolete, M.A.**, Ribeiro, R., Singru, P., Fekete, C., da Silva, W.S., Gordon, D.F., Huang, S.A., Crescenzi, A., Harney, J.W., Ridgway, E.C., et al. 2006. Atypical expression of type 2 iodothyronine deiodinase in thyrotrophs explains the thyroxine-mediated pituitary thyrotropin feedback mechanism. Endocrinology 147:1735-1743.
2. Fekete, C., Singru, P.S., Sanchez, E., Sarkar, S., **Christoffolete, M.A.**, Riberio, R.S., Rand, W.M., Emerson, C.H., Bianco, A.C., and Lechan, R.M. 2006. Differential effects of central leptin, insulin, or glucose administration during fasting on the hypothalamic-pituitary-thyroid axis and feeding-related neurons in the arcuate nucleus. Endocrinology 147:520-529.
3. Miyoshi, H., Souza, S.C., Zhang, H.H., Strissel, K.J., **Christoffolete, M.A.**, Kovsan, J., Rudich, A., Kraemer, F.B., Bianco, A.C., Obin, M.S., et al. 2006. Perilipin promotes hormone-sensitive lipase-mediated adipocyte lipolysis via phosphorylation-dependent and -independent mechanisms. J Biol Chem 281:15837-15844.
4. Watanabe, M., Houten, S.M., Mataki, C., **Christoffolete, M.A.**, Kim, B.W., Sato, H., Messaddeq, N., Harney, J.W., Ezaki, O., Kodama, T., et al. 2006. Bile acids induce energy expenditure by promoting intracellular thyroid hormone activation. Nature 439:484-489.
5. Fekete, C., Sarkar, S., **Christoffolete, M.A.**, Emerson, C.H., Bianco, A.C., and Lechan, R.M. 2005. Bacterial lipopolysaccharide (LPS)-induced type 2 iodothyronine deiodinase (D2) activation in the mediobasal hypothalamus (MBH) is independent of the LPS-induced fall in serum thyroid hormone levels. Brain Res 1056:97-99.
6. Gouveia, C.H., **Christoffolete, M.A.**, Zaitune, C.R., Dora, J.M., Harney, J.W., Maia, A.L., and Bianco, A.C. 2005. Type 2 iodothyronine selenodeiodinase is expressed throughout the mouse skeleton and in the MC3T3-E1 mouse osteoblastic cell line during differentiation. Endocrinology 146:195-200.
7. Kim, S.W., Ho, S.C., Hong, S.J., Kim, K.M., So, E.C., **Christoffolete, M.**, and Harney, J.W. 2005. A novel mechanism of thyroid hormone-dependent negative regulation by thyroid hormone receptor, nuclear receptor corepressor (NCoR), and GAGA-binding factor on the rat cD44 promoter. J Biol Chem 280:14545-14555.
8. Zavacki, A.M., Ying, H., **Christoffolete, M.A.**, Aerts, G., So, E., Harney, J.W., Cheng, S.Y., Larsen, P.R., and Bianco, A.C. 2005. Type 1 iodothyronine deiodinase is a sensitive marker of peripheral thyroid status in the mouse. Endocrinology 146:1568-1575.

9. **Christoffolete, M.A.**, Linardi, C.C.G., de Jesus, L.A., Ebina, K.N., Carvalho, S.D., Ribeiro, M.O., Rabelo, R., Curcio, C., Martins, L., Kimura, E.T., et al. 2004. Mice with targeted disruption of the Dio2 gene have cold-induced overexpression of uncoupling protein 1 gene but fail to increase brown adiose tissue lipogenesis and adaptive thermogenesis. Diabetes 53:577-584.
10. Bianco, A.C., Maia, A.L., da Silva, W.S., and **Christoffolete, M.A**. 2005. Adaptive activation of thyroid hormone and energy expenditure. Biosci Rep 25:191-208.
11. Dentice, M., Bandyopadhyay, A., Gereben, B., Callebaut, I., **Christoffolete, M.A.**, Kim, B.W., Nissim, S., Mornon, J.P., Zavacki, A.M., Zeold, A., et al. 2005. The Hedgehog-inducible ubiquitin ligase subunit WSB-1 modulates thyroid hormone activation and PTHrP secretion in the developing growth plate. Nat Cell Biol 7:698-705.
12. Curcio-Morelli, C., Zavacki, A.M., **Christofollete, M.**, Gereben, B., de Freitas, B.C., Harney, J.W., Li, Z., Wu, G., and Bianco, A.C. 2003. Deubiquitination of type 2 iodothyronine deiodinase by von Hippel-Lindau protein-interacting deubiquitinating enzymes regulates thyroid hormone activation. J Clin Invest 112:189-196.

IX – Referências Bibliográficas

1. Bianco, A.C., Salvatore, D., Gereben, B., Berry, M.J., and Larsen, P.R. 2002. Biochemistry, cellular and molecular biology and physiological roles of the iodothyronine selenodeiodinases. *Endocrine Reviews* 23:38-89.
2. Larsen, P.R., Davies, T.F., and Hay, I.D. 1998. The Thyroid Gland. In *Williams Textbook of Endocrinology*. J.D. Wilson, D.W. Foster, H.M. Kronenberg, and P.R. Larsen, editors. Philadelphia: W.B. Saunders Co. 389-515.
3. Bianco, A.C. 2004. Triplets! Unexpected structural similarity among the three enzymes that catalyze initiation and termination of thyroid hormone effects. *Arq Bras Endocrinol Metabol* 48:16-24.
4. Croteau, W., Whittemore, S.L., Schneider, M.J., and St Germain, D.L. 1995. Cloning and expression of a cDNA for a mammalian type III iodothyronine deiodinase. *J Biol Chem* 270:16569-16575.
5. Berry, M.J., Kieffer, J.D., Harney, J.W., and Larsen, P.R. 1991. Selenocysteine confers the biochemical properties of the type I iodothyronine deiodinase. *J Biol Chem* 266:14155-14158.
6. Buettner, C., Harney, J.W., and Larsen, P.R. 2000. The role of selenocysteine 133 in catalysis by the human type 2 iodothyronine deiodinase. *Endocrinology* 141:4606-4612.
7. Oppenheimer, J.H., Schwartz, H.L., and Surks, M.I. 1972. Propylthiouracil inhibits the conversion of L-thyroxine to L-triiodothyronine: An explanation of the antithyroxine effect of propylthiouracil and evidence supporting the concept that triiodothyronine is the active thyroid hormone. *J Clin Invest* 51:2493-2497.
8. Fekkes, D., Hennemann, G., and Visser, T.J. 1982. Evidence for a single enzyme in rat liver catalyzing the deiodination of the tyrosyl and the phenolic ring of iodothyronines. *Biochem J* 201:673-676.
9. Leonard, J.L., and Rosenberg, I.N. 1978. Thyroxine 5'-deiodinase activity of rat kidney: Observations on activation by thiols and inhibition by propylthiouracil. *Endocrinology* 103:2137-2144.
10. Visser, T.J., van der Does-Tobe, I., Docter, R., and Hennemann, G. 1976. Subcellular localization of a rat liver enzyme converting thyroxine into triiodothyronine and possible involvement of essential thiol groups. *Biochem J* 157:479-482.
11. Visser, T.J., Fekkes, D., Docter, R., and Hennemann, G. 1978. Sequential deiodination of thyroxine in rat liver homogenate. *Biochem J* 174:221-229.
12. Chopra, I.J. 1978. Sulfhydryl groups and the monodeiodination of thyroxine to triiodothyronine. *Science* 199:904-905.
13. Leonard, J.L., and Rosenberg, I.N. 1980. Characterization of essential enzyme sulfhydryl groups on thyroxine 5'-deiodinase from rat kidney. *Endocrinology* 106:444-451.
14. St. Germain, D.L., and Galton, V.A. 1997. The deiodinase family of selenoproteins. *Thyroid* 7:655-668.

15. Galton, V.A. 1988. Iodothyronine 5'-deiodinase activity in the amphibian Rana catesbeiana at different stages of the life cycle. *Endocrinology* 122:1746-1750.
16. Becker, K.B., Stephens, K.C., Davey, J.C., Schneider, M.J., and Galton, V.A. 1997. The type 2 and type 3 iodothyronine deiodinases play important roles in coordinating development in Rana catesbeiana tadpoles. *Endocrinology* 138:2989-2997.
17. Campos-Barros, A., Hoell, T., Musa, A., Sampaolo, S., Stoltenburg, G., Pinna, G., Eravci, M., Meinhold, H., and Baumgartner, A. 1996. Phenolic and tyrosyl ring iodothyronine deiodination and thyroid hormone concentrations in the human central nervous system. *J Clin Endocrinol Metab* 81:2179-2185.
18. Nishikawa, M., Toyoda, N., Yonemoto, T., Ogawa, Y., Tabata, S., Sakaguchi, N., Tokoro, T., Gondou, A., Yoshimura, M., Yoshikawa, N., et al. 1998. Quantitative measurements for type 1 deiodinase messenger ribonucleic acid in human peripheral blood mononuclear cells: mechanism of the preferential increase of T3 in hyperthyroid Graves' disease. *Biochem Biophys Res Commun* 250:642-646.
19. Baqui, M.M., Botero, D., Gereben, B., Curcio, C., Harney, J.W., Salvatore, D., Sorimachi, K., Larsen, P.R., and Bianco, A.C. 2003. Human type 3 iodothyronine selenodeiodinase is located in the plasma membrane and undergoes rapid internalization to endosomes. *J Biol Chem* 278:1206-1211.
20. Silva, J.E., and Larsen, P.R. 1977. Pituitary nuclear 3,5,3'-triiodothyronine and thyrotropin secretion: an explanation for the effect of thyroxine. *Science* 198:617-620.
21. Larsen, P.R., and Frumess, R.D. 1977. Comparison of the biological effects of thyroxine and triiodothyronine in the rat. *Endocrinology* 100:980-988.
22. Cheron, R.G., Kaplan, M.M., and Larsen, P.R. 1979. Physiological and pharmacological influences on thyroxine to 3,5,3'- triiodothyronine conversion and nuclear 3,5,3'-triiodothyronine binding in rat anterior pituitary. *J Clin Invest* 64:1402-1414.
23. Visser, T.J., Leonard, J.L., Kaplan, M.M., and Larsen, P.R. 1982. Kinetic evidence suggesting two mechanisms for iodothyronine 5'- deiodination in rat cerebral cortex. *Proc Natl Acad Sci USA* 79:5080-5084.
24. Leonard, J.L. 1988. Dibutyryl cAMP induction of Type II 5'deiodinase activity in rat brain astrocytes in culture. *Biochem Biophys Res Commun* 151:1164-1172.
25. Crantz, F.R., and Larsen, P.R. 1980. Rapid thyroxine to 3,5,3'-triiodothyronine conversion and nuclear 3,5,3'-triiodothyronine binding in rat cerebral cortex and cerebellum. *J Clin Invest* 65:935-938.
26. Silva, J.E., and Larsen, P.R. 1983. Adrenergic activation of triiodothyronine production in brown adipose tissue. *Nature* 305:712-713.
27. Molinero, P., Osuna, C., and Guerrero, J.M. 1995. Type II thyroxine 5'-deiodinase in the rat thymus. *J Endocrinol* 146:105-111.
28. Song, S., Sorimachi, K., Adachi, K., and Oka, T. 2000. Biochemical and molecular biological evidence for the presence of type II iodothyronine deiodinase in mouse mammary gland. *Mol Cell Endocrinol* 160:173-181.
29. Kamiya, Y., Murakami, M., Araki, O., Hosoi, Y., Ogiwara, T., Mizuma, H., and Mori, M. 1999. Pretranslational regulation of rhythmic type II iodothyronine

deiodinase expression by beta-adrenergic mechanism in the rat pineal gland. *Endocrinology* 140:1272-1278.
30. Galton, V.A., Martinez, E., Hernandez, A., St Germain, E.A., Bates, J.M., and St Germain, D.L. 2001. The type 2 iodothyronine deiodinase is expressed in the rat uterus and induced during pregnancy. *Endocrinology* 142:2123-2128.
31. Mizuma, H., Murakami, M., and Mori, M. 2001. Thyroid hormone activation in human vascular smooth muscle cells: expression of type II iodothyronine deiodinase. *Circ Res* 88:313-318.
32. Bates, J.M., St Germain, D.L., and Galton, V.A. 1999. Expression profiles of the three iodothyronine deiodinases, D1, D2, and D3, in the developing rat. *Endocrinology* 140:844-851.
33. Campos-Barros, A., Amma, L.L., Faris, J.S., Shailam, R., Kelley, M.W., and Forrest, D. 2000. Type 2 iodothyronine deiodinase expression in the cochlea before the onset of hearing. *Proc Natl Acad Sci USA* 97:1287-1292.
34. Ng, L., Goodyear, R.J., Woods, C.A., Schneider, M.J., Diamond, E., Richardson, G.P., Kelley, M.W., Germain, D.L., Galton, V.A., and Forrest, D. 2004. Hearing loss and retarded cochlear development in mice lacking type 2 iodothyronine deiodinase. *Proc Natl Acad Sci U S A* 101:3474-3479.
35. Forrest, D., Ng, L., Kelley, M., Schneider, M.J., St. Germain, D.L., and Galton, V.A. 2001. Cochlear defects and deafness in mice lacking type II selenodeiodinase. In *73rd Meeting of the American Thyroid Association*. Washington DC.
36. Guadano-Ferraz, A., Obregon, M.J., St Germain, D.L., and Bernal, J. 1997. The type 2 iodothyronine deiodinase is expressed primarily in glial cells in the neonatal rat brain. *Proc Natl Acad Sci U S A* 94:10391-10396.
37. Riskind, P.N., Kolodny, J.M., and Larsen, P.R. 1987. The regional hypothalamic distribution of type II 5'-monodeiodinase in euthyroid and hypothyroid rats. *Brain Res* 420:194-198.
38. Tu, H.M., Kim, S.W., Salvatore, D., Bartha, T., Legradi, G., Larsen, P.R., and Lechan, R.M. 1997. Regional distribution of type 2 thyroxine deiodinase messenger ribonucleic acid in rat hypothalamus and pituitary and its regulation by thyroid hormone. *Endocrinology* 138:3359-3368.
39. Fekete, C., Mihaly, E., Herscovici, S., Salas, J., Tu, H., Larsen, P.R., and Lechan, R.M. 2000. DARPP-32 and CREB are present in type 2 iodothyronine deiodinase-producing tanycytes: implications for the regulation of type 2 deiodinase activity. *Brain Res* 862:154-161.
40. Diano, S., Naftolin, F., Goglia, F., Csernus, V., and Horvath, T.L. 1998. Monosynaptic pathway between the arcuate nucleus expressing glial type II iodothyronine 5'-deiodinase mRNA and the median eminence-projective TRH cells of the rat paraventricular nucleus. *J Neuroendocrinol* 10:731-742.
41. Salvatore, D., Bartha, T., Harney, J.W., and Larsen, P.R. 1996. Molecular biological and biochemical characterization of the human type 2 selenodeiodinase. *Endocrinology* 137:3308-3315.
42. Bartha, T., Kim, S.W., Salvatore, D., Gereben, B., Tu, H.M., Harney, J.W., Rudas, P., and Larsen, P.R. 2000. Characterization of the 5'-flanking and 5'-

untranslated regions of the cyclic adenosine 3',5'-monophosphate-responsive human type 2 iodothyronine deiodinase gene. *Endocrinology* 141:229-237.
43. Salvatore, D., Tu, H., Harney, J.W., and Larsen, P.R. 1996. Type 2 iodothyronine deiodinase is highly expressed in human thyroid. *J Clin Invest* 98:962-968.
44. Murakami, M., Araki, O., Hosoi, Y., Kamiya, Y., Morimura, T., Ogiwara, T., Mizuma, H., and Mori, M. 2001. Expression and regulation of type II iodothyronine deiodinase in human thyroid gland. *Endocrinology* 142:2961-2967.
45. Imai, Y., Toyoda, N., Maeda, A., Kadobayashi, T., Wang, F., Kuma, K., Mitsushige, N., and Iwasaka, T. 2001. Type 2 iodothyronine deiodinase expression is upregulated by protein kinase A-dependent pathway and is downregulated by the protein kinase C-dependent pathway in cultured human thyroid cells. *Thyroid* 11:899-907.
46. Baqui, M.M., Gereben, B., Harney, J.W., Larsen, P.R., and Bianco, A.C. 2000. Distinct subcellular localization of transiently expressed types 1 and 2 iodothyronine deiodinases as determined by immunofluorescence confocal microscopy. *Endocrinology* 141:4309-4312.
47. Larsen, P.R., Silva, J.E., and Kaplan, M.M. 1981. Relationships between circulating and intracellular thyroid hormones: physiological and clinical implications. *Endocr Rev* 2:87-102.
48. Silva, J.E., and Larsen, P.R. 1978. Contributions of plasma triiodothyronine and local thyroxine monodeiodination to triiodothyronine to nuclear triiodothyronine receptor saturation in pituitary, liver, and kidney of hypothyroid rats. Further evidence relating saturation of pituitary nuclear triiodothyronine receptors and the acute inhibition of thyroid- stimulating hormone release. *J Clin Invest* 61:1247-1259.
49. Bianco, A.C., and Silva, J.E. 1987. Nuclear 3,5,3'-triiiodothyronine (T3) in brown adipose tissue: receptor occupancy and sources of T3 as determined by *in vivo* techniques. *Endocrinology* 120:55-62.
50. Crantz, F.R., Silva, J.E., and Larsen, P.R. 1982. Analysis of the sources and quantity of 3,5,3'-triiodothyronine specifically bound to nuclear receptors in rat cerebral cortex and cerebellum. *Endocrinology* 110:367-375.
51. Bianco, A.C., Maia, A.L., da Silva, W.S., and Christoffolete, M.A. 2005. Adaptive activation of thyroid hormone and energy expenditure. *Biosci Rep* 25:191-208.
52. Heaton, G.M., Wagenvoord, R.J., Kemp, A., Jr., and Nicholls, D.G. 1978. Brown-adipose-tissue mitochondria: photoaffinity labelling of the regulatory site of energy dissipation. *Eur J Biochem* 82:515-521.
53. Ricquier, D., Lin, C., and Klingenberg, M. 1982. Isolation of the GDP binding protein from brown adipose tissue mitochondria of several animals and amino acid composition study in rat. *Biochem Biophys Res Commun* 106:582-589.
54. Enerback, S., Jacobsson, A., Simpson, E.M., Guerra, C., Yamashita, H., Harper, M.E., and Kozak, L.P. 1997. Mice lacking mitochondrial uncoupling protein are cold-sensitive but not obese. *Nature* 387:90-94.
55. Bianco, A.C., and Silva, J.E. 1987. Intracellular conversion of thyroxine to triiodothyronine is required for the optimal thermogenic function of brown adipose tissue. *J Clin Invest* 79:295-300.

56. Bianco, A.C., and Silva, J.E. 1987. Optimal response of key enzymes and uncoupling protein to cold in BAT depends on local T3 generation. *Am J Physiol* 253:E255-E263.
57. Obregon, M.J., Pitamber, R., Jacobsson, A., Nedergaard, J., and Cannon, B. 1987. Euthyroid status is essential for the perinatal increase in thermogenin mRNA in brown adipose tissue of rat pups. *Biochem Biophys Res Commun* 148:9-14.
58. Carvalho, S.D., Kimura, E.T., Bianco, A.C., and Silva, J.E. 1991. Central role of brown adipose tissue thyroxine 5'-deiodinase on thyroid hormone-dependent thermogenic response to cold. *Endocrinology* 128:2149-2159.
59. Carvalho, S.D., Negrao, N., and Bianco, A.C. 1993. Hormonal regulation of malic enzyme and glucose-6-phosphate dehydrogenase in brown adipose tissue. *Am J Physiol* 264:E874-881.
60. McCormack, J.G. 1982. The regulation of fatty acid synthesis in brown adipose tissue by insulin. *Prog Lipid Res* 21:195-223.
61. Young, J.B., Saville, E., and Landsberg, L. 1982. Effect of thyroid state on norepinephrine (NE) turnover in rat brown adipose tissue (BAT): potential importance of the pituitary. *Clin Res* 32:407 (Abstract).
62. Himms-Hagen, J. 1990. Brown adipose tissue thermogenesis: interdisciplinary studies. *Faseb J* 4:2890-2898.
63. Jockers, R., Issad, T., Zilberfarb, V., de Coppet, P., Marullo, S., and Strosberg, A.D. 1998. Desensitization of the beta-adrenergic response in human brown adipocytes. *Endocrinology* 139:2676-2684.
64. de Jesus, L.A., Carvalho, S.D., Ribeiro, M.O., Schneider, M., Kim, S.-W., Harney, J.W., Larsen, P.R., and Bianco, A.C. 2001. The type 2 iodothyronine deiodinase is essential for adaptive thermogenesis in brown adipose tissue. *J Clin Invest* 108:1379-1385.
65. Schneider, M.J., Fiering, S.N., Pallud, S.E., Parlow, A.F., St. Germain, D.L., and Galton, V.A. 2001. Targeted disruption of the type 2 selenodeiodinase gene (Dio2) results in a phenotype of pituitary resistance to T4. *Mol Endocrinol* 15:2137-2148.
66. Gereben, B., Kollar, A., Harney, J.W., and Larsen, P.R. 2002. The mRNA structure has potent regulatory effects on type 2 iodothyronine deiodinase expression. *Mol Endocrinol* 16:1667-1679.
67. Burmeister, L.A., Pachucki, J., and St. Germain, D.L. 1997. Thyroid hormones inhibit type 2 iodothyronine deiodinase in the rat cerebral cortex by both pre- and posttranslational mechanisms. *Endocrinology* 138:5231-5237.
68. St. Germain, D.L. 1988. The effects and interactions of substrates, inhibitors, and the cellular thiol-disulfide balance on the regulation of type II iodothyronine 5'-deiodinase. *Endocrinology* 122:1860-1868.
69. Leonard, J.L., Kaplan, M.M., Visser, T.J., Silva, J.E., and Larsen, P.R. 1981. Cerebral cortex responds rapidly to thyroid hormones. *Science* 214:571-573.
70. Koenig, R.J., Leonard, J.L., Senator, D., Rappaport, N., Watson, A.Y., and Larsen, P.R. 1984. Regulation of thyroxine 5'-deiodinase activity by T3 in cultured rat anterior pituitary cells. *Endocrinology* 115:324-329.

71. Silva, J.E., and Leonard, J.L. 1985. Regulation of rat cerebrocortical and adenohypophyseal type II 5'- deiodinase by thyroxine, triiodothyronine, and reverse triiodothyronine. *Endocrinology* 116:1627-1635.
72. Halperin, Y., Shapiro, L.E., and Surks, M.I. 1994. Down-regulation of type II L-thyroxine, 5'-monodeiodinase in cultured GC cells: different pathways of regulation by L-triiodothyronine and 3,3',5'-triiodo-L-thyronine. *Endocrinology* 135:1464-1469.
73. Leonard, J.L., Silva, J.E., Kaplan, M.M., Mellen, S.A., Visser, T.J., and Larsen, P.R. 1984. Acute posttranscriptional regulation of cerebrocortical and pituitary iodothyronine 5'-deiodinases by thyroid hormone. *Endocrinology* 114:998-1004.
74. Obregon, M.J., Larsen, P.R., and Silva, J.E. 1986. The role of 3,3',5'-triiodothyronine in the regulation of type II iodothyronine 5'-deiodinase in the rat cerebral cortex. *Endocrinology* 119:2186-2192.
75. Steinsapir, J., Bianco, A.C., Buettner, C., Harney, J., and Larsen, P.R. 2000. Substrate-induced down-regulation of human type 2 deiodinase (hD2) is mediated through proteasomal degradation and requires interaction with the enzyme's active center. *Endocrinology* 141:1127-1135.
76. Kim, B.W., Zavacki, A.M., Curcio-Morelli, C., Dentice, M., Harney, J.W., Larsen, P.R., and Bianco, A.C. 2003. ER-associated degradation of the human type 2 iodothyronine deiodinase (D2) is mediated via an association between mammalian UBC7 and the carboxyl region of D2. *Mol Endocrinol* 17:2603-2612.
77. Coux, O., Tanaka, K., and Goldberg, A.L. 1996. Structure and functions of the 20S and 26S proteasomes. *Annu Rev Biochem* 65:801-847.
78. Hershko, A., and Ciechanover, A. 1998. The ubiquitin system. *Annu Rev Biochem* 67:425-479.
79. Dentice, M., Bandyopadhyay, A., Gereben, B., Callebaut, I., Christoffolete, M.A., Kim, B.W., Nissim, S., Mornon, J.P., Zavacki, A.M., Zeold, A., et al. 2005. The Hedgehog-inducible ubiquitin ligase subunit WSB-1 modulates thyroid hormone activation and PTHrP secretion in the developing growth plate. *Nat Cell Biol* 7:698-705.
80. Curcio-Morelli, C., Zavacki, A.M., Christofollete, M., Gereben, B., de Freitas, B.C., Harney, J.W., Li, Z., Wu, G., and Bianco, A.C. 2003. Deubiquitination of type 2 iodothyronine deiodinase by von Hippel-Lindau protein-interacting deubiquitinating enzymes regulates thyroid hormone activation. *J Clin Invest* 112:189-196.
81. Moreno, M., Berry, M.J., Horst, C., Thoma, R., Goglia, F., Harney, J.W., Larsen, P.R., and Visser, T.J. 1994. Activation and inactivation of thyroid hormone by type I iodothyronine deiodinase. *FEBS Lett* 344:143-146.
82. Salvatore, D., Low, S.C., Berry, M., Maia, A.L., Harney, J.W., Croteau, W., St. Germain, D.L., and Larsen, P.R. 1995. Type 3 lodothyronine deiodinase: cloning, in vitro expression, and functional analysis of the placental selenoenzyme. *J Clin Invest* 96:2421-2430.
83. Kaplan, M.M., and Yaskoski, K.A. 1980. Phenolic and tyrosyl ring deiodination of iodothyronines in rat brain homogenates. *J Clin Invest* 66:551-552.
84. Bates, J.M., Spate, V.L., Morris, J.S., St. Germain, D.L., and Galton, V.A. 2000. Effects of selenium deficiency on tissue selenium content, deiodinase activity, and

thyroid hormone economy in the rat during development. *Endocrinology* 141:2490-2500.
85. Roti, E., Braverman, L.E., Fang, S.L., Alex, S., and Emerson, C.H. 1982. Ontogenesis of placental inner ring thyroxine deiodinase and amniotic fluid 3,3',5'-triiodothyronine concentration in the rat. *Endocrinology* 111:959-963.
86. Kaplan, M.M., McCann, U.D., Yaskoski, K.A., Larsen, P.R., and Leonard, J.L. 1981. Anatomical distribution of phenolic and tyrosyl ring iodothyronine deiodinases in the nervous system of normal and hypothyroid rats. *Endocrinology* 109:397-402.
87. Galton, V.A., McCarthy, P.T., and St Germain, D.L. 1991. The ontogeny of iodothyronine deiodinase systems in liver and intestine of the rat. *Endocrinology* 128:1717-1722.
88. Richard, K., Hume, R., Kaptein, E., Sanders, J.P., van Toor, H., De Herder, W.W., den Hollander, J.C., Krenning, E.P., and Visser, T.J. 1998. Ontogeny of iodothyronine deiodinases in human liver. *J Clin Endocrinol Metab* 83:2868-2874.
89. Tu, H.M., Legradi, G., Bartha, T., Salvatore, D., Lechan, R.M., and Larsen, P.R. 1999. Regional expression of the type 3 iodothyronine deiodinase messenger ribonucleic acid in the rat central nervous system and its regulation by thyroid hormone. *Endocrinology* 140:784-790.
90. Squire, L.R. 1986. Mechanisms of memory. *Science* 342:1612-1619.
91. Puymirat, J., Miehe, M., Marchand, R., Sarlieve, L., and Dussault, J.H. 1991. Immunocytochemical localization of thyroid hormone receptors in the adult rat brain. *Thyroid* 1:173-184.
92. Puymirat, J. 1992. Thyroid receptors in the rat brain. *Prog Neurobiol* 39:281-294.
93. McCann, U.D., Shaw, E.A., and Kaplan, M.M. 1984. Iodothyronine deiodination reaction types in several rat tissues: effects of age, thyroid status, and glucocorticoid treatment. *Endocrinology* 114:1513-1521.
94. Huang, T.S., Chopra, I.J., Beredo, A., Solomon, D.H., and Chua Teco, G.N. 1985. Skin is an active site for the inner ring monodeiodination of thyroxine to 3,3',5'-triiodothyronine. *Endocrinology* 117:2106-2113.
95. Fay, M., Roti, E., Fang, S.L., Wright, G., Braverman, L.E., and Emerson, C.H. 1984. The effects of propylthiouracil, iodothyronines, and other agents on thyroid hormone metabolism in human placenta. *J Clin Endocrinol Metab* 58:280-286.
96. Roti, E., Fang, S.L., Green, K., Emerson, C.H., and Braverman, L.E. 1981. Human placenta is an active site of thyroxine and 3,3',5-triiodothyronine tyrosyl ring deiodination. *J Clin Endocrinol Metab* 53:498-501.
97. Castro, M.I., Braverman, L.E., Alex, S., Wu, C.F., and Emerson, C.H. 1985. Inner-ring deiodination of 3,5,3'-triiodothyronine in the *in situ* perfused guinea pig placenta. *J Clin Invest* 76:1921-1926.
98. Hidal, J.T., and Kaplan, M.M. 1985. Characteristics of thyroxine 5'-deiodination in cultured human placental cells: regulation by iodothyronines. *J Clin Invest* 76:947-955.
99. Galton, V.A., Martinez, E., Hernandez, A., St Germain, E.A., Bates, J.M., and St Germain, D.L. 1999. Pregnant rat uterus expresses high levels of the type 3 iodothyronine deiodinase. *J Clin Invest* 103:979-987.

100. Friesema, E.C., Kuiper, G.G., Jansen, J., Visser, T.J., and Kester, M.H. 2006. Thyroid hormone transport by the human monocarboxylate transporter 8 and its rate-limiting role in intracellular metabolism. *Mol Endocrinol*.
101. Huang, S.A., Tu, H.M., Harney, J.W., Venihaki, M., Butte, A.J., Kozakewich, H.P., Fishman, S.J., and Larsen, P.R. 2000. Severe hypothyroidism caused by type 3 iodothyronine deiodinase in infantile hemangiomas. *N Engl J Med* 343:185-189.
102. Wasco, E.C., Martinez, E., Grant, K.S., St Germain, E.A., St Germain, D.L., and Galton, V.A. 2003. Determinants of iodothyronine deiodinase activities in rodent uterus. *Endocrinology* 144:4253-4261.
103. Huang, S.A., Dorfman, D.M., Genest, D.R., Salvatore, D., and Larsen, P.R. 2003. Type 3 Iodothyronine Deiodinase is Highly Expressed in the Human Uteroplacental Unit and in Fetal Epithelium. *J Clin Endocrinol and Metabolism* 88:1384-1388.

Livros Grátis

(http://www.livrosgratis.com.br)

Milhares de Livros para Download:

Baixar livros de Literatura
Baixar livros de Literatura de Cordel
Baixar livros de Literatura Infantil
Baixar livros de Matemática
Baixar livros de Medicina
Baixar livros de Medicina Veterinária
Baixar livros de Meio Ambiente
Baixar livros de Meteorologia
Baixar Monografias e TCC
Baixar livros Multidisciplinar
Baixar livros de Música
Baixar livros de Psicologia
Baixar livros de Química
Baixar livros de Saúde Coletiva
Baixar livros de Serviço Social
Baixar livros de Sociologia
Baixar livros de Teologia
Baixar livros de Trabalho
Baixar livros de Turismo